

Revista Română de Inginerie Civilă
Indexată în bazele de date internaționale (BDI)
ProQuest, INSPEC, EBSCO
INDEX COPERNICUS, ULRICH'S și JOURNALSEEK

Volumul 6 (2015), Numărul 1
ISSN 2068-3987

Preliminary study of PTC use for human body heating dissipation mannequin	<i>1-10</i>
<i>Tiberiu Adrian Salaoru, Marina Andrei</i>	
<hr/>	
Numerical study of air cooling photovoltaic panels using heat sinks	<i>11-20</i>
<i>Sebastian Hudisteanu, Theodor-Dorin Mateescu, Nelu-Cristian Chereches, Catalin-George Popovici</i>	
<hr/>	
Analysis of the Flow Structure and its Influence on the Operation of a Wastewater Pumping Station	<i>21-25</i>
<i>Nicolae Ioan Alboiu, Costin Ioan Coșoiu, Anton Anton</i>	
<hr/>	
Etude thermique d'un capteur solaire innovant à circulation d'air	<i>26-35</i>
<i>Cristiana Croitoru, Amina Meslem, Ramy Atta</i>	
<hr/>	
Application of multivariate statistical analysis to evaluate parameters in a wastewater treatment	<i>36-42</i>
<i>Marius-Daniel Roman</i>	
<hr/>	
Modelarea sistemelor cu purtători multipli de energie în clădiri	<i>43-50</i>
<i>Pavel Atănăsoae</i>	
<hr/>	
Daylight in retrofitting office building design	<i>51-62</i>
<i>Alexandru Mircea Iatan, Angel Madalin Dogeanu</i>	
<hr/>	
Aiming to achieve net zero energy lighting in buildings	<i>63-78</i>
<i>Cosmin Ticleanu</i>	
<hr/>	
Fluid flow and heat transfer simulations for a box double-skin façade in Brasov, Romania	<i>79-86</i>
<i>Gabriel Nastase, Robert Gavriiliuc, Alexandru Serban, Ioan Boian</i>	
<hr/>	
Ecoshopping: energy efficient & cost competitive retrofitting solutions for retail buildings	<i>87-100</i>
<i>A. J. Lewry, E. Suttie</i>	

COLEGIUL EDITORIAL

Prof.dr.ing. Ioan BOIAN, *Universitatea Transilvania Braşov*
Prof.dr.ing. Alexandru CĂTĂRIG, *Universitatea Tehnică Cluj Napoca*
Conf.dr.ing. Victoria COTOROBAL, *Universitatea Tehnică Gh. Asachi Iaşi*
Prof. dr. mat. Rodica DĂNEŢ, *Universitatea Tehnică de Construcţii Bucureşti*
Prof.dr.ing. Carlos Infante FERREIRA, *Delft University of Technology, The Netherlands*
Prof.dr.ing. Dragoş HERA, *Universitatea Tehnică de Construcţii Bucureşti – redactor şef*
Prof.dr.ing. Ovidiu IANCULESCU, *director editorial*
Prof.dr.ing. Gheorghe Constantin IONESCU, *Universitatea Oradea*
Prof.dr.ing. Florin IORDACHE, *Universitatea Tehnică de Construcţii Bucureşti*
Prof.dr.ing. Vlad IORDACHE, *Universitatea Tehnică de Construcţii Bucureşti*
Prof.dr.ing. Carmen Elena MAFTEI, *Universitatea Ovidius Constanţa*
Prof.dr.ing. Ion MIREL, *Universitatea Politehnică Timişoara*
Prof.dr.ing. Dan GEORGESCU, *Universitatea Tehnică de Construcţii Bucureşti*
Prof.dr.ing. Mircea PETRINA, *Universitatea Tehnică Cluj Napoca*
Conf.dr.ing. Dorel PLĂTICĂ, *Universitatea Tehnică Gh. Asachi Iaşi*
Prof.dr.ing. Nicolae POSTĂVARU, *Universitatea Tehnică de Construcţii Bucureşti-redactor şef*
Prof.dr.ing. Daniela PREDA, *Universitatea Tehnică de Construcţii Bucureşti*
Prof.dr.ing. Ioan SÎRBU, *Universitatea Politehnică Timişoara*
Prof.dr.ing. Ioan TUNS, *Universitatea Transilvania Braşov*

ISSN 2068-3987

MATRIX ROM
OP CHIAJNA CP 2
077040 – ILFOV
Tel. 021 4113617 Fax. 021 4114280
e-mail: office@matrixrom.ro
www.matrixrom.ro

Preliminary study of PTC use for human body heating dissipation mannequin*

Tiberiu Adrian Salaoru*¹, Marina Andrei¹

*Corresponding author

*1INCAS - National Institute for Aerospace Research "Elie Carafoli"

B-dul Iuliu Maniu 220, Bucharest 061136, Romania

E-mail: salaoru.tiberiu@incas.ro

Abstract. *An important field of research for improving the efficiency of the Heating, Ventilation and Air Conditioning (HVAC) systems and for reducing the number of deaths occurred during the surgical procedures of the patients under effect of full anesthesia is the study of the human body heat losses mechanisms. A useful way to perform these studies is to manufacture a human body manikin which has maintained constant its surface temperature on a value close to real human body temperature. For heating the surface of the manikin can be used PTC (Positive Temperature Coefficient) thermistors mounted on the entire surface of the manikin. In this paper are presented preliminary results of the study performed on these devices, of the transient heating regime and the temperature stability.*

Key words: *PTC, thermistors, thermal mannequin, temperature stability*

1. Introduction

An important issue of the air conditioning systems is to ensure the indoor ambient quality for the best comfort of the users of these systems. Unfortunately there are two demands which are opposite: one is to comply with new air quality standards and the other is to save the energy. The main problem is to satisfy both of these by trying to optimise the systems which at the moment it seems they are not optimised enough. One of the main problems is the cooling of the rooms in hot season when the cold air supplied by the system is tumbling due to the gravitational forces causing the "cold", "draft" and sore throat sensations to the people. This problem is caused by the poor quality of cooling and warm air mixture quality. On the other hand, the energy consumption seems to rise in the past decade mainly due to the hotter summers. A solution to these issues it seems to work on the optimisation of the design for the air recirculation terminal devices related to the ambient air.

It is seems that taking into account the convection air currents generated by the surrounding heat sources as human body will change dramatically the air flows

* Lucrare inclusă în programul conferinței EENVIRO 2014

configuration [1]. Unfortunately at the moment are considered the configuration of the air flows generated only by recirculation devices.

An important issue is to study the distribution of the air speed which is influenced by the heat sources, mainly the position of the peak values of the air speed [1]. Human body being an important heat source, has been developed a series of its models having various complexity used on the CFD type studies [2-4].

The thermal perception of the internal environment can be influenced by some specific parameters such as shape, size, metabolism, dressing level or physical activity [5].

Using a thermal mannequin for simulating the human body thermal behaviour [6-8] is a good solutions for validating experimentally the numerical models because the experiments involving human subjects are expensive, time consuming and difficult to be validated.

Has been developed a series of five low cost thermal mannequins prototypes made by Universitatea Tehnica de Construcții Bucuresti [10-13] team in the EQUATOR[9] project frame and we want to carry on further optimisations of better future prototypes. The main requirement for these mannequins is to have the real shape and size of an adult person, having its surface split in distinct areas, [7] each of them being maintained at a slightly different temperature from each other but close to the human body temperature [14].

A method for heating the surface of the mannequin is to mount Positive Temperature Coefficient (PTC) thermistors on the surface.

These thermistors have a self regulation temperature feature embedded which allow to maintain the mannequin surface on a controlled constant temperature. In this paper is presented a series of preliminary results of a study for evaluating the use of PTC for making thermal mannequins.

2. Experimental system setup

The block diagram for the experimental system made for testing the temperature stability and for measuring the consumed power is shown in the Figure 1. Each PTC thermistor which has been tested has been mounted on a square shape aluminium plate.

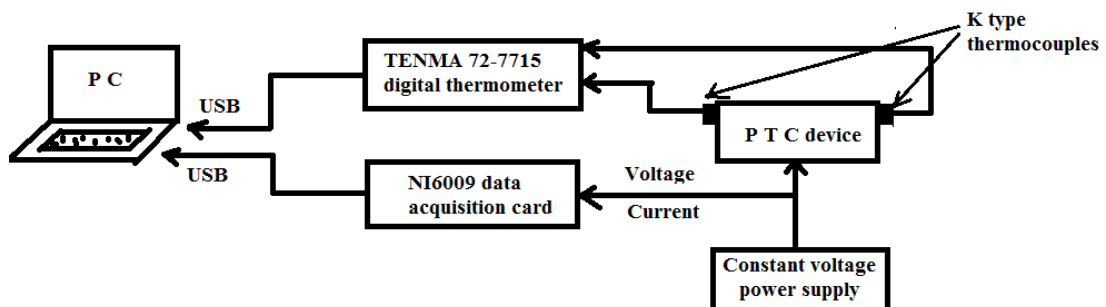


Figure 1. Block diagram of the measurement system

Preliminary study of PTC use for human body heating dissipation mannequin

The power supply TENMA 72-10500, 30V/3A is applying a constant voltage to the PTC thermistor and to the first analogue input channel of the National Instruments NI6009 data acquisition card for measuring its value. The current intensity value which is flowing from the power supply thru PTC thermistor is measured using the second analogue channel of the same data acquisition card. On the same aluminium plate where is mounted the PTC device are attached two K type thermocouples connected to the TENMA 72-7115 digital thermometer for monitoring the temperature. Both data acquisition card and the digital thermometer are connected to the PC thru USB ports for data transfer.

Have been tested a number of PTC thermistors, HP03 1/04, HP03-1/08, HP05-1/22, HP06-2/22, HP06-2/13 made by DBK Technitherm Ltd and A60 B59060A0040A010 made by EPCOS (Figure 3)[16]

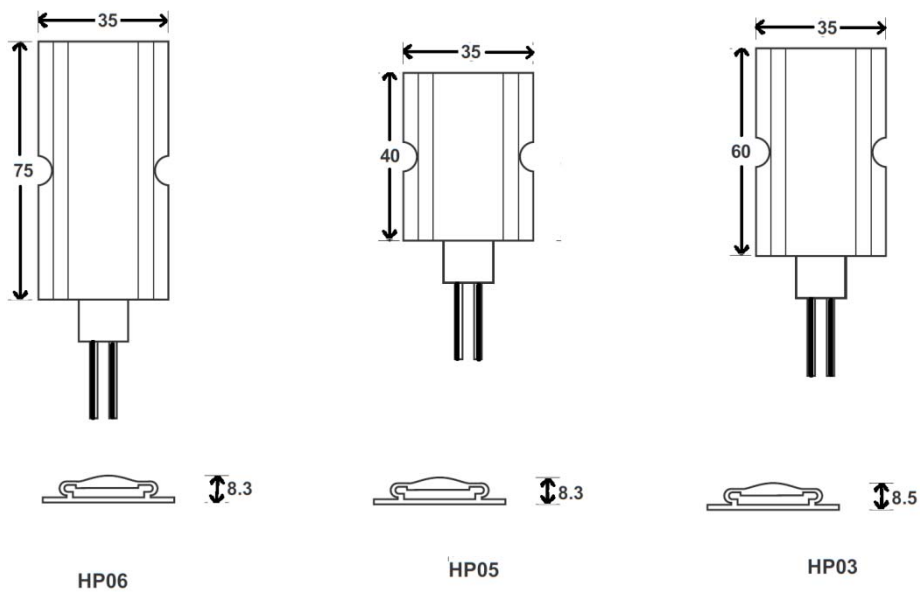


Figure 2. PTC dimensions produced by DBK Technitherm

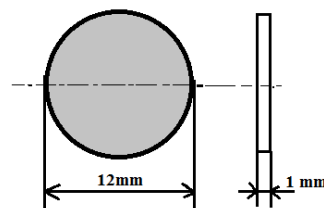


Figure 3. PTC dimensions of A60 B59060A0040A010 produced by EPCOS

Each of these thermistors have been mounted each on a 100 x 100mm square aluminium plate and 1.5mm thickness. The attaching mode of the HP03 – HP06 to the aluminium plate is shown in the Figure 4.

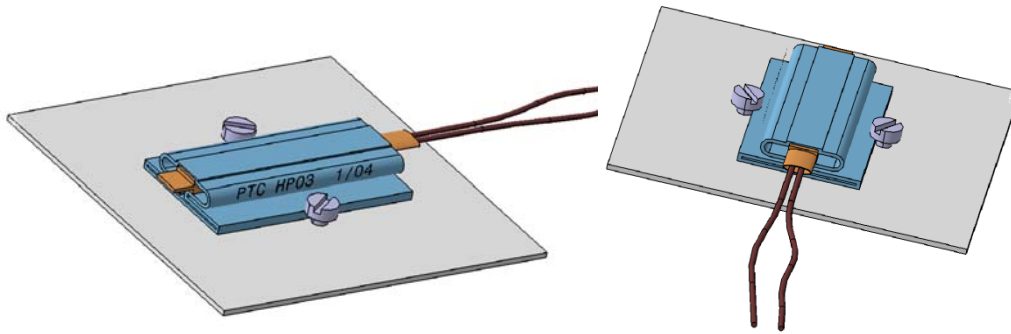


Figure 4. HP03 thermistor attached to the aluminium plate

For the purpose of monitoring the temperature, have been attached to the aluminium plate, two K type thermocouples which are connected to TENMA 72-7715 thermometer.

The A60 B59060A0040A010 PTC thermistor having a shape of a disk without any terminals as it appears in Figure 3, is requiring a system for attaching it to the aluminium plate and for electrical connections. This system is made by a smaller rectangular plate which is pressing the PTC against the aluminium plate using two screws (Figure 4).

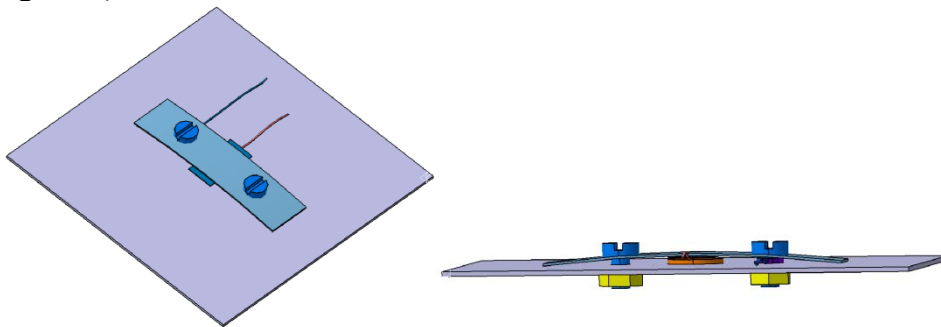


Figure 4. A60 B59060A0040 thermistor attachment system to the aluminium plate

The main element of the electrical circuit diagram of the PTC thermistors testing system is the NI 6009 data acquisition card which is measuring simultaneously the applied voltage and the electrical current which is flowing thru the PTC thermistor (Figure 5). In this way can be monitored continuously the consumed power of the device.

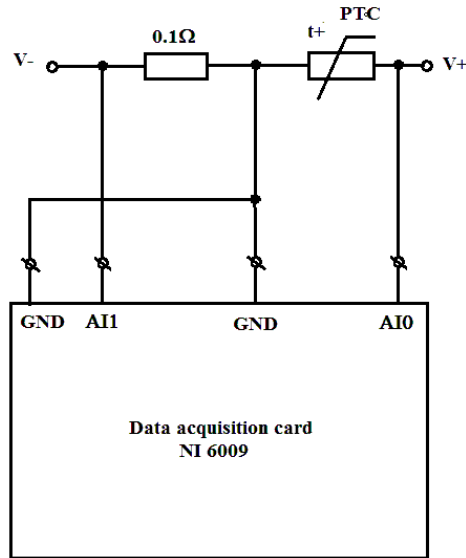


Figure 5. Circuit diagram for PTC testing

Applied voltage to the thermistor is measured by AI0 channel from the data acquisition card which is set in the range of 0 – 10V and the current intensity (I) is measured by using a 0.1Ω resistor connected in series with the PTC device. The dropping voltage on this resistor is offering the information about the electrical current intensity which is passing thru it. This voltage (U) is measured by AI1 channel of the data acquisition card and the measurement range is set in 0 – 1V range. Knowing the value of the resistor, the current intensity is calculated by:

$$I = U / 0.1 \quad (2.1)$$

Knowing the applied voltage and the current intensity can be easily calculated the power (P) consumed by the PTC thermistor:

$$P = U \cdot I \quad (2.2)$$

These calculations are done in a Labview code which is controlling system data acquisition and storage.

3. Experimental method

For studying the behaviour of each PTC device regarding temperature stability, has been applied a constant voltage during each test having the value in the range between 4.5 – 8.5V using 1V step. For each value of the voltage has been measured every second the current intensity and plate temperature variation in time for 30 minutes.

This time interval of 30 minutes has been chosen for allowing the system to reach thermal equilibrium.

The data acquisition rate of 1 measurement/second has been proved to be fast enough for sensing the fastest temperature and current intensity variation for the studied system.

For preventing any significant external perturbation from the environmental conditions such as air draughts, the system has been shielded and the ambient temperature has been maintained to 23°C.

4. Results and discussions

After analysing all the experimental results has been selected those from two PTC thermistors: A60 B59060A0040A010 and HP03 1/04 which seems to have the best characteristics such as the temperature stability for this voltage range applied.

By applying a constant voltage to the PTC device will produce a flowing current thru it which will heat the device quickly at beginning producing a rapid temperature rise which will have as result dropping of the current intensity.

This current intensity variation for A60 B59060A0040A010 thermistor is shown in the figure 6 and for HP03 1/04 is presented in figure 7.

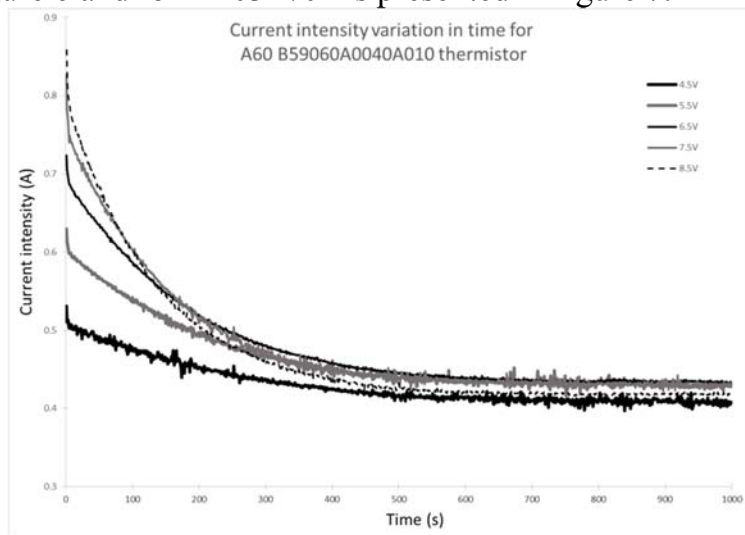


Figure 6. Current intensity variation for A60 B59060A0040A010 thermistor

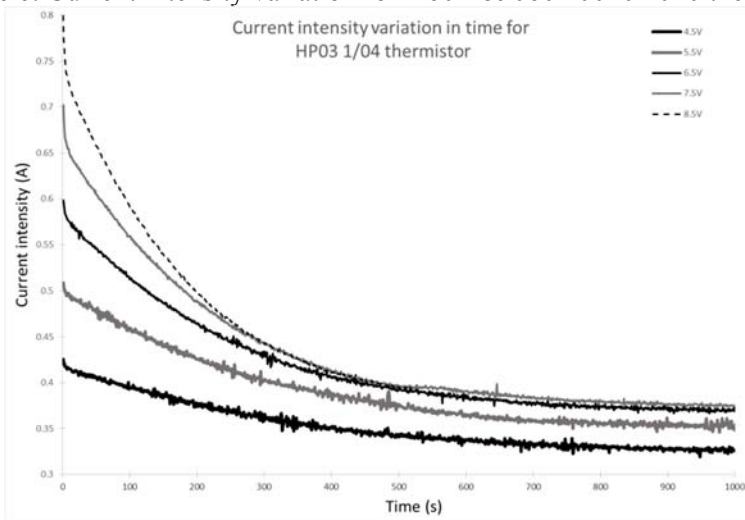


Figure 7. Current intensity variation for HP03 1/04 thermistor

The applied voltage being constant, the variation of the current intensity is caused by the variation of the resistance of the PTC device, which is rising quickly at the beginning and slower after.

The time variation of the resistance for A60 B59060A0040A010 thermistor is presented in the figure 8 and for HP03 1/04 in figure 9.

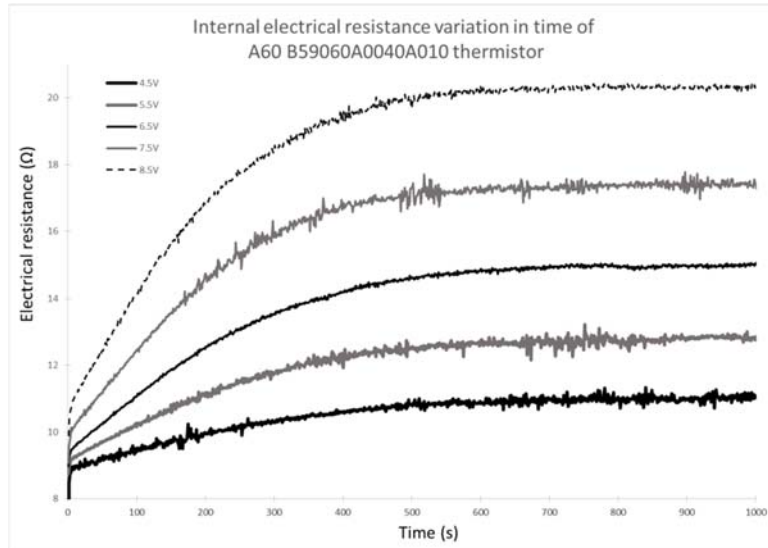


Figure 8. Variation of the internal electrical resistance of A60 B59060A0040A010 thermistor

For both thermistors, the internal electrical resistance is rising significantly in the first 5 minutes and then the rise slope is lowering in time becomes nearly constant after 15 minutes.

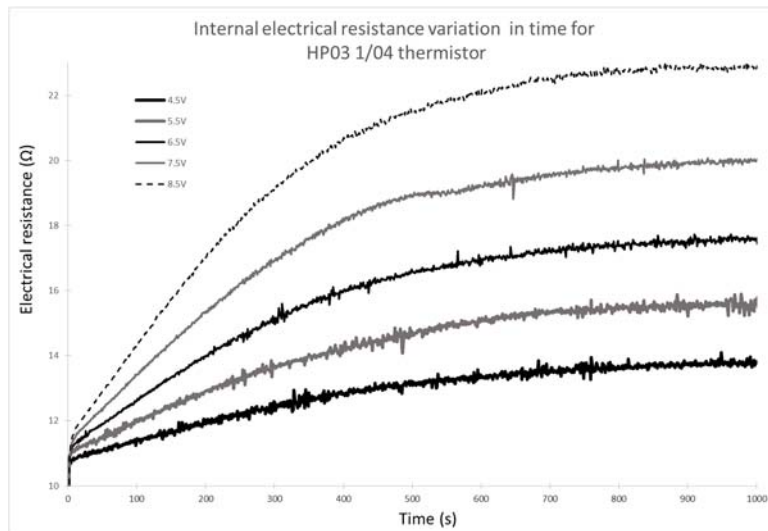


Figure 9. Variation of the electrical internal resistance of HP03 1/04 thermistor

The stability of the current intensity and of the electrical internal resistance after 15 minutes has as result a stability of the temperature which can be seen in the figures 10 and 11.

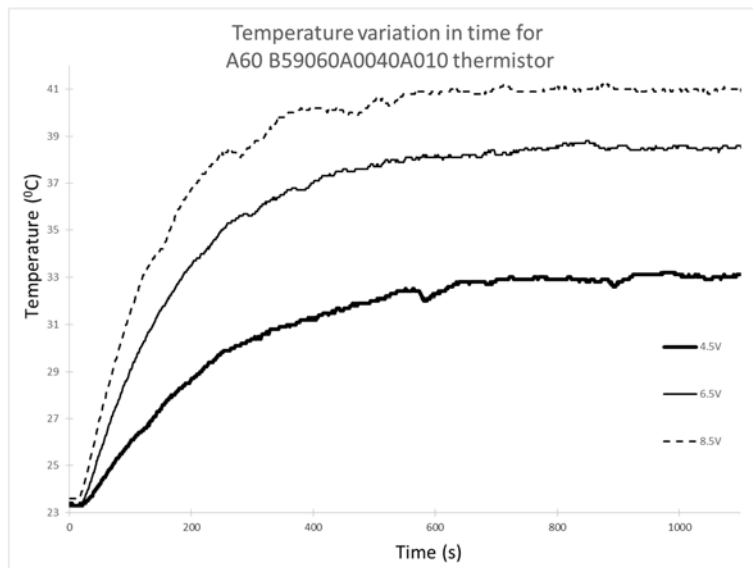


Figure 10. Temperature variation for A60 B59060A0040A010

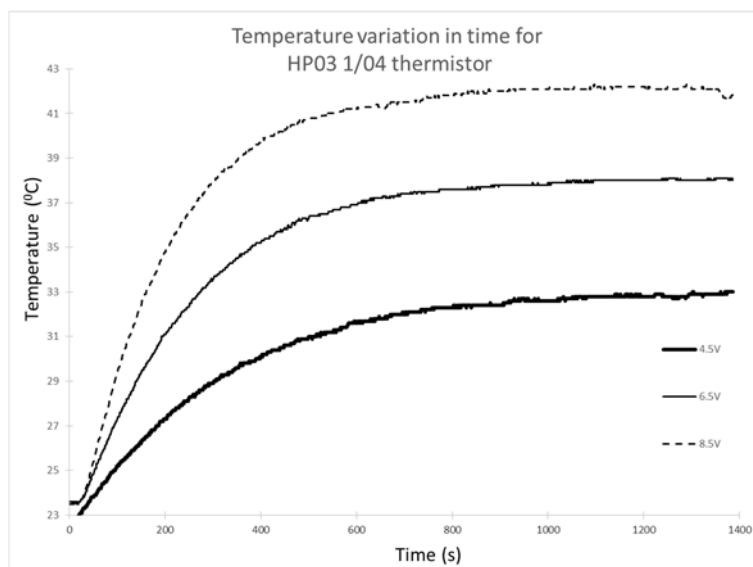


Figure 11. Temperature variation for HP03 1/04

All results shown above reveal a clear correlation between variations of the internal electrical resistance, current and temperature. Any change of temperature of the thermistor will have as results a change of its electrical resistance causing a variation of the intensity of current. For each characteristics, the power supply voltage has been maintained constant.

5. Future directions of development

One of the useful direction for improving using the PTC device as heating element for mannequin will be to try to reduce the relaxation time of the thermistor.

This is necessary to reach quicker the equilibrium temperature and to improve the temperature stability in time. This could be done by connecting this type of thermistor into a higher complexity circuit, where the applied voltage will be controlled by another devices during transient processes, maintaining it constant only during the thermal equilibrium.

6. Conclusions

The preliminary studies presented in this paper was performed for evaluation the use of the PTC devices for heating the thermal mannequin surface. The advantage of this devices is the low cost and simplicity of installing and using them. They require only to be mounted of the mannequin's surface and be supplied by a constant voltage power supply.

They present an intrinsic self regulating temperature feature when they are powered from a constant voltage power supply.

Their current temperature stability added with the possibility of improving it by connecting them in a higher performance circuits recommend the PTC thermistors as an excellent component for maintaining constant temperature of the external surface of the thermal mannequins.

Acknowledgements

This work was supported by the grant of the Romanian National Authority for Scientific Research, CNCS – UEFISCDI, project numbers: PN-II-PT-PCCA-2011-3.2-1212.

References

- [1] R. Kosonen, et al., *Impact of heat load location and strength on air flow pattern with a passive chilled beam system*, *Energy and Buildings*, ISSN: 0378-7788 **42**(1): p. 34-42, doi: 10.1016/j.enbuild.2009.07.008, 2010.
- [2] D. N. Sorensen and L. K. Voigt, *Modeling airflow and heat transfer around a seated human body by computational dynamics*, *Building and Environment*, ISSN: 0360-1323, **38**(6): p. 753-762, 2003.
- [3] S. Murakami, S. Kato and J. Zeng, *Combined simulation of airflow, radiation and moisture transport for heat release from a human body*, *Building and Environment*, ISSN: 0360-1323, **35**(6): p. 489-500, 2000.
- [4] S. Murakami, S. Kato and J. Zeng, *CFD analysis of thermal environment around human body*. *Indoor air '96*, **2**: p. 479-484, 1996.
- [5] C. Croitoru, et al., *Numerical and experimental modeling of airflow and heat transfer of a human body*. in Roomvent 2011 Conference, Trondheim, Norway.
- [6] A. Dogeanu, et al., *Conception of a simplified seated thermal manikin for CFD validation purposes*. *Romanian Journal of Civil Engineering*, 2013, (december 2013).
- [7] A. Dogeanu, et al. *Conception of an advanced thermal manikin for thermal comfort assessment in buildings and vehicles*. in Young Researchers Conference 2013, UTCB, 2013.

- [8] I. A. Cruceanu, *Studiul mișcării aerului în sistemele de ventilare personalizate*, Thesis, UTCB. 2013.
- [9] ***, ISO 9972 :2006 Thermal performance of buildings - Determination of air permeability of buildings - Fan pressurization method.
- [10] ***, *HP Series of PTC Heaters, datasheet catalog*,
<http://www.dbktechnitherm.ltd.uk/brochures/hpebht/Overview.pdf>,
<http://www.farnell.com/datasheets/477436.pdf>.

Numerical study of air cooling photovoltaic panels using heat sinks*

Sebastian Hudisteanu¹, Theodor-Dorin Mateescu¹, Nelu-Cristian Chereches¹, Catalin-George Popovici¹

¹Technical University "Gheorghe Asachi" of Iasi, Faculty of Civil Engineering and Building Services, Department of Building Services Engineering 13, bd Dimitrie Mangeron, 700050, Iasi
E-mail: seby_hudisteanu@yahoo.com

Abstract. *In this paper is presented a numerical study for the air cooling of the photovoltaic panels integrated in buildings. The studied cases assume the integration of photovoltaic panel on a double skin façade. Numerical simulations were achieved in ANSYS-Fluent software, for 3D model, in forced convection and turbulent flow. The improvement of the air cooling is studied for different inlet velocities and also in case of using a heat sink with ribs. The investigation is focused on the influence of different heights of the ribs on the heat transfer between photovoltaic panel and circulating air. The results are aimed on the conversion efficiency of the photovoltaic cells that is dependent on the average temperature of it.*

Key words: photovoltaic panel, passive cooling, numerical modeling, heat sink, ventilated façade

1. Introduction

A photovoltaic (PV) panel is composed from several photovoltaic cells that are designed to convert solar radiation into electric energy. The performance of photovoltaic panels is quantified as conversion efficiency, or how much solar radiation [W/m^2] is transformed into electric power [W/m^2] in certain conditions. Currently, this efficiency has maximum values between 14% and 17% for mono-crystalline silicon solar cell. The other 80% of solar radiation is transformed almost completely into heat.

The absorption of photons in far layers of p-n junction, that causes the recombination of free electrons, also generates extra heat inside the cells. Another heat source for photovoltaic cell is represented by the absorption of photons at lower energetic levels, without releasing electrons. The heat generated by Joule effect is also influencing the temperature of the PV panel.

In literature there are many studies talking about the dependence between the conversion efficiency and the temperature of photovoltaic cell [9]. The conclusion is that the efficiency is decreasing when the temperature of PV cell is rising, and the variation of maximum power production with temperature is considered almost linear.

* Lucrare inclusă în programul conferinței EENVIRO 2014

In fig. 1 it can be remarked that the I_{sc} (short-circuit current) value is rising once the temperature of the cell is greater but the V_{oc} (open circuit voltage) value is dropping abruptly, and in consequence the P_{max} (maximum power) is dropping too. The reduction of efficiency can be considered as approximately 0.3%...0.5% for each degree of temperature rise over 25 °C.

In this regard, the best conversion efficiency would be realized into the space, where the average temperature is near 0 K.

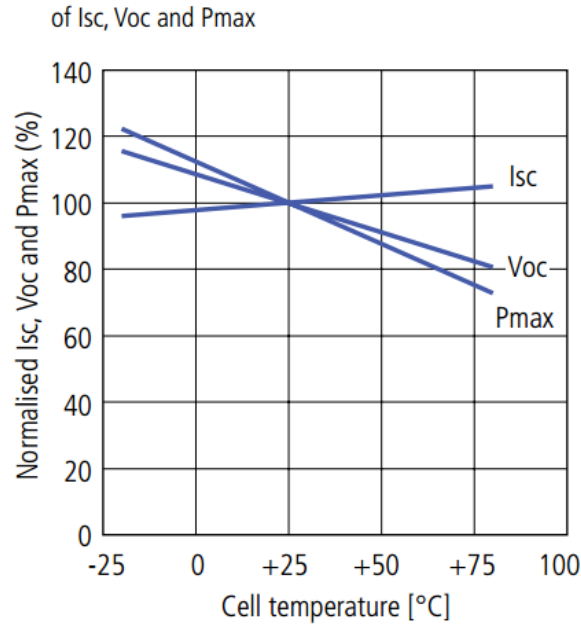


Fig. 1. The influence of temperature over conversion efficiency [1]

Skoplaki E. et al. [2] present different methods and relations for calculating the dependence between conversion efficiency and temperature of PV cells.

Because the power of a PV cell is dependent on temperature changes and solar irradiation level, in literature [10], are defined the standard parameters that are generating the Watt-peak (Wp). Therefore, the electrical power produced by a photovoltaic panel, measured in Wp, is defined for an average temperature of the cell of 25 °C, wind speed of 1 m/s and intensity of solar radiation of 1000 W/m².

In literature are presented many solutions for cooling the photovoltaic panels, by using the air, water or phase changing materials.

Cuce et al. [3] studied a method for improving the temperature of photovoltaic panels by using the air as a passive cooling. In that study the efficiency of PV panels is considered in three ways: energetic efficiency, efficiency of the conversion power and exergetic efficiency.

Another important study of the air cooling of photovoltaic panels was realized by Tonui et al. [4]. The cooling is obtained by realizing a ventilated channel of 10 cm width behind the photovoltaic panel. That study presents the PV/T technology that represents an optimized way of using photovoltaic panels with an additional role of

producing thermal energy. This aspect is very important because are produced two of the most used types of energy and the proper functioning of each one brings benefits to the other. It must be mentioned that in case of using PV/T systems the priority is represented by electrical energy production.

2. Case description

In this paper is studied the air cooling solution for PV panels by adding a ventilated channel behind them, that represents an interesting solution in case of integration of photovoltaic panels into buildings. For the buildings equipped with double skin façade, the PV panels can be inserted as exterior glazing and the channel of the façade can be used for air cooling. The ventilation of the channel can be realized naturally, determined by the thermal circulation or pressure differences, or mechanically for achieving velocities over 0.5 m/s.

The usual photovoltaic panels have some different layers depending on the technology of conception and producer. An example of structure for PV panels is presented and studied by Armstrong et al. in [5]. Thus, the main layers are: exterior glass, ARC (anti reflexive coating), PV cells, EVA (ethylene-vinyl acetate), metal rear contact and tedlar (realized from PVF). The thermo-physical properties of these layers are presented in table 1 [5].

Table 1

Thermo-physical properties of the PV panel layers

Layer	Thickness (m)	Thermal conductivity (W/mK)	Density (kg/m ³)	Specific heat Capacity (J/kgC)
1. Glass	0.003	1.8	3000	500
2. ARC	100 x 10 ⁻⁹	32	2400	691
3. PV Cells	225 x 10 ⁻⁶	148	2330	677
4. EVA	500 x 10 ⁻⁶	0.35	960	2090
5. Rear contact	10 x 10 ⁻⁶	237	2700	900
6. Tedlar	0.0001	0.2	1200	1250

In this paper, the photovoltaic panel is considered as a single layer with thermal characteristics of the PV cells. For realizing a better heat transfer from the photovoltaic cell, a heat sink with ribs is connected behind it. The heat sink must be realized from metals with high conductivity like copper.

3. Numerical Modeling

For this study, a small scale photovoltaic panel of 500mm x 500mm was considered. Since the temperature of photovoltaic cell is decisive regarding conversion efficiency, we considered the solution of air cooling the cells by using a heat sink connected to the PV panel. The heat sink is designed like a ribbed wall (fig. 2.), using ANSYS-Design Modeler, with the following dimensional characteristics:

- h – rib height (1...5 cm);
- s – step between ribs (5 cm);
- L, H – length and width of heat sink ($L = H = 500$ mm);
- g – thickness of heat sink base (2 mm);
- g_n – thickness of ribs (2 mm);
- l_n – length of ribs (480 mm);

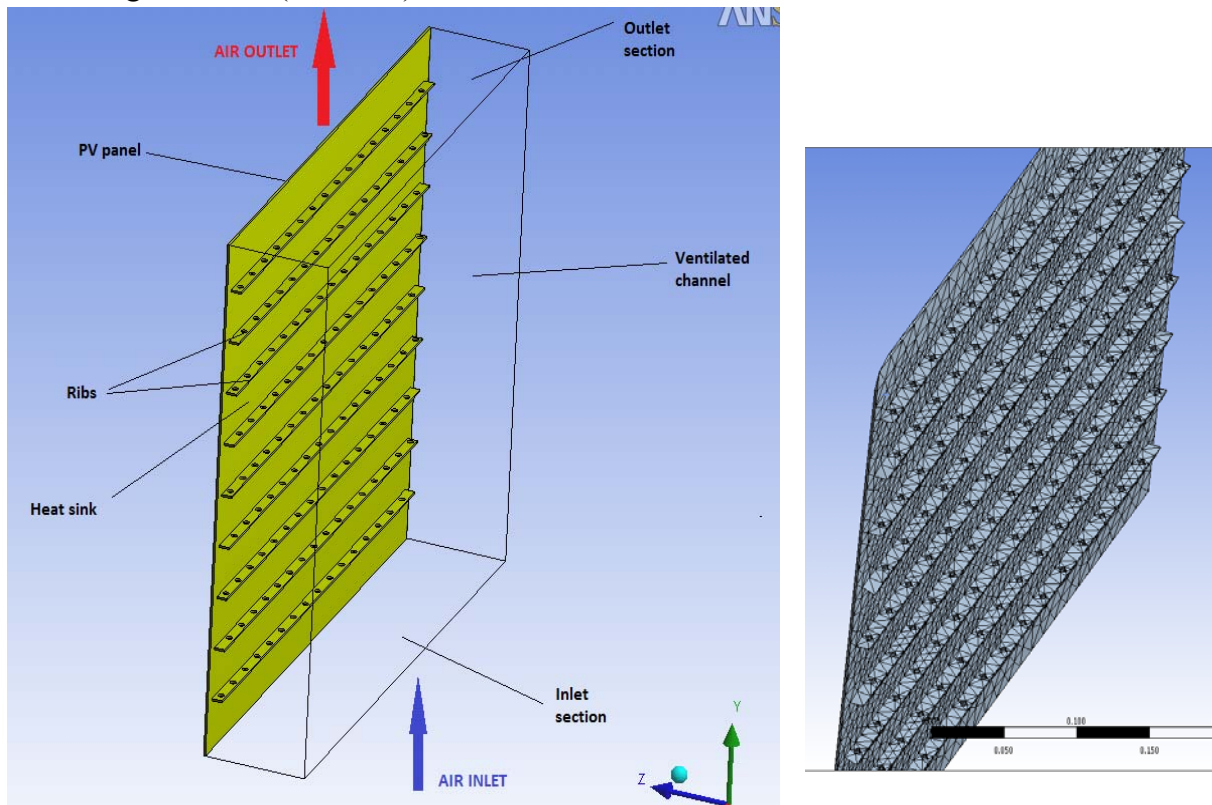


Fig. 2. Geometry and mesh of the model

The mesh – fig. 2 was realized with different refinement for the heat sink and ventilation channel. Hence, the minimum size of the finite element is about 2 mm for the heat sink and ribs and about 8 mm for the air channel. This fact was necessary taking into account the time needed for simulations. The mesh was created using ANSYS-Meshing and resulted a number of 194921 tetrahedral cells and 382888 interior faces.

The double skin facade system is created behind this ensemble and consists of a ventilated channel of 10 cm width. In this way, the heat sink is placed inside the channel and can be cooled using the ventilation system of the double skin facade.

The ribs of the heat sink have circular holes of 3 mm radius, placed at 30 mm distance one to another in order to improve the air circulation near the heat sink and extract more heat from the PV panel.

The different cases studied in this paper were realized by modifying the height of ribs from 1 cm to 5 cm with the step of 1 cm. Once the height is growing another row of holes is added on the rib.

The numerical simulation was realized using ANSYS-Fluent software. It was determined the average temperatures of photovoltaic panel in steady regime for the five configurations of heat sink for inlet velocities of 0.5 m/s, 1 m/s, 1.5 m/s and exterior temperature of 35 °C. In this study the variation of the height is considered in terms of h/s ratio. The sunlight conditions were considered for a summer day, without clouds, near Iasi and for a vertical position of photovoltaic panel. Hence, the maximum solar radiation for these conditions is about 500 W/m².

The flow regime considered is the turbulent one. The model of turbulence used in numerical simulations was k-ε RNG that is the most realistic for air flow inside channels [6].

The turbulence intensity I can be estimated as:

$$I = 0.16 \cdot \text{Re}^{\frac{1}{8}} \quad [7]$$

The characteristic values used as input for turbulence model was:

I – turbulence intensity of 5.5 %, 5 % and 4.8 % respectively for inlet velocities of 0.5 m/s, 1 m/s and 1.5 m/s;

D_H – hydraulic diameter of 0.166 m;

The results of simulations, for numerical model, are obtained for a solar radiation of 500 W/m². To the outer surface of photovoltaic panel, exposed to the sun, was considered a convective heat transfer with the exterior air with following values: α = 8 W/m²K and exterior temperature.

The optical parameters of photovoltaic panel, as ensemble, were synthesized in the software model as the coefficient of absorption of solar radiation of α = 0.7 [8]. The model used to simulate the solar radiation was the Fluent specific tool Solar Ray Tracing.

To resolve the continuity, the momentum and the energy equations, a computational program named Fluent based on the control volume method have been used with a SIMPLE algorithm. This method uses a relationship between velocity and pressure corrections to enforce mass conservation and to obtain the pressure field. In order to reduce the time necessary for simulations the soft was set for First Order Upwind in equation solver. A fully implicit numerical scheme is employed, in which upwind differences are used for the convective terms and central differences for the diffusion terms. The calculation is an iterative one, the chosen convergence criteria are 10⁻⁶ for the energy equation and 10⁻³ for the pressure, velocities and continuity equations.

4. Results and discussion

The results are presented as velocities and temperatures spectra and as parametric curves like:

$$t_{\text{medPV}} = f(h/S; v_{\text{in}}) \quad [^{\circ}\text{C}]$$

The first step consisted in determining the most favorable velocity regime in order to obtain a good cooling for the photovoltaic panel. Thus, for a constant ratio h/S of $1/5$ and inlet temperature of $35\text{ }^{\circ}\text{C}$ we realized a variation of inlet velocity of the air and the results are presented in fig. 3.

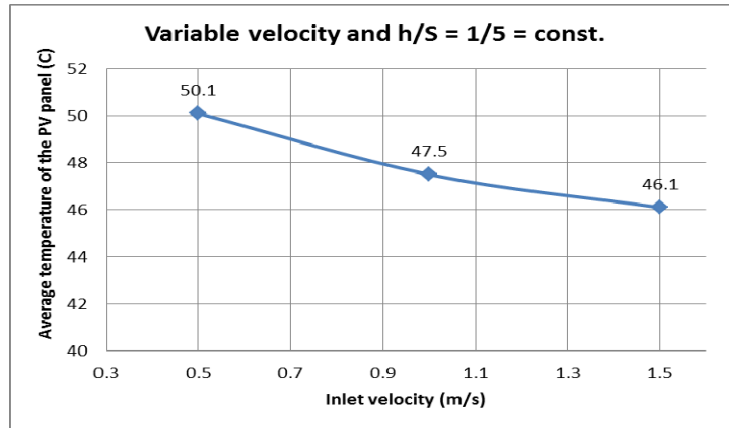


Fig. 3. Variation of PV panel temperature (interior surface) for different inlet velocities

It can be observed – fig. 3, that for this configuration, the lowest temperature of PV panel is achieved for the inlet velocity of 1.5 m/s . This value is used in the following simulations as constant for determining the relation between the average temperature of PV panel and h/s ratio.

By increasing the height of the ribs and maintaining constant the other parameters, the following cases are resulting:

- Case 1: $h/s = 1/5$
- Case 2: $h/s = 2/5$
- Case 3: $h/s = 3/5$
- Case 4: $h/s = 4/5$
- Case 5: $h/s = 5/5$

In fig. 4 are presented the results obtained in all five studied cases, for similar temperature and solar radiation conditions, considering the inlet velocity $v = 1.5\text{ m/s}$, same for all simulations.

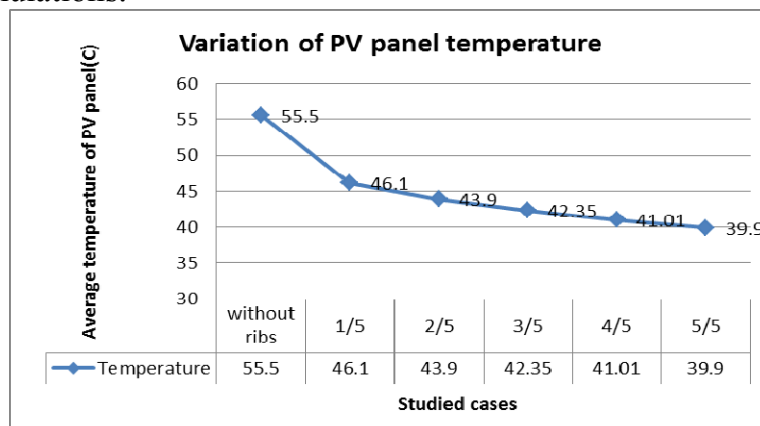


Fig. 4. Average temperature of PV panel for different h/S values

It can be observed - fig. 4 that the average temperature of photovoltaic panel has the tendency to decrease once the height of the ribs is growing. For the studied cases, an improvement of PV average temperature can be remarked with a ratio of minimum 1 °C for each centimeter raise of height.

For the base case, without using ribs, the location of the PV panel is similar to other studied cases, but there is no heat sink connected behind it. A reducing of almost 10 °C is recorded when there are used the smallest ribs of 1 cm height comparing to the case without ribs, and 15 °C for the case with 5 cm height – fig. 4.

For a better view over the phenomena inside the channel and near the ribs of the heat sink, in the following images are presented the temperature and velocity spectra.

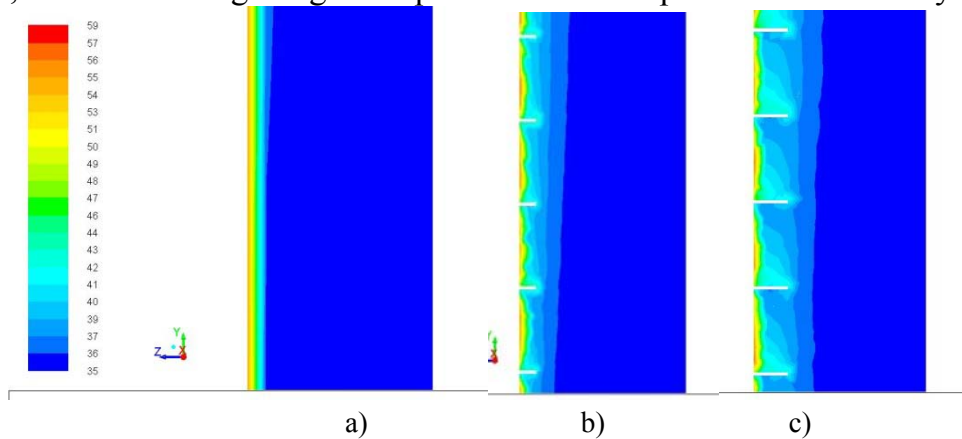


Fig. 5. Temperature spectra for cases: a) without ribs; b) h=1 cm; c) h = 2 cm

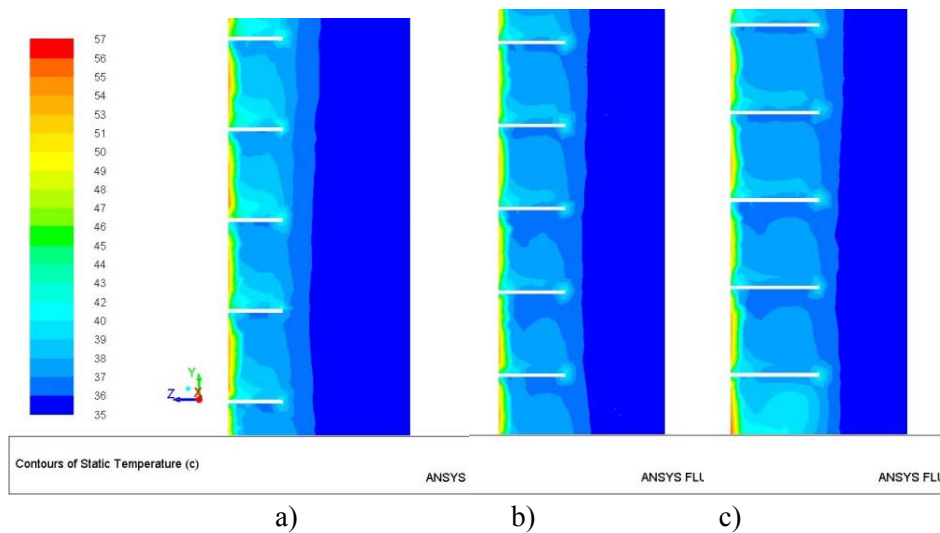


Fig. 6. Temperature spectra for cases: a) h = 3 cm; b) h = 4 cm; c) h = 5 cm

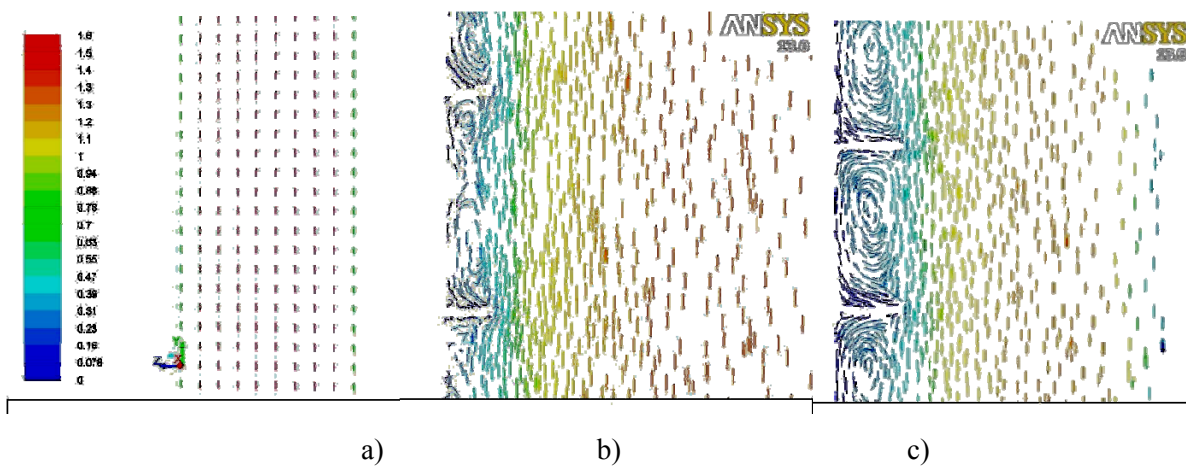


Fig. 7. Velocity magnitude for cases: a) without ribs; b) $h=1$ cm; c) $h = 2$ cm

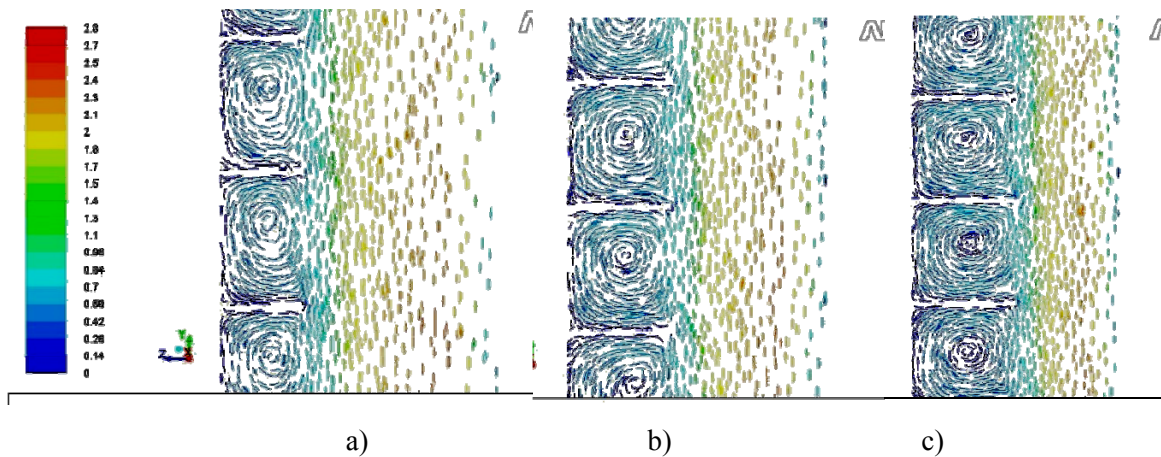


Fig. 8. Velocity magnitude for cases: a) $h = 3$ cm; b) $h = 4$ cm; c) $h = 5$ cm

The temperature spectra, fig. 5,6, highlights that the heat transfer from the heat sink to the air inside the channel is becoming more intense once the height of the ribs becomes larger. It can be observed that the warm air near the heat sink is combining better with the colder one that is circulating inside the channel, and so there is obtained a more efficient cooling of the PV panel.

Figures 7,8 confirm the precedent affirmations, the heat transfer being better because of the amplified turbulence phenomena determined by the ribs presence. Also, the recirculation between ribs becomes more important when the ribs are higher and the efficiency of the heat sink is increasing.

According to fig. 1, the efficiency of photovoltaic panel has a strong variation depending on the temperature of PV silicon cell. The performance can be represented by the main parameters of photovoltaic panel like the voltage and intensity of the current produced, globally expressed as maximum produced power. In this way, it can be seen that for a temperature of 55.5 °C, the electrical power produced by solar cell becomes approximately 85 % of the nominal one. These values of power percentage depending on temperatures are presented in table 2.

Table 2

Influence of temperature on the efficiency of PV panels for studied cases

Case	t_p [°C]	*[%] of P_N	η	** $P_{el\text{spec}}$ [W/m ²]	S [m ²]	P_{el} [W]	Increase compared to base case [%]
base***	55.5	86	0.1376	68.8	0.25	17.2	-
h/S=1/5	46.1	89	0.1424	71.2	0.25	17.8	3.48
h/S=2/5	43.9	91	0.1456	72.8	0.25	18.2	5.82
h/S=3/5	42.35	92	0.1472	73.6	0.25	18.4	6.98
h/S=4/5	41.01	93	0.1488	74.4	0.25	18.6	8.14
h/S=5/5	39.9	94	0.1504	75.2	0.25	18.8	9.31
Nominal	25	100	0.16	80	0.25	20	16.28

* According to fig. 1

** For solar radiation of 500 W/m²

*** Case without ribs

Where: t_p – average temperature of PV panel [°C];
 P_N – nominal produced power at 25 °C [W];
 η – conversion efficiency;
 $P_{el\text{spec}}$ – specific electric power [W/m²];
 S – Surface of PV panel [m²];
 P_{el} – electrical power produced by the studied PV panel [W];

5. Conclusions

For a nominal conversion efficiency of 16%, in table 2 are also presented the respectively performances for different cases: η . A performance of 16% can be expressed as an electric energy production of 160 W/m², in nominal conditions that requires 1000 W/m² of solar radiation. In this paper, in the studied models we used the maximum value of solar radiation of 500 W/m² as constant and the surface of PV panel of 0.25 m². But the maximum power produced by a photovoltaic cell also depends of the value of solar radiation, most often linearly and proportionally. So, the maximum power that can be produced by studied panel in our imposed conditions can reach 80 W/m², for a temperature of 25 °C.

It can be concluded that the purpose of decreasing the average temperature of PV panel is very important. Though for the studied case, a small dimension photovoltaic panel of 0.5m x 0.5m, the difference between the cases with no ribs to the cases when the ribs are used is about 0.6 to 1.6 W of electrical power produced, the problem must be traced deeper. In this way, we can focus on the percentage of increase that is from 3.5% to 9.3%. From this point of view, the improvement is more significant in case of using of a large scale building integrated photovoltaic system with installed power of several kWp. In this case every percent of extra power produced is very important, taking into account the investment that is quite expensive.

References

- [1] <http://www.lorenz.de/en/products/pv-modules.html>
- [2] *E. Skoplaki et al.*, “On the temperature dependence of photovoltaic module electrical performance: A review of efficiency/power correlations”, *Solar Energy* 83, 614–624, 2009
- [3] *Erdem Cuce et al.*, “Effects of passive cooling on performance of silicon photovoltaic cells”, *International Journal of Low-Carbon Technologies*
- [4] *J.K. Tonui et al.*, “Improved PV/T solar collectors with heat extraction by forced or natural air circulation”, *Renewable Energy* 32, 623–637, 2007
- [5] *S. Armstrong et al.*, “A thermal model for photovoltaic panels under varying atmospheric conditions”, *Applied Thermal Engineering* 30, 1488-1495, 2010
- [6] ANSYS Fluent Documentation
- [7] *Abu Karvinen et al.*, “Comparison of turbulence models in case of three-dimensional diffuser”
- [8] *Rudi Santbergen*, “Optical Absorption Factor of Solar Cells for PVT Systems”, ISBN: 978–90–386–1467–0
- [9] *V.Jafari Fesharaki, Majid Dehghani, J. Jafari Fesharaki*, ”The Effect of Temperature on Photovoltaic Cell Efficiency”, *Proceedings of the 1st International Conference on Emerging Trends in Energy Conservation - ETEC Tehran, Tehran, Iran, 20-21 November 2011*
- [10] http://www.wouterlood.com/solar_htmls/page_13_uk.html

Analysis of the Flow Structure and its Influence on the Operation of a Wastewater Pumping Station*

Nicolae Ioan Alboiu¹, Costin Ioan Coșoiu¹, Anton Anton¹

¹Technical University of Civil Engineering of Bucharest
E-mail: nalboiu@hidraulica.utcb.ro; nalboiu@yahoo.com

Abstract. *The hydraulic phenomena occurring at the entrance of a pumping station are crucial in order to ensure the required operation conditions. Under the circumstances of an undesired flow regime a faulty functioning of the pump units can occur. Such a case was studied by the authors of the present paper. As a consequence of the hydraulic system particularities and due to the local conditions at the inlet of the pumping station, the designed operation parameters were only occasionally achieved. Additionally, shortly after commissioning, the pump rotors were damaged. Starting this point on the Technical University of Civil Engineering Bucharest team studied, based on field measurement and using the expert software Fluent for CFD, the phenomena which caused the aforementioned operation problems. Thus, the streamlines and the velocity field in the given situation were modeled and analyzed. Based on this study several conclusions about the flow characteristics were driven, and a clearly point of view about the causes that are responsible for the poor operation parameter was issued.*

Key words: flow structure, sewerage system, Fluent CFD, pumping station

1. Background and aims

Short after the commissioning for the pumping station serving the first treatment line of a municipal wastewater treatment plant, operation problems were reported. Mainly these are related to the designed pumping capacity (10 m³/s) that is achieved only for short operation periods.

In their efforts to identify and remediate the problems that could lead to this situation the owner of the pumping station together with the designer and the contractor of the works developed several investigations. The conclusions of these studies revealed rotor damages that could be caused by erosion and/or cavitation. Also the low quality materials used for the pumps (unprotected cast iron) have favored the erosion process.

For identifying the real causes which can be responsible for such phenomenon and to eliminate them, the operator of the sewerage system requested to the Technical University of Civil Engineering of Bucharest (TUCEB) a new expertise on the

* Lucrare inclusă în programul conferinței EENVIRO 2014

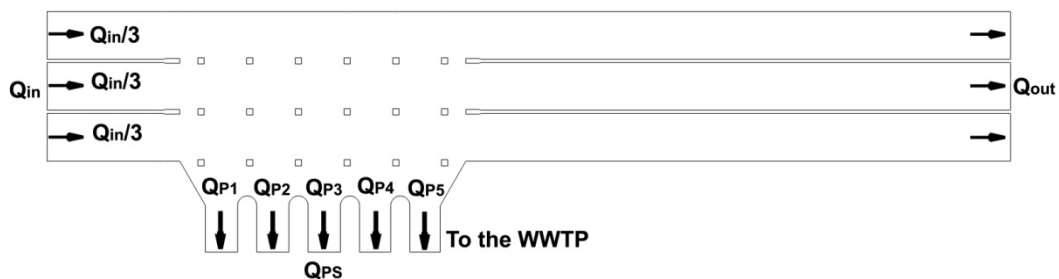
operation of the pumping station which aimed the solutions for solving the reported problems. To achieve these objectives the technical expertise pursuit the development of studies in the hydraulics field focused on all the possible causes leading to the malfunction of the pumping station.

Beside the data and technical documents provided by the operation personnel of the sewage system, a onsite monitoring campaign was carried out by the TUCEB team. The developed technical analyses has revealed a very complex hydraulic system which consists of the main collector, a three way rectangular gallery, a junction were the flow splits, part of the wastewater flows to the pumping station and part downstream to be discharged in the emissary. In the discharge section is a sharp crested weir controlling the water levels upstream.

One of the expertise topics carried out by the TUCEB team is related to the influences of the local conditions and their effects on the flow structure. In order to analyze these problems a numerical model was carried out. The obtained results offered a view of the flow phenomena occurring at the suction chambers inlet. Based on the results of the study several conclusions on the causes leading to the mentioned problems were driven

2. Model description, modeling conditions and obtained results

The domain of interest for the numerical study is the junction between the main collector and the suction chambers inlet (figure 1). In order to analyze the flow conditions and the flow structure, a steady state 2D model using the ANSYS FLUENT code was developed.



Q_{in} – the flow rate upstream junction 1; Q_{out} – the flow rate downstream junction 1; Q_{PS} – the flow rate pumped to the waste water treatment plant (WWTP); $Q_{P1} \dots Q_{P5}$ – the flow rate pumped by each pump

Fig. 1. The analyzed domain; main collector - pumping station junction.

The fluid used in the modeling process is water, considered to be incompressible for the associated conditions of the study. The pumped flow rate was assumed to be half of the total quantity ($10 \text{ m}^3/\text{s}$) and equally distributed to the five pumps. The other half leaves the junction and flows downstream.

The Reynolds number value obtained using the characteristic length of the main collector reveals the turbulent character of the motion. Therefore, for the simulations, the Navier-Stokes and the continuity equations in the Reynolds-averaged manner (RANS) were used. For the closure problem the Boussinesq linear approximation was

used. Thus, for the turbulent viscosity modeling two additional equations were solved. One for the turbulent kinetic energy transport (k) and the other for its specific dissipation rate (ω) [1].

The adopted turbulence model was the $k-\omega$ SST, a hybrid between the $k-\varepsilon$ and the $k-\omega$ model [1]. The model uses a $k-\varepsilon$ formulation for the free flow domain, avoiding thus the disadvantages of the $k-\omega$ from the initial conditions point of view and a $k-\omega$ for the boundary layer. This is achieved by expressing the $k-\varepsilon$ model in a $k-\omega$ manner. The gradual transition between the two areas is provided by defining of area depended “mixing” functions which activate the $k-\omega$ or $k-\varepsilon$ formulation and also by introducing of an diffusive term in the transport relationship of ω [2].

The used software integrates the above mentioned equations using the finite volume method [3]. The chosen solver is a pressure based one. For the momentum, continuity and the specific turbulence model equations discretization a second order scheme was used.

The domain of interest includes the junction, the upstream and three way rectangular galleries and the pumping station inlet. For the numerical study the considered domain dimensions are three specific lengths upstream and fifteen specific lengths downstream the junction.

The incoming flow rate is considered to be equal distributed on the entire upstream boundary of the considered domain. Each pumping unit ensures a $2 \text{ m}^3/\text{s}$ maximum flow rate. For each of the three flow paths, at the downstream limit, a constant head boundary condition was considered. Figure 2 shows the grid and the considered boundary conditions, used for the modeling of the fluid domain.

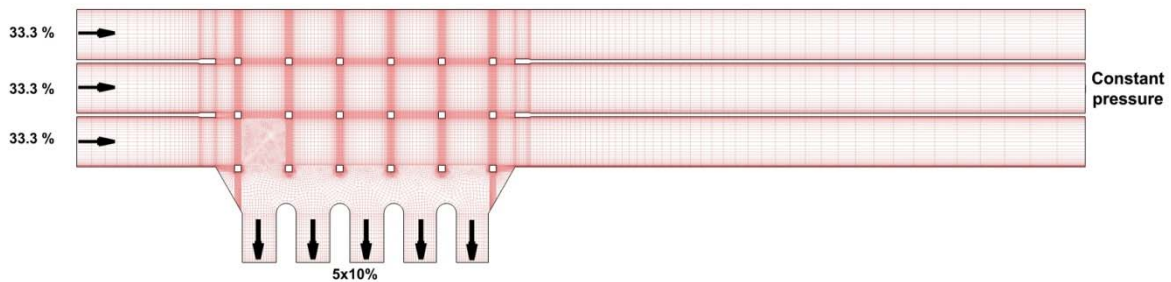


Fig. 2. The grid and the boundary conditions.

The model was calibrated using the on-site measurements carried out by the TUCEB team and the data delivered by the operator.

The pumped flow rate is uniformly distributed to the five pumps and is half of the incoming to the junction flow rate. The data obtained from the modeling process shows a velocity field similar to figure 3.

Analyzing figure 3, a strongly non-uniform velocity distribution at the pumping station inlet can be observed. For the given flow conditions, the obtained velocity values are covering a quite large interval. Responsible for this are both the junction geometry and the presence of the structural elements (pillars) influencing the flow

structure. The presences of sub-domains with low velocities are leading to favorable conditions for the formation of solid material deposits [4]. In the Romanian technical literature the minimum recommended velocity value for avoiding the formation of solid material deposits in sewerage systems is 0.7 m/s [5]. For larger flow rates, especially in the rainy season, the settled solid material will be transported downstream most of it to the suction chambers.

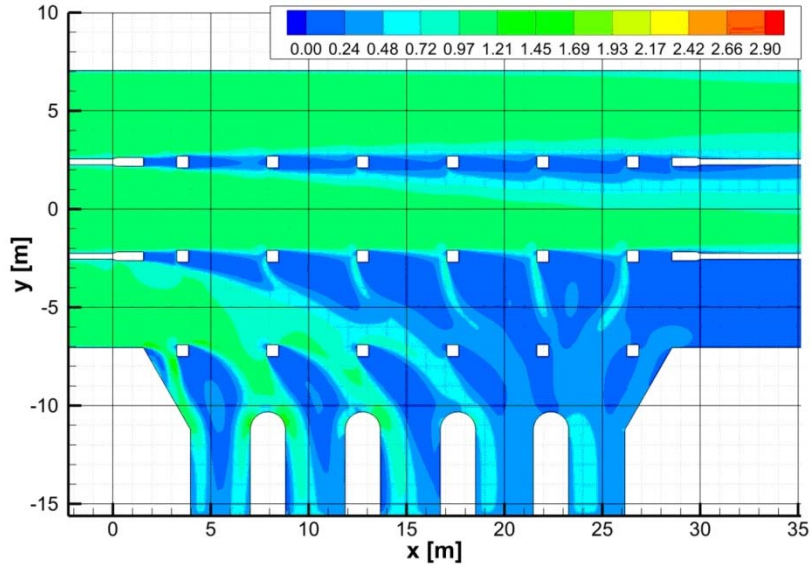


Fig. 3. The velocity field for the main collector - pumping station junction flow domain.

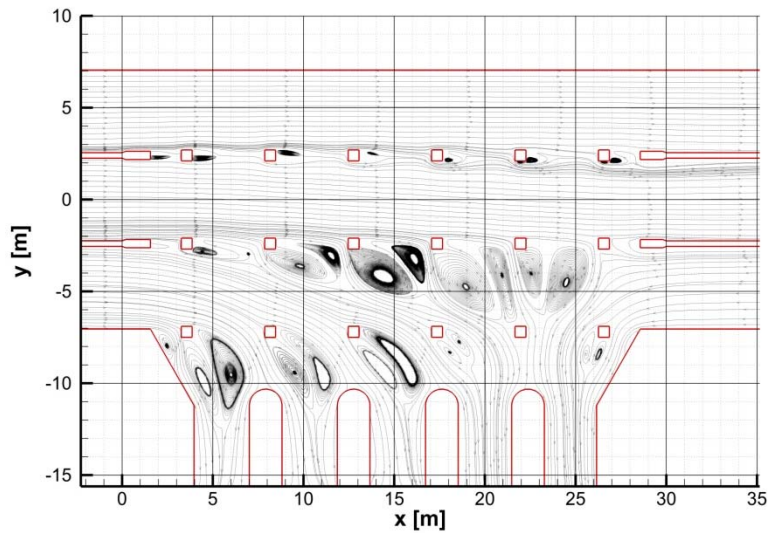


Fig. 4. The streamline structure for the main collector - pumping station junction flow domain.

The streamline representation, plotted in figure 4, show the formation and propagation of von Karman vortices. This is a consequence of the presence of the twelve pillars. After their formation the vortices are spreading downstream, mostly to

the coarse screens preceding the suction chambers. The coarse screens are modifying the flow structures formed upstream, and are eliminating also the trapped air in these structures.

3. Conclusions

Based on the modeling of the flow phenomena occurring in the main collector – pumping station junction several conclusions regarding the possible causes leading to the malfunction of the pumping station and the observed rotor damages were driven.

Speaking in terms of hydrodynamics, the entrances in the suction chambers for pumps number four and five (see figure 1) are more “facile”. As shown in figure 4, at the inlet of the last two suction chambers the stream lines are less disturbed and the velocity distribution is more uniform leading to lower velocity values (see figure 3).

At the suction chambers inlet of pumps number 1, 2 and 3 the presence of vortices produces flow irregularities which leads to supplementary head losses to those normally caused by the coarse screens. As a consequence the water level in the aforementioned suction chambers will decrease more. At low wastewater levels in the sewer system, this, together with the designing failures of the suction pipes will lead to the occurrence of air in the pumps, a major cause of damages.

Another reason of concern regarding the pump’s rotor integrity was the presence in the pumping facilities of coarse solid particles. Figure 3 highlights the presence of low velocity domains, a necessary condition for solid particles settling.

The non-uniform flow regime and the low water levels at the inlet in the suction chambers leading to a cavitation operation regime are more susceptible for rotor damages than the presence of coarse solid particles.

To avoid the mentioned drawbacks, several measures for improving the flow structure, namely a uniform distribution at the suction chamber inlet for all five pumps, and increasing the water depth in the suction chambers are necessary.

References

- [1] Menter, F.R., 1994. Two-Equation Eddy-Viscosity Turbulence Models for Engineering Applications. *AIAA Journal*. 32(8). 1598–1605.
- [2] Coșoiu C.I., Georgescu A.M., Degeratu M., Hlevca D., Numerical predictions of the flow around a profiled casing equipped with passive flow control devices, *Journal of Wind Engineering and Industrial Aerodynamics*, vol. 114, March 2013, pp. 48-61, 2013
- [3] ***ANSYS Inc. 2010, *Fluent 13.0 Users Guide*
- [4] Luca O., Tatu G. *Environmental Impact of Free Surface Flows*; Editura Orizonturi Universitare, ISBN 973-8391-34-2; Timișoara 2002
- [5] Ionescu Gh. C. *Instalații de canalizare*; Editura didactică și pedagogică, ISBN: 973-30-5009-1; 1997
- [6] Karassik I.J., Messina J.P., Cooper P., Heald C.C. *Pump Handbook*; McGRAW-HILL, ISBN: 9780071460446; 2008

Etude thermique d'un capteur solaire innovant à circulation d'air*

Thermal study of a innovative solar collector with air circulation

Cristiana Croitoru¹, Amina Meslem², Ramy Atta²

CAMBI Research Center, Technical University of Civil Engineering in Bucharest, Building Services Faculty.

Avenue Pache Protopescu 66, Bucharest, Romania

E-mail: cristianaveronacroitoru@gmail.com

² LaSIE, University of La Rochelle, Pôle Sciences et Technologie,
Avenue Michel Crépeau, 17042 La Rochelle, France

Rezumat. *L'utilisation des énergies renouvelables est une solution attractive pour satisfaire deux exigences: la qualité à l'intérieur et l'efficacité énergétique. Les systèmes solaires passifs sont faciles à mettre en œuvre et efficace dans les zones à fort potentiel solaire. Le mur solaire transpiré non vitré (UTSW) est en bardage métallique avec perforations, installé à plusieurs centimètres du mur du bâtiment, créant ainsi une cavité. Cette étude est une approche d'analyse préliminaire sur l'importance de la forme de l'orifice du panneau perforé pour le transfert de chaleur. L'article présente des données extraites de recherche expérimentale du transfert de chaleur entre la plaque perforée et la circulation de l'air. La comparaison entre deux géométries de perforations en termes de transfert de chaleur a montré de différence significative. La forme innovante de l'orifice lobes a été trouvée plus efficace en ce qui concerne le transfert thermique entre la plaque chauffée et l'air, grâce aux structures tourbillonnaires longitudinales caractéristiques.*

Cuvinte cheie: énergie solaire; mur solaire transpiré non vitré; transfert de chaleur;

Abstract. *The use of renewable energy is an attractive solution to fulfill two requirements: quality indoor and energy efficiency. Passive solar systems are easy to implement and effective in areas with high solar potential. The unglazed transpired solar wall (UTSW) is perforated with metal siding, installed several inches from the building wall, creating a cavity. This study is a preliminary analysis approach to the importance of the shape of the orifice of the perforated panel to the heat transfer. The article presents data from experimental research of heat transfer between the perforated plate and the flow of air. The evaluation between two geometries of perforations in terms of heat transfer showed significant difference. The innovative shape of the lobes orifice has been found more efficient as regards heat transfer between the heated plate and the air, thanks to the longitudinal vortex structures characteristics.*

Key words: solar energy; unglazed transpired solar wall; heat transfer;

* Lucrare inclusă în programul conferinței EENVIRO 2014

1. Introduction

Les demandes des occupants sont de plus en plus exigeantes et atteindre le confort intérieur est l'un des défis les plus importants pour les ingénieurs civils. En général, le secteur du bâtiment consomme 35,3% de la demande totale d'énergie [1, 2]. Cette demande d'énergie est due aux systèmes CVC (Chauffage, Ventilation et Climatisation). Les conditions locales climatiques influent directement sur la consommation d'énergie des bâtiments par des systèmes CVC, s'il y a une demande un chauffage ou de refroidissement. Pendant la saison froide dans les pays froids, la demande de chaleur du bâtiment représente le plus fort pourcentage du montant total de la demande d'énergie, alors que pendant l'été, la ventilation ou le traitement d'air est un grand consommateur d'énergie électrique. Par exemple, au Royaume-Uni, l'énergie utilisée pour la demande de chaleur intérieure était d'environ 50% de la consommation totale d'énergie en 2004. D'autre part, les systèmes de refroidissement à air utilisent plus de 40% de la charge de pointe en été chaud à Shanghai. Tous ces consommations d'énergie, qu'il s'agisse de chauffage ou de refroidissement, peuvent être traduits en termes d'émissions de CO₂ [1, 3, 4].

Dans ce contexte, l'utilisation des énergies renouvelables est une solution attractive pour satisfaire deux exigences: La qualité intérieure et l'efficacité énergétique. Parmi ces énergies renouvelables, les systèmes solaires passifs sont faciles à mettre en œuvre et efficace du point de vue de l'accessibilité dans les zones à fort potentiel solaire [5]. Ces systèmes ont une contribution significative pour atteindre de l'haute performance des enveloppes et dans le même temps économiser de l'énergie pour que ce soit pour le chauffage en hiver ou de climatisation en été. La multitude de solutions pour l'utilisation de l'énergie thermique du soleil présente des avantages importants mais aussi des inconvénients qui maintiennent la recherche dans ce domaine. Parmi eux, les murs thermiques peuvent être divisées en quelques catégories (ex. murs Trombe, les murs solaires eutectiques, autres systèmes qui stockent l'énergie)[6]. Une des solutions les plus intéressantes est, de notre point de vue, les murs capteurs solaires ou Unglazed Transpired Solar Walls (UTSW).

Un UTSW est fait d'une feuille en métal avec des perforations, installée à plusieurs centimètres de la paroi du bâtiment, créant ainsi une cavité. Le dessin schématique de ce type de capteur solaire est tel qu'illustré à la Figure 1. La plaque métallique est chauffée par le rayonnement solaire, et à l'aide d'un ventilateur, on crée une pression négative dans la cavité, l'air étant aspiré et chauffé à travers le panneau perforé. L'air est généralement prise sur le haut du mur (en raison des gradients de température dans la cavité) pour assurer que toute la chaleur solaire produite est recueillie, et en ensuite, distribuée dans le bâtiment par le système de ventilation.

D'autre part, les techniques de mélange passif appliquées aux unités de diffusion pour HVAC ont été fortement développés au cours des dernières années, depuis que des équipes de recherche en collaboration l'Université de La Rochelle et UTCB ont effectué nombreuses études consacrées à ces dispositifs [7-16]. Une nouvelle direction de recherche a été lancé l'année dernière à l'Université de La Rochelle (ULR) en ce qui concerne la possibilité d'utiliser le contrôle passif pour

améliorer le transfert de chaleur pour des jets impactants [17]. Toutes ces études utilisent une géométrie spéciale, qui est appelé "géométrie lobée». Un exemple d'une telle géométrie est l'orifice lobé. La Figure 1 b présenté un panneau percé d'orifices lobes (ou orifices en forme de croix à 4 lobes). Pour la même aire (même diamètre équivalent) le périmètre du jet lobé est beaucoup plus grand que celui de l'orifice circulaire, en augmentant la limite de contact entre le flux d'air passant à travers l'orifice et l'épaisseur de l'orifice. Sous nombres de Reynolds faibles ou modérés, comme celle qui caractérise les écoulements dans le UTSW, l'analyse de la buse lobée élémentaire et orifice jets montre que la forme lobée présente de cisaillement transversal sur les creux du lobe [12, 18-20].

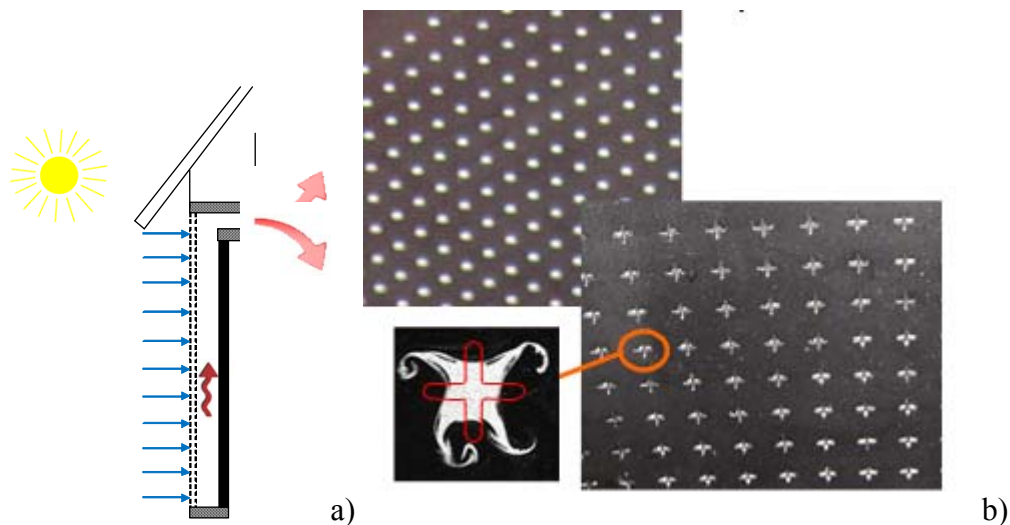


Fig. 1 a) Schéma de UTSW (unglazed transpired solar wall), b) Panneau perforé innovant développé au ULR [21]

Notre idée consiste à introduire orifices lobées innovantes en panneaux perforés utilisés pour UTSW afin d'améliorer dans ces dispositifs passifs de récupération de chaleur solaires. En quelques études récentes [56, 57] certaines caractéristiques intéressantes de l'écoulement en amont de l'orifice lobes ont été mises en évidence: la contrainte de cisaillement à la paroi et les distributions de tourbillons sur le plan amont d'orifice générés dans un jet lobé, à partir de simulations LES, suggèrent la possibilité d'utiliser la géométrie lobée aux UTSW pour un transfert de chaleur élevé.

Cette étude est une première approche des tests expérimentaux pour essayer d'évaluer si les panneaux perforés sont appropriées pour être intégrés dans UTSW.

2. Méthode expérimentale

L'enquête expérimentale a été réalisée dans des conditions contrôlées en laboratoire où la température et l'humidité relative ont été surveillées en permanence. Deux types de panneaux perforés ont été testés. Le panneau de base est de forme ronde et les perforations du panneau innovantes a lobé perforations en forme de croix. Le De diamètre équivalent de deux géométries d'orifices était 5mm. Deux porosités

différentes ont été testées pour chaque type de panneau, en faisant varier la distance entre les deux orifices adjacents de 3 et 4 D_e .

L'ensemble est composé d'une plaque perforée en acier galvanisé appelée absorbeur.



Fig. 2 Photo de la manipulation: le panneau perforé et les lampes de radiation

L'air extérieur est préchauffé dès lors qu'il passe au travers de l'absorbeur, lui-même chauffé par le rayonnement solaire incident, d'une cavité d'air, fermée à toutes ses extrémités, créée par le volume entre l'absorbeur et sa structure support : l'air préchauffé y circule et est canalisé jusqu'au système de traitement de l'air. Un banc expérimental à échelle réduite a été conçu et est présenté. Il s'agit d'une boîte en panneaux bois de 150mm de profondeur et environ 700mm de côté, fermée sur une de ses faces par la plaque perforée à tester.

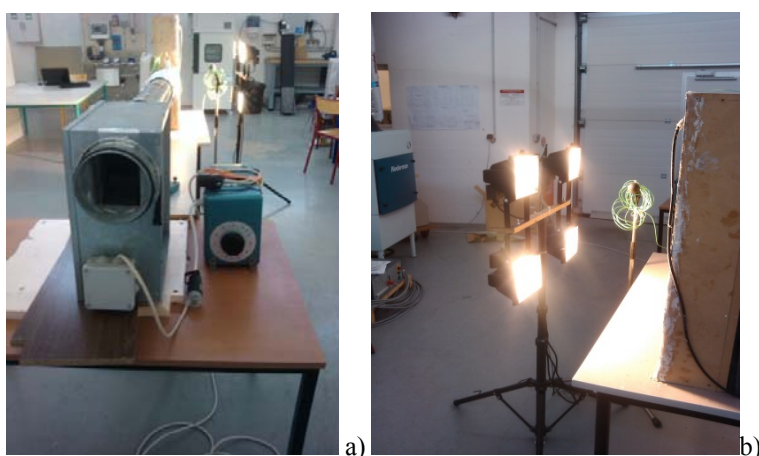


Fig. 3 a) Le ventilateur fonctionnant en aspiration de marque EAB VARIAC et à débit variable; b) L'éclairage solaire simulé par 4 lampes halogène de 400W situées à 50 cm de la plaque

La boîte est reliée à un ventilateur fonctionnant en aspiration. L'éclairage solaire est simulé par quatre lampes halogène de 400W chacune, placées à une distance de 50 cm. Plusieurs couples de plaques perforées circulaire/lobée existent et seront à comparer. Le banc expérimental est instrumenté (capteurs de température, capteur de vitesse), ce qui permet de mesurer la puissance extraite pour chaque plaque perforée. Le débit d'air extrait sera à faire varier et les courbes $Y = \text{Puissance extraite}$ en fonction de $X = \text{débit d'air extrait}$, seront à comparer pour chaque couple de panneaux. Le panneau reçoit presque 800 W/m^2 du flux de chaleur émis par la source ([22]).

Trois sondes de température (thermocouples de type K) ont été utilisés pour mesurer la température de l'air ambiant (T_{amb}), la température de l'air à l'intérieur de la boîte (T_{box}) et la température de l'air à l'entrée de la conduite d'aspiration (T_{pipe}).

Le débit volumétrique extrait a varié entre 10 et 150 m^3 / h . Le débit a été évalué en utilisant des sondes de vitesse omnidirectionnelles de TSI qui a été placé à l'intérieur du tuyau.

3. Résultats et Discussion

Les études réalisées sur les systèmes de murs solaires montrent de bons résultats en termes d'efficacité énergétique. Dans ce contexte, l'utilisation de systèmes solaires passifs est encouragée par les réglementations nationales, car ils peuvent avoir une contribution significative à atteindre des performances élevées et des économies d'énergie pour le chauffage en hiver et en été pour refroidir. Le tableau 1 résume certaines des études de cas disponibles dans la littérature.

Tableau 1

Etudes de cas sur UTSW

Référence	Type	Débit air [$\text{m}^3/\text{h}/\text{m}^2$]	Delta t	Efficienc	Economie d'énergie
[23]	1877 m^2 ; mur vertical; 2% porosité; 1% canopée;	125	12.5 °C	57%	917 kWh/ m^2/an
[23], [24]	420 m^2 aire; 2%porosité; 1% canopée	72	13 °C	52%	754 kWh/ m^2/an
[23]	27.9 m^2 ; 2% porosité	N/A	N/A	63-68%	N/A
[25]	335 m^2 ; aluminium ondulé	N/A	N/A	N/A	195 700 kWh/ m^2
[25]	Solarwall panneau aire=1.1664 m^2 ; PV cellules couvertes 24% de la superficie totale	100	N/A	Efficienc thermique 48% Efficienc combinée 51%	500-1000 kWh/ m^2/an En total
[26]	2 m^2 ; mur solaire perforé	117	13.2°C		
Cet étude	0.47 m^2 ; mur solaire perforé; 0.6 % - 10% porosité; panneau noir en aluminium	10-150 [$\text{m}^3/\text{h}/\text{m}^2$]	9°C-30°C	60-70% pour débits d'air plus grands que 50 [$\text{m}^3/\text{h}/\text{m}^2$]	N/A

Un rapide sondage nous permet d'être au courant des possibilités énormes de tels dispositifs de récupération d'énergie. Par exemple, l'étude CFD de Arulanadam et al.[27] conclut que non seulement les panneaux métalliques pourraient être utilisés pour l'absorbeur perforé mais même les matériaux à faible conductivité peuvent conduire à une efficacité thermique acceptable du système, ou de faible porosité des absorbeurs de plaques transpiré ou pour faibles débits etc. Mais des études comme celles de Van Decker et al. [28], Gunnewieck et al. [29, 30] est très intéressante de notre point de vue, compte tenu de l'information connexe sur les possibilités directes d'amélioration de ces dispositifs. L'étude numérique de début de Gunnewieck et al. [29] souligne l'importance d'un écoulement non uniforme et d'une faible vitesse sur l'efficacité des dispositifs de chauffage solaire de l'air transpiré non vitrés de grande surface. Van Decker et al. [28] montre que en conditions sans vent, environ 62% de la hausse de la température finale de l'air est prévu pour le devant de plat, 28% dans le trou et 10% à l'arrière de la plaque.

Cordeau and Barrington [31] dans leur étude sur UTSW utilisé pour amener de l'air frais dans une grange de poulets, révèlent que l'efficacité de l'air en pré-chauffe solaire a atteint 65% pour des vitesses de vent de 2 m/s, mais a chuté sous 25% pour des vitesses de vent supérieures à 7 m / s, avec un retour sur investissement annuel de l'an de 4,7%. Différentes autres études de cas de UTSW [22, 29-39] soulignent l'efficacité énergétique du système de 52% à 68%, soit un bénéfice important en termes de consommation d'énergie fossile.

Dans la présente étude, la chaleur transférée de la plaque à l'air (P) a été quantifiée par l'augmentation de la température de l'air, en utilisant:

$$P = m_{air} * c_p * (T_{pipe} - T_{amb}) \quad (1)$$

m_{air} : débit massique de l'air ;

$c_{p,air}$: chaleur massique de l'air à pression atmosphérique et à température ambiante ;

Quatre cas ont été étudiés par rapport à la configuration standard d'un panneau perforé pour les systèmes commerciaux UTSW. Les cas étudiés sont: 3R - orifices ronds avec $S = 3DE$, 4R - orifices ronds avec $S = 4DE$, 3C - orifices en forme de croix avec $S = 3DE$ et 4C orifices en forme croix avec $S = 4DE$.

Le rendement du panneau a été défini comme:

$$\varepsilon = \frac{P}{I_T A_{pl}} \quad (2)$$

Où P est la chaleur transférée de la plaque à l'air, I c'est l'irradiation fournie par les lampes au niveau de la plaque et A est la surface de la plaque de 0.47 m^2 .

In Fig. 4 nous avons représenté l'évolution du rendement thermique pour les quatre cas étudiés, en comparaison avec le résultat obtenu en utilisant un UTSW commercial et les deux modèles proposés par Belusko et al. et Shukla et al. pour UTSW sans vent et avec des perforations circulaires de même diamètre que dans notre cas [37, 40].

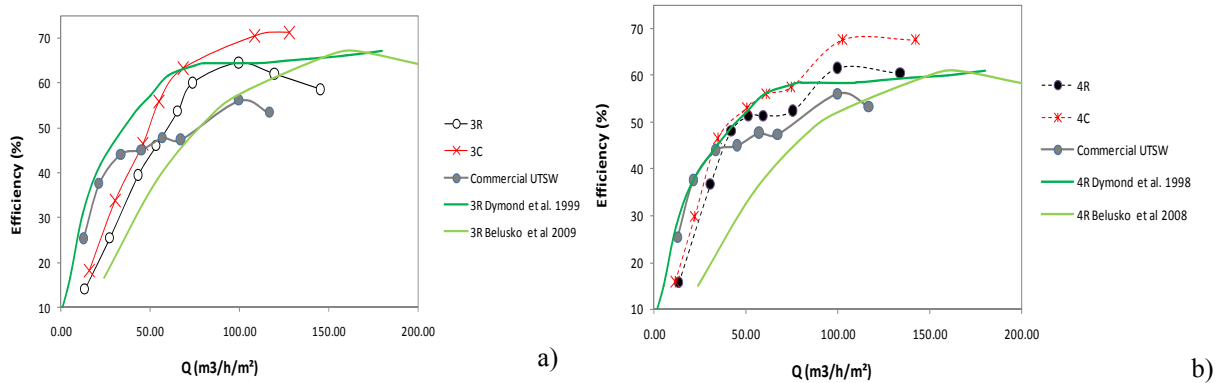


Fig. 4 Efficacité de l'UTSW pour différents débits: a) S=3De, b) S=4De

Pour les deux taux de perforation étudiés dans la présente campagne expérimentale, nous pouvons voir l'avantage de la plaque perforée innovante avec orifices lobés par rapport aux panneaux avec orifices ronds de base. En outre, ils présentent un avantage évident pour des débits élevés par rapport aux modèles analytiques de Belusko et al. et Shukla et al. pour des panneaux ayant des perforations circulaires.

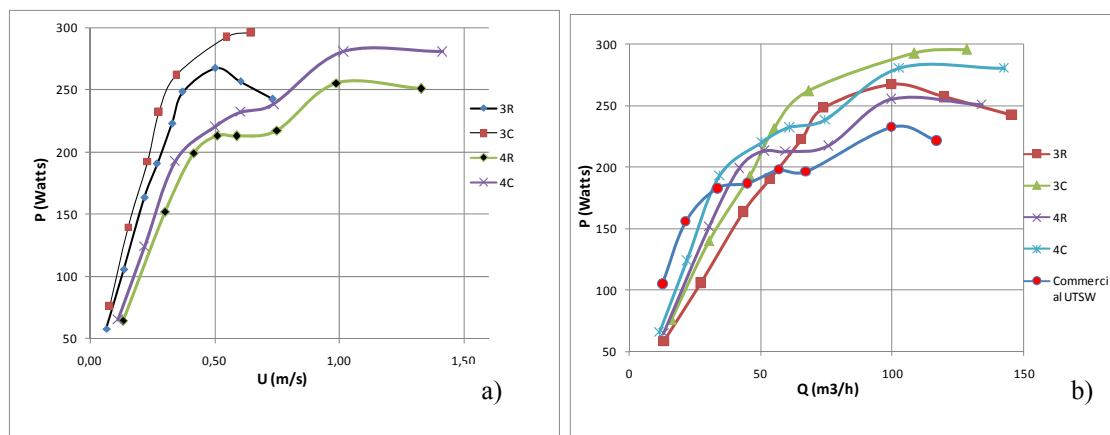


Fig. 5 a) Evolution de transfert de chaleur en fonction de la vitesse dans la conduite, b) l'évolution de transfert de chaleur en fonction du débit de l'air

La même conclusion peut être extraite de la variation de la chaleur transférée par la vitesse sur le trou. Les trous en forme de croix ont un rendement supérieur par rapport aux orifices ronds, jusqu'à 30 W pour chaque type de porosité. Plus la vitesse est élevée, plus la chaleur transférée de la plaque à l'air est grande.

D'autre part, la différence entre la température ambiante et la température du flux d'air qui a traversé la plaque perforée diminue avec l'augmentation de la vitesse ou de débit d'air. Pour le cas 3C et 3R nous avons fait plusieurs mesures pour évaluer plus correctement le transfert de chaleur de ces deux cas.

Tableau 2

Range de débits pour le cas 3C et 3R

Qtube	P_3C	P_3R	Efficacité
m ³ /h	W	W	%
20	144,96	120,71	20,08%
40	218,42	183,90	18,77%
60	261,40	220,87	18,35%
80	291,89	247,09	18,13%
100	315,54	267,44	17,99%
120	334,87	284,06	17,89%
140	351,20	298,11	17,81%
160	365,36	310,28	17,75%
180	377,84	321,02	17,70%
200	389,01	330,63	17,66%
220	399,11	339,31	17,62%
240	408,33	347,25	17,59%
260	416,82	354,54	17,56%
280	424,67	361,30	17,54%
300	431,98	367,59	17,52%

Pour évaluer l'efficacité de la plaque 3C, on la compare avec les puissances obtenues sur la plaque 3R (Tableau 2).

En considérant ces valeurs, on voit sur le graphique l'évolution de la puissance en fonction de la gamme des débits. On peut voir que l'efficacité du panneau avec perforations lobées se préserve tout au long de la courbe de variation (Fig. 6).

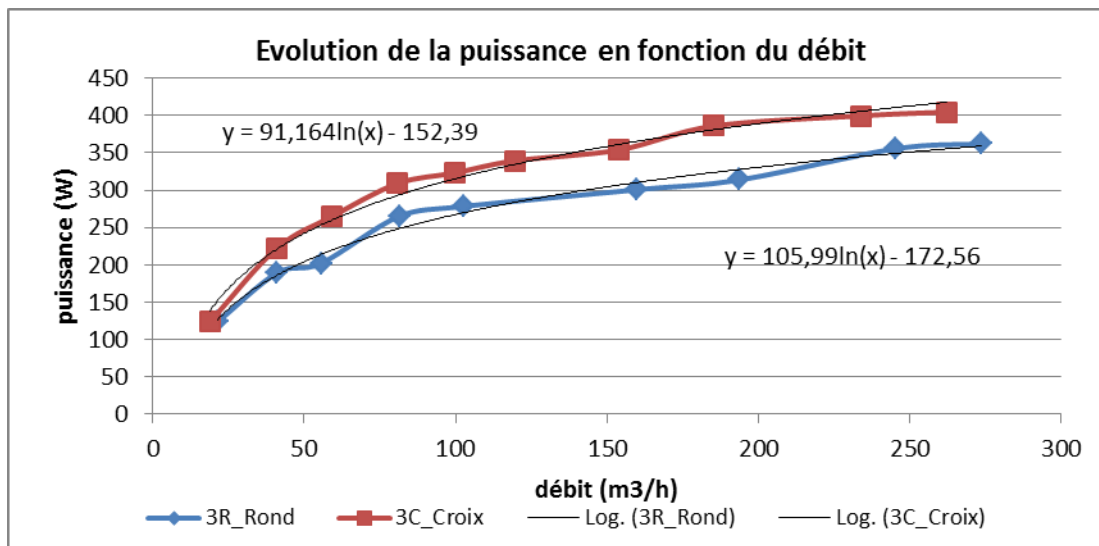


Fig. 6 Evolution de la puissance en fonction du débit

4. Conclusions

L'étude a été un premier test sur un capteur solaire non vitré transpiré (UTSW) qui est équipé de perforations de forme de croix. Le modèle physique utilisé montre de bons résultats en accord avec la littérature. Plus de cela, la comparaison d'un UTSW classique avec un nouveau avec des géométries de perforation innovantes conduit à des résultats intéressants. La géométrie lobée est plus efficace et le cas 3C est le meilleur. Nous pouvons voir que le gain de puissance en choisissant la plaque 3C varie entre 17,5% et 20% ce qui est un rendement assez élevé. Ce gain est seulement testé sur une petite surface de plaque (0,47 m²). A l'échelle d'un bâtiment, cela génère une source d'économie très intéressante.

Les résultats nous laissent supposer que plus la température surfacique de la plaque est basse, plus le rendement de la puissance est meilleur.

Remerciements (Acknowledgements)

CNCS – UEFISCDI, Project numéro PN-II-RU-PD-2012-3-0144.

Références

1. IEA, *Renewables for heating and cooling: untapped potential*. France: OECD/IEA; 2007.
2. Chan, H.-Y., S.B. Riffat, and J. Zhu, *Review of passive solar heating and cooling technologies*. Renewable and Sustainable Energy REviews, 2010. **14**(2): p. 781-789.
3. IEA, *World energy outlook 2007: China and India insights*. France: OECD/IEA; 2007.
4. IEA, *Worldwide trends in energy use and efficiency: key insights from IEA indicator analysis*. France: OECD/IEA. 2008.
5. IEA. *Solar's Untapped Potential*. 2005; Available from: <http://www.iea-shc.org/solarenergy/potential.htm>.
6. Hami, K., B. Draoui, and O. Hami, *The thermal performances of a solar wall*. Energy, 2012. **39**(1): p. 11-16.
7. Meslem, A., I. Nastase, and F. Allard, *Passive mixing control for innovative air diffusion terminal devices for buildings*. Building and Environment, 2010. **45** (2679-2688).
8. Meslem, A., I. Nastase, and K. Abed-Meraim, *Experimental investigation of a lobed jet flow mixing performance*. Journal of Engineering Physics and Thermophysics, 2007. **81**(1).
9. Meslem, A., M. El-Hassan, and I. Nastase, *Analysis of jet entrainment mechanism in the transitional regime by time-resolved PIV*. Journal of Visualization, 2010. **online first**: p. 1-12.
10. Meslem, A., et al., *A comparison of three turbulence models for the prediction of parallel lobed jets in perforated panel optimization*. Building and Environment, 2011. **46**(11): p. 2203-2219.
11. Nastase, I., et al., *Lobed grilles for high mixing ventilation - An experimental analysis in a full scale model room*. Building and Environment, 2011. **46**(3): p. 547-555.
12. Nastase, I., A. Meslem, and P. Gervais, *Primary and secondary vortical structures contribution in the entrainment of low Reynolds number jet flows*. Experiments in Fluids, 2008. **44**(6): p. 1027-1033.
13. Nastase, I., A. Meslem, and M. El Hassan, *Image processing analysis of vortex dynamics of lobed jets from three-dimensional diffusers*. Fluid Dynamics Research, 2011. **43**(6).
14. Nastase, I. and A. Meslem, *Vortex Dynamics and mass entrainment in turbulent lobed jets with and without lobe deflection angles*. Experiments in Fluids, 2010. **48**(4): p. 693-714.

15. Nastase, I. and A. Meslem, *Vortex dynamics and entrainment mechanisms in low Reynolds orifice jets*. Journal of Visualization, 2008. **11**(4).
16. Nastase, I. and A. Meslem. *Lobed jets for improving air diffusion performance in buildings*. in *The 29th AIVC Conference*. 2008. Kyoto, Japon.
17. Kristiawan, M., et al., *Wall shear rates and mass transfer in impinging jets: Comparison of circular convergent and cross-shaped orifice nozzles*. International Journal of Heat and Mass Transfer, 2012. **55**(1-3): p. 282-293.
18. Nastase, I. and A. Meslem, *Vortex Dynamics and Entrainment Mechanisms in Low Reynolds Orifice Jets*. Journal of Visualisation, 2008. **11**(4): p. 309-318.
19. Nastase, I. and A. Meslem, *Vortex dynamics and mass entrainment in turbulent lobed jets with and without lobe deflection angles*. Experiments in Fluids, 2010. **48**(4): p. 693-714.
20. El-Hassan, M. and A. Meslem, *Time-resolved stereoscopic PIV investigation of the entrainment in the near-field of circular and daisy-shaped orifice jets*. Physics of Fluids, 2010. **22**.
21. Meslem, A., I. Nastase, and F. Allard, *Passive mixing control for innovative air diffusion terminal devices for buildings*. Building and Environment, 2010. **45**: p. 2679-2688.
22. Leon, M.A. and S. Kumar, *Mathematical modeling and thermal performance analysis of unglazed transpired solar collectors*. Solar Energy, 2007. **81**(1): p. 62-75.
23. Cali, A., Kutscher, C.F., Dymond, C.S., Pfluger, R., Hollick, J., Kokko, J., et al. , *A report of Task 14 Air Systems Working Group: low cost high performance solar airheating systems using perforated absorbers*, in 1999, International Energy Agency (IEA): Washington.
24. Hollick, J.C., *Unglazed solar wall air heaters*. Renewable Energy, 1994. **5**: p. 415-21.
25. Hollick, J.C., *World's largest and tallest solar recladding*. Renewable Energy, 1996. **9**: p. 703-7.
26. Chan, H.Y., S. Riffat, and J. Zhu, *Experimental performance of unglazed transpired solar collector for air heating*, in *World Renewable Energy Congress*. 2011: Sweden.
27. Arulanandam, S.J., K.G.T. Hollands, and E. Brundrett, *A CFD heat transfer analysis of the transpired solar collector under no-wind conditions*. Solar Energy, 1999. **67**(1-3): p. 93-100.
28. Van Decker, G.W.E., K.G.T. Hollands, and A.P. Brunger, *Heat-exchange relations for unglazed transpired solar collectors with circular holes on a square or triangular pitch*. Solar Energy, 2001. **71**(1): p. 33-45.
29. Gunnewiek, L.H., E. Brundrett, and K.G.T. Hollands, *Flow distribution in unglazed transpired plate solar air heaters of large area*. Solar Energy, 1996. **58**(4-6): p. 227-237.
30. Gunnewiek, L.H., K.G.T. Hollands, and E. Brundrett, *Effect of wind on flow distribution in unglazed transpired-plate collectors*. Solar Energy, 2002. **72**(4): p. 317-325.
31. Cordeau, S. and S. Barrington, *Performance of unglazed solar ventilation air pre-heaters for broiler barns*. Solar Energy, 2011. **85**(7): p. 1418-1429.
32. Hollick, J.C., *Unglazed solar wall air heaters*. Renewable Energy, 1994. **5**(1-4): p. 415-421.
33. Hollick, J.C., *Solar cogeneration panels*. Renewable Energy, 1998. **15**(1-4): p. 195-200.
34. Konttinen, P., T. Salo, and P.D. Lund, *Degradation of unglazed rough graphite-aluminium solar absorber surfaces in simulated acid and neutral rain*. Solar Energy, 2005. **78**(1): p. 41-48.
35. Sopian, K., et al., *Performance of a non-metallic unglazed solar water heater with integrated storage system*. Renewable Energy, 2004. **29**(9): p. 1421-1430.
36. Nábilek, B., et al., *Performance of an unglazed textile-plastic solar absorber*. Renewable Energy, 1999. **16**(1-4): p. 635-638.
37. Belusko, M., W. Saman, and F. Bruno, *Performance of jet impingement in unglazed air collectors*. Solar Energy, 2008. **82**(5): p. 389-398.
38. Molineaux, B., B. Lachal, and O. Guisan, *Thermal analysis of five unglazed solar collector systems for the heating of outdoor swimming pools*. Solar Energy, 1994. **53**(1): p. 27-32.
39. Kumar, S. and S.C. Mullick, *Wind heat transfer coefficient in solar collectors in outdoor conditions*. Solar Energy, 2010. **84**(6): p. 956-963.
40. Shukla, A., et al., *A state of art review on the performance of transpired solar collector*. Renewable and Sustainable Energy Reviews, 2012. **16**(6): p. 3975-3985.

Application of multivariate statistical analysis to evaluate parameters in a wastewater treatment

Aplicarea analizei statistice multivariate pentru evaluarea parametrilor la o stație de epurare a apei

Marius-Daniel Roman

Technical University of Building Services Engineering Department
Boulevard December 21, no. 128-130, 400604, Cluj-Napoca, ROMÂNIA
E-mail: Marius.ROMAN@insta.utcluj.ro

Rezumat. *Autorul lucrării de față prezintă rezultatele în urma aplicării analizei componentelor principale (PCA). Datele colectate de la influentul și efluentul stației de epurare a apelor uzate Gherla în perioada (mai 2013- mai 2014), au fost analizate pentru a găsi o relație între parametrii fizico-chimici. PCA este conceput pentru a transforma variabilele originale în noi variabile necorelate (axe), numite componente principale, care sunt combinații liniare ale variabilelor originale. Noile axe se află de-a lungul direcției de variație maximă. PCA oferă o modalitate obiectivă de a găsi indicii de acest tip, astfel încât variația în date să poată fi pe cât posibil concisă. Aplicarea PCA este utilizată pentru a obține, pe lângă datele statistice, imaginile care pot fi studiate și interpretate vizual.*

Cuvinte cheie: PCA, analiza cluster, parametrii, apă uzată.

Abstract. *The author of the present paper presents the results following the application of Principal Components Analysis (PCA). The collected data of influent and effluent from Gherla's wastewater treatment plant during (May 2013- May 2014), were analyzed to find a relationship between physical-chemical parameters. PCA is designed to transform the original variables into new, uncorrelated variables (axes) called the principal components, that are linear combinations of the original variables. The new axes lie along the directions of maximum variance. PCA provides an objective way of finding indices of this type so that the variation in the data can be accounted for as concisely as possible. The application of PCA used to obtain, besides statistical data, the images which can be studied and interpreted visual.*

Key words: PCA, cluster analysis, parameters, wastewater.

1. Introduction

The characteristics of municipal wastewaters are varied, depending upon the sources of discharge, the effluents from industries, land uses and groundwater levels [4].

Municipal wastewater characteristics properties its essential as well as concentrations of suspended and dissolved inorganic and organic pollutants. Among the organic pollutants present in sewage are phenols, hydrocarbons, biological oxygen demand (BOD), carbohydrates, lignin, fats, soaps, synthetic detergents, proteins and their decomposition products, as well as various natural and synthetic organic chemicals from the process industries [1]. Inorganic pollutants comprises of compounds of trace minerals, nitrogen and phosphorous.

A major role of wastewater treatment is to restore and maintain the chemical, physical and biological integrity of waters. There is a rapid growth in the re-use of municipal wastewater for irrigation and ground water recharge, which necessitates enhanced treatment to remove nutrients (nitrogen and phosphorus), suspended solids, and other contaminants. The changing of the environmental parameters may change the life cycle of populations from an entire species.

In the present paper, a series of physical-chemical parameters of wastewater, before and after water treatment at Gherla's WWTP, recorded over one year were included into analysis, in order to find relevant relationships between them.

2. Problem formulation

Principal component analysis (PCA) is a vector space transformation often used to transform multivariable space into a subspace which preserves maximum variance of the original space in minimum number of dimensions. The measured process variables are usually correlated to each other. PCA finds linear combinations of variables that describe major trends in data set. Mathematically, PCA is based on an orthogonal decomposition of the covariance matrix of the process variables along the directions that explain the maximum variation of the data.

The collected data at every month at Gherla's wastewater treatment plant (WWTP) include pH, total suspended matter (MTS), biochemical oxygen demand in five days – BOD₅, chemical oxygen demand – COD, and ammonium (NH₄-N) are presented in table 1. Values exceeding maximum standard limits (according to NTPA 001/2005 and NTPA 002/2005, respectively) in table 1.

Table 1

Evolution of parameters in wastewater treatment plant of Gherla, during 2013-2014

Year	Mo	pH		MTS		BOD ₅		COD		NH ₄ -N	
		infl.	effl.	infl.	effl.	infl.	effl.	infl.	effl.	infl.	effl.
2013	May	7,53	7,51	233	21,26	184,42	6,26	267,35	53,87	15,0	1,15
	Jun	7,58	7,54	100,90	20,03	134,97	4,57	204,16	50,83	11,4	0,90
	Jul	7,54	7,53	106,19	20,48	148,39	5,06	229,54	71,33	10,6	0,77
	Aug	7,26	7,10	156,35	22,77	187,63	7,74	264,48	58,42	10	0,62
	Sept	7,34	7,18	139,50	16,70	227,43	9,10	325,12	59	10,9	0,82
	Oct	7,38	7,29	155,42	14,74	237,48	9,66	421,35	54,41	11,0	0,93
	Nov	7,41	7,27	166,97	16,47	213,50	8,73	433,92	56,64	10,2	0,70
	Dec	7,35	6,95	246,77	19,13	246,58	7,32	458,19	64,98	14,9	1,12
2014	Jan	7,35	7,01	221,87	17,42	245,90	8,61	416,43	63,41	12,01	0,72
	Feb	7,37	7,06	165,45	21,76	200,50	7,68	364,63	61,64	11,78	0,97
	Mar	7,01	7,01	241,58	17,19	204,61	7,35	397,59	51,74	10,5	0,57
	Apr	6,79	7,04	220,45	16,87	259,60	10,87	451,30	42,87	10,3	0,48
	May	6,86	7,12	178,98	17,98	254,07	12,97	400,83	37,25	10,5	0,30

4. Problem solution

There are several multivariate statistical methods for the analysis of process. Some of this methods have recently been used successfully for monitoring parameters [3]. These methods are useful because reduces the dimensionality of the original historical data by projecting it onto a lower dimensionality space.

Cluster analysis is a powerful exploratory technique for discovering groups of similar observations within a data set. The idea of cluster analysis is to use values of variables to devise a scheme for grouping objects in such a way that similar objects will belong to the same group (in some sense or another) to each other than to those in other groups.

The association analysis was conducted with 1-r as classification measure, where r represents the Pearson's correlation coefficient [2]. The results are depicted in figure 1.

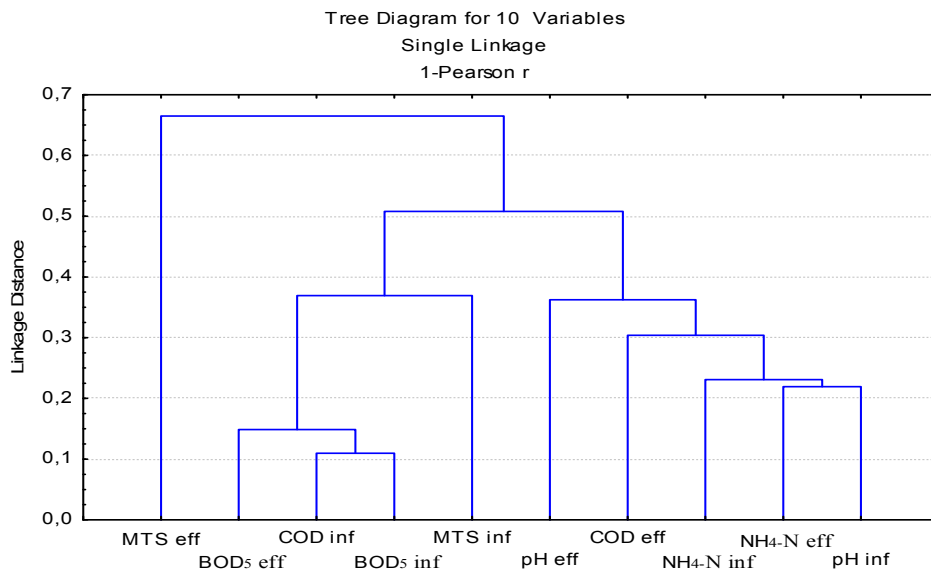


Fig. 1. Single linkage influent and effluent values of the observed variables

The results from figure 1 shows that variables were also included in order to reveal if periodicity is the main factor in the given observable. The strongest association is between BOD₅ (biochemical oxygen demand at 20°C in 5 days) and COD (chemical oxygen demand) values at the effluent of WWTP (being below 0.2 degree of dissimilarity). The next link is at about 0.3 degree of dissimilarity (about 0.5 correlations) and is established between the same observable, but at the influent of the treatment plant. An interesting association is established between the values of CBO₅ and COD at the effluent of the plant and the value of NH₄-N at the influent of the plant, suggesting that somehow the efficiency of the treatment in the WWTP is not affected by the ammonium in treated wastewater.

Total suspended matter at influent (MTS) of WWTP also connects with the cluster formed by BOD₅ influent and COD influent (almost 0.4 degree of dissimilarity), suggesting the influence of season on the quality of inflow. That means that quantity of total suspended matter, which increases along with increase of rain amount, affects oxygen exchange within surface water.

The next figure (fig. 2) shows the explanatory degree of the principal components in the values of the variables depending on the number of the components.

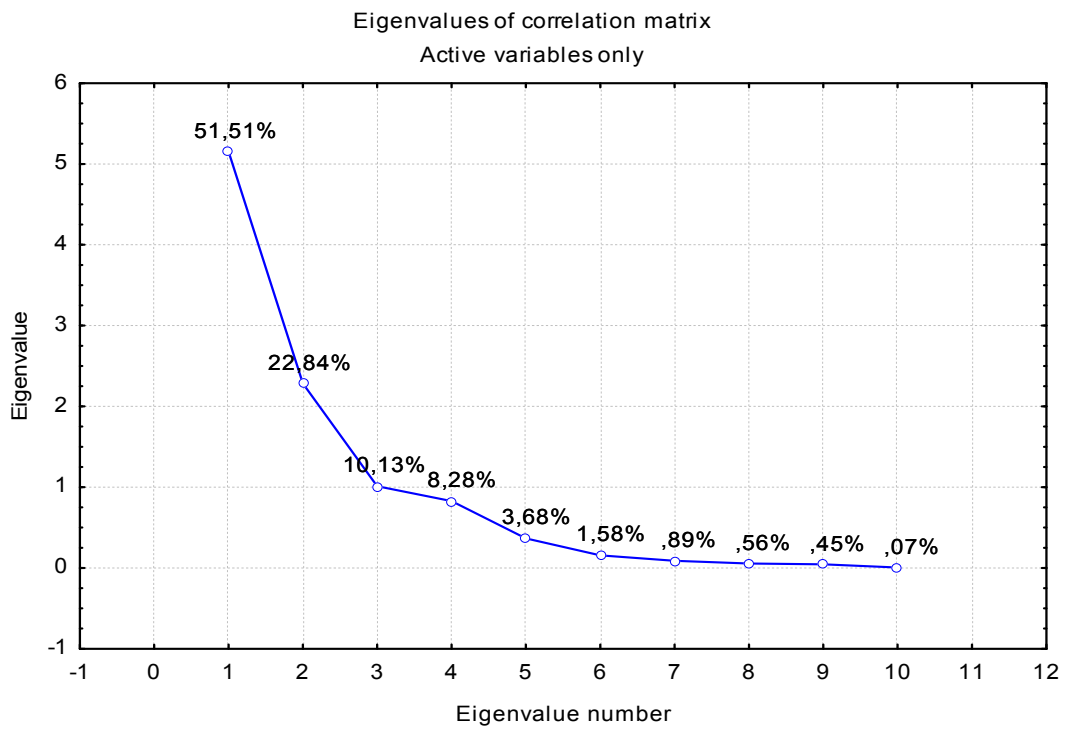


Fig. 2. Explained variance by each consecutive component in principal component analysis

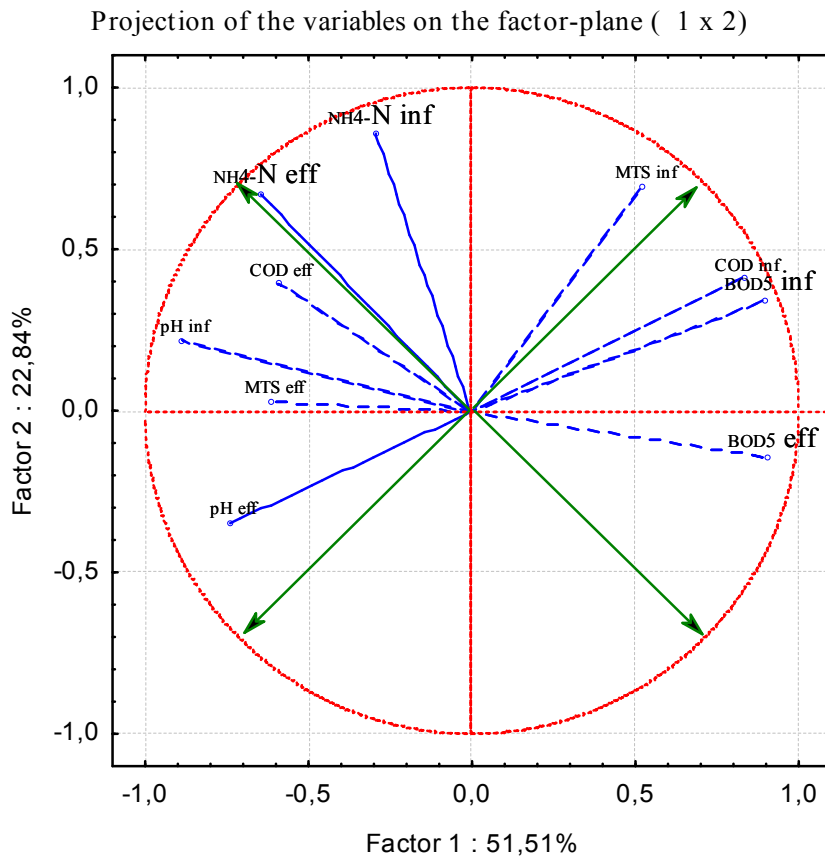


Fig. 3. Projection of the variables in the plane of the first two principal components

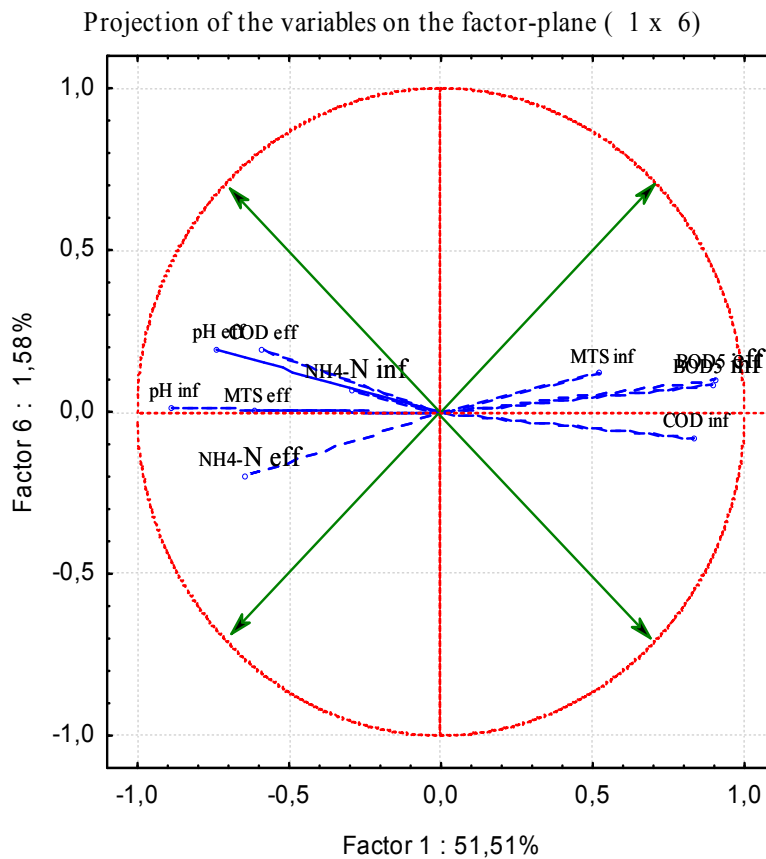


Fig. 4. Projection of the variables in the plane of the first and six principal components

The values from figure 2 reveals that no more than three principal components should be assigned to the deterministic factors in monitored parameters. It is easy to see how the factors starting from factor 3 (with explained variance of 10,13 %) until factor 10 (with explained variance of 0.07 %) fit to a straight line and their explanatory variance is only an expression of overfitting.

The next figure (fig. 3) depicts the projection of the variables on the plane of the first two principal components (explaining over 60 % of the variance present in the observed values of the active variables).

The analysis of the projections given in figure 3 reveals a strong association of the influent value of the pH at the influent of the WWTP with the BOD₅ factor as well as that both are along the first component of the total variability. This result suggests that the main factor giving variation in the observed variables is the value of pH, and this factor is a slow changing one, varying in approximately good agreement with the BOD₅ of the observation. The analysis of the projections given in figure 4 reveals a strong association of the influent value of the COD at the influent of the WWTP with the ammonium NH₄-N from influent.

6. Conclusions

Statistical methods revealed a strong relationship between chemical and biochemical demand, especially for the effluent of WWTP, which explains why the efficiency of BOD₅ and COD reduction represents a criterion for assessing wastewater treatment degree. These results correlated with the exceeding values reported during the monitored period (May 2013- May 2014) show the influence of ammonium on the efficiency of wastewater treatment process.

Season represents one of the main variation factor, especially concerning the change in suspended matter (MTS) content.

Projection of the variables on the factor plane is able to effluent in detail around which observables gather the identified variation factors.

The obtained statistically significant model allows an analytical expression of intrinsic link between the physical-chemical parameters.

Comparing the values observed in different observation points (influent and effluent) in different times (month, year) are able to highlight on the one hand the extent that the treatment process caused differences in values of environmental parameters controlled and monitored in WWTP and how much systematic changes appeared year to year to influence the water quality if untreated and treated, respectively.

The result of analyzed collected data shows that there is some interrelationship among wastewater parameters. The parameters interrelationship can be assembled into two groups by PCA results. The first group is BOD₅ and COD and the second group is NH₄-N and COD.

Acknowledgements:

This paper is supported by the Sectoral Operational Programme Human Resources Development POSDRU/159/1.5/S/137516 financed from the European Social Fund and by the Romanian Government.

References

- [1] Jäntschi, L., S.D. Bolboacă, „The Jungle of Linear Regression Revisited”, Leonardo Electronic Journal of Practices and Technologies, 2007, 6(10):169-187.
- [2] Pearson, K. (1900). On the criterion that a given system of deviations from the probable in the case of a correlated system of variables is such that it can be reasonably supposed to have arisen from random sampling. Philosophical Magazine 5th Ser 50:157-175.
- [3] POP, H.F, EINAX, J.W., Sârbu, C., Classical and Fuzzy Principal Component Analysis of Some Environmental Samples Concerning the Pollution with Heavy Metals, Chemometrics and Intelligent Laboratory Systems, 2009, 97(1), 25-32.
- [4] R. R. Bansode, „Treatment of organic and inorganic pollutants in municipal wastewater by agricultural by-product based granular activated carbons” [M.S. thesis], The Department of Food Science, Louisiana State University and Agricultural and Mechanical College, Baton Rouge, La, USA, 2002.

Modelarea sistemelor cu purtători multipli de energie în clădiri*

Modelling of systems with multiple energy carriers in buildings

Pavel Atănăsoae

Universitatea „Ștefan cel Mare” Suceava
Str. Universității 13, 720229, Suceava
E-mail: atanasoae@eed.usv.ro

Rezumat. În lucrare se prezintă un exemplu de modelare a sistemelor cu purtători multipli de energie bazat pe conceptul de hub energetic. Modelul a fost personalizat pentru a putea fi utilizat în etapa de proiectare sau reabilitare a unei clădiri. Această abordare permite configurarea optimă a diferitelor surse de energie disponibile, inclusiv a surselor regenerabile, pentru alimentarea cu energie a clădirilor.

Cuvinte cheie: purtători multipli de energie, hub energetic, modelarea sistemelor

Abstract. The paper presents an example of modeling for systems with multiple energy carriers based on the concept of energy hub. The model was personalized to be used in the design or refurbishment stage of a building. This approach enables optimal configuration of the various available energy resources, including renewable sources, for the power supply of buildings.

Key words: multiple energy carriers, energy hub, systems modelling

1. Introducere

În cele mai multe cazuri, sursele de alimentare cu energie a unei clădiri sunt luate în considerare și analizate individual. Tratarea în comun și nu individual poate să conducă la o serie de beneficii. Aceste beneficii pot fi sintetizate în: continuitatea în alimentare cu energie, flexibilitatea în alimentare și potențialul de optimizare.

Disponibilitatea de energie pentru sarcina cerută nu mai este dependentă de o singură infrastructură având în vedere mai multe intrări în hub-ul energetic care pot fi utilizate pentru a satisface cererea de ieșire.

Creșterea flexibilității în alimentare se datorează căilor redundante care oferă un anumit grad de libertate în acoperirea curbei de sarcină.

Potențialul de optimizare derivă din faptul că mai multe surse și diferite combinații ale acestora pot fi utilizate pentru a satisface cerințele de consum cu un cost cât mai scăzut. Sursele utilizate pot fi caracterizate prin costuri diferite, emisiile aferente, disponibilitate și alte criterii.

* Lucrare inclusă în programul conferinței RCEPB 2014

De regulă, metodele de optimizare sunt utilizate pe sisteme cu o singură formă de energie: energie electrică, gaze naturale sau rețeaua de termoficare. În ultimul timp se constată o creștere a preocupărilor privind modelarea și analiza combinată a sistemelor cu surse multiple de energie [1-5].

2. Descrierea problemei

Alimentarea cu energie a unei clădiri se realizează din diverse surse, prin intermediul purtătorilor de energie, fie direct fie prin intermediul sistemelor de conversie care transformă energia dintr-o formă de energie în alta.

Luarea în considerare a interacțiunilor dintre aceste sisteme de energie s-a realizat după conceptul de hub energetic. Un hub energetic reprezintă interfața dintre infrastructura de transport (rețele), surse locale și consumurile (sarcinile) de energie din clădire. Elemente de bază ale unui hub energetic sunt: conexiunile directe și convertoarele (sursele locale) de energie.

De exemplu, energia electrică necesară consumatorilor din clădire poate fi asigurată fie din rețeaua electrică publică fie poate fi produsă local într-o centrală de cogenerare sau utilizând surse regenerabile de energie (solară, eoliană). Similar, pentru celelalte utilități necesare clădirii (încălzire, răcire) pot fi luate în considerare diverse soluții de alimentare (fig.1).

Astfel, necesarul de energie în clădire poate fi asigurat direct de la intrarea corespunzătoare sau poate fi generat parțial sau total în interiorul hub-ului. Printr-o astfel de abordare poate fi substituit sau chiar eliminat un purtător de energie neatractiv, de exemplu cu cost ridicat.

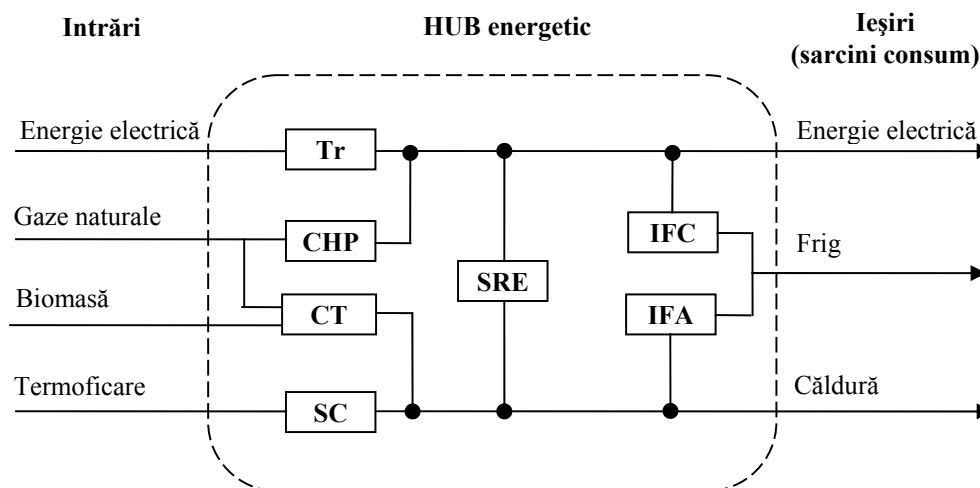


Fig.1. Exemplu privind structura unui hub energetic

Tr-transformator de putere coborât; CHP-centrală de cogenerare; CT-centrală termică; SC-schimbător de căldură; SRE-surse de energie regenerabile; IFC-instalație frigorifică cu compresie; IFA-instalație frigorifică cu absorbție.

Ecuția matricială care reprezintă un sistem cu purtători multipli de energie are forma următoare:

$$\underbrace{\begin{bmatrix} L_{\alpha} \\ L_{\beta} \\ \vdots \\ L_{\omega} \end{bmatrix}}_L = \underbrace{\begin{bmatrix} c_{\alpha\alpha} & c_{\beta\alpha} & \cdots & c_{\omega\alpha} \\ c_{\alpha\beta} & c_{\beta\beta} & \cdots & c_{\omega\beta} \\ \vdots & \vdots & \ddots & \vdots \\ c_{\alpha\omega} & c_{\beta\omega} & \cdots & c_{\omega\omega} \end{bmatrix}}_C \cdot \underbrace{\begin{bmatrix} P_{\alpha} \\ P_{\beta} \\ \vdots \\ P_{\omega} \end{bmatrix}}_P \quad (1)$$

unde:

$\alpha, \beta, \dots, \omega$ – sunt diferiți purtători de energie;

L – matricea sarcinilor (consumurilor din clădire);

P – matricea purtătorilor de energie care intră în contur (hub);

C – matricea de cuplaj între purtătorii de energie.

Coefficienții de cuplaj caracterizează eficiența energetică a conversiei și au valori cuprinse între:

$$0 \leq c_{ij} \leq 1 \quad (2)$$

Matricea de cuplaj între purtătorii de energie reflectă gradele de libertate în alimentare ce pot fi utilizate pentru optimizarea satisfacerii necesarului de energie în clădire.

3. Exemplu de aplicare

Pentru exemplificare, se consideră un consumator cu profilurile de consum prezentate în figura 2 pentru consumul anual de energie termică și respectiv în figura 3 pentru consumul anual de energie electrică.

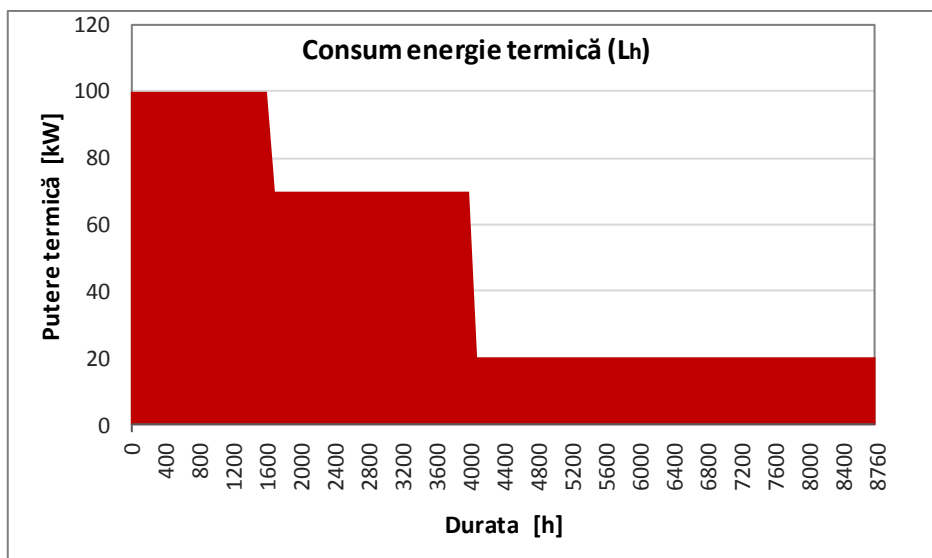


Fig.2. Curba clasată a consumului anual de energie termică

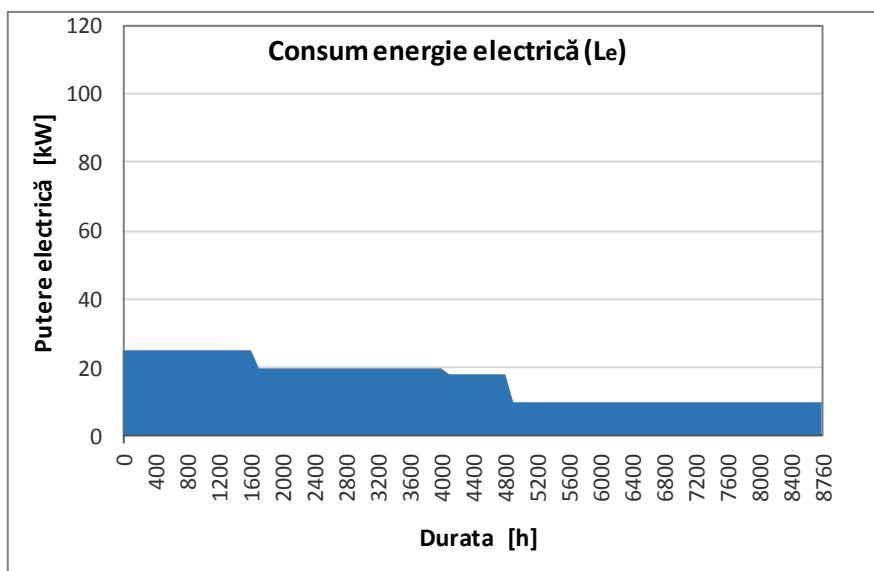


Fig.3. Curba clasată a consumului anual de energie electrică

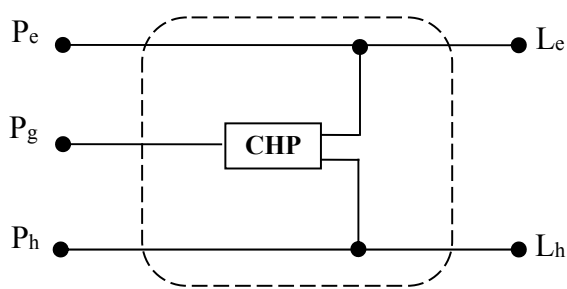


Fig.4. Scenariul 1

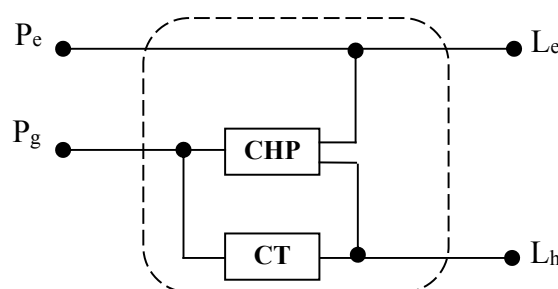


Fig.5. Scenariul 2

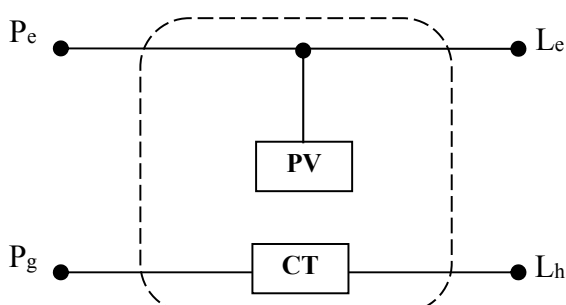


Fig.6. Scenariul 3

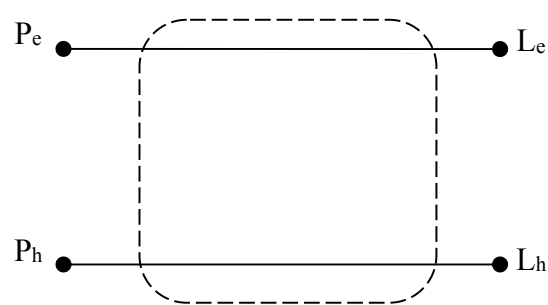


Fig.7. Scenariul 4

Pentru satisfacerea consumurilor de energie, aferente clădirii analizate, s-au luat în considerare următoarele scenarii:

1. Scenariul 1 (figura 4): alimentarea cu energie din rețelele publice de utilități (energie electrică și energie termică) și instalarea la consumator a unei centrale de cogenerare (CHP) pe combustibil gaze naturale;

2. Scenariul 2 (figura 5): alimentarea cu energie electrică din rețeaua publică și instalarea la consumator a unei centrale de cogenerare (CHP) și a unei centrale termice (ca sursă de vârf), ambele utilizând combustibil gaze naturale;
3. Scenariul 3 (figura 6): alimentarea din rețeaua publică și instalarea unei surse de energie regenerabilă (panouri fotovoltaice) pentru asigurarea consumului de energie electrică iar pentru consumul de energie termică instalarea unei centrale termice pe combustibil gaze naturale;
4. Scenariul 4 (figura 7): alimentarea cu energie din rețelele publice de utilități (energie electrică și energie termică) fără alte surse la consumator.

Performanțele diferitelor surse luate în considerare la analiza scenariilor se prezintă în tabelul 1 iar tarifele pentru energia consumată din rețelele publice se prezintă în tabelul 2.

Tabelul 1

Performanțele diferitelor surse luate în considerare la analiza scenariilor

	Putere electrică nominală [kW]	Putere termică nominală [kW]	Randament		Factor de utilizare a capacității nominale	Investiția specifică [Euro/kW]	Operare și mentenanță [%] din investiție
			electric [%]	termic [%]			
CHP	10	20	28	56	-	1500	3
CT	-	80 în S2	-	90	-	53	1,5
		100 în S3					
PV	8	-	-	-	0,16	2500	1

Tabelul 2

Tarifele pentru energia consumată din rețelele publice

Energie electrică [Euro/kW]	Gaze naturale [Euro/kW]	Energie termică [Euro/kW]
0,107	0,027	0,030

Scenariul 1:

Ecuția (1) particularizată pentru secenariul 1:

$$\begin{bmatrix} L_e \\ L_h \end{bmatrix} = \begin{bmatrix} c_{ee} & c_{ge} & c_{he} \\ c_{eh} & c_{gh} & c_{hh} \end{bmatrix} \cdot \begin{bmatrix} P_e \\ P_g \\ P_h \end{bmatrix} \quad (3)$$

Prin înlocuirea coeficienților de cuplaj, ecuația devine:

$$\begin{bmatrix} L_e \\ L_h \end{bmatrix} = \begin{bmatrix} 1 & \eta_{CHPe} & 0 \\ 0 & \eta_{CHPh} & 1 \end{bmatrix} \cdot \begin{bmatrix} P_e \\ P_g \\ P_h \end{bmatrix} \quad (4)$$

Rezultă următoarele ecuații:

$$\begin{cases} L_e = P_e + \eta_{CHPe} \cdot P_g \\ L_h = \eta_{CHPh} \cdot P_g + P_h \end{cases} \quad (5)$$

Pentru rezolvare se ține seama de indicele de cogenerare (raportul putere electrică/putere termică):

$$y = \frac{P_{CHPe}}{P_{CHPh}} \left[\frac{kW}{kW} \right] \quad (6)$$

Se impune P_{CHPh} (prin alegerea instalației de cogenerare) și se rezolvă sistemul de ecuații (4) rezultând necunoscutele P_e , P_g și P_h (tabelul 3).

Tabelul 3

Puterile purtătorilor de energie în scenariul 1

Sarcini necesare [kW]		Durata [h/an]									
L_e	25	1600	L_e	20	2400	L_e	18	800	L_e	10	3960
L_h	100		L_h	70		L_h	20		L_h	20	
P_e	15		P_e	10		P_e	8		P_e	0	
P_g	35,71		P_g	35,71		P_g	35,71		P_g	35,71	
P_h	80		P_h	50		P_h	0		P_h	0	

Scenariul 2:

Ecuția (1) particularizată pentru scenariul 2:

$$\begin{bmatrix} L_e \\ L_h \end{bmatrix} = \begin{bmatrix} 1 & \eta_{CHPe} & 0 \\ 0 & \eta_{CHPh} & \eta_{CT} \end{bmatrix} \cdot \begin{bmatrix} P_e \\ P_{gCHP} \\ P_{gCT} \end{bmatrix} \quad (7)$$

Rezultă următoarele ecuații:

$$\begin{cases} L_e = P_e + \eta_{CHPe} \cdot P_{gCHP} \\ L_h = \eta_{CHPh} \cdot P_{gCHP} + \eta_{CT} \cdot P_{gCT} \end{cases} \quad (8)$$

Pentru rezolvare, se procedează similar ca în cazul scenariului 1, rezultând necunoscutele P_e și P_g (tabelul 4), unde P_g :

$$P_g = P_{gCHP} + P_{gCT} \quad (9)$$

Tabelul 4

Puterile purtătorilor de energie în scenariul 2

Sarcini necesare [kW]		Durata [h/an]	Sarcini necesare [kW]		Durata [h/an]	Sarcini necesare [kW]		Durata [h/an]	Sarcini necesare [kW]		Durata [h/an]
L_e	25	1600	L_e	20	2400	L_e	18	800	L_e	10	3960
L_h	100		L_h	70		L_h	20		L_h	20	
P_e	15		P_e	10		P_e	8		P_e	0	
P_g	124,60		P_g	91,27		P_g	35,71		P_g	35,71	

Scenariul 3:

Ecuția (1) particularizată pentru scenariul 3:

Modelarea sistemelor de energie cu purtători multipli de energie

$$\begin{bmatrix} L_e \\ L_h \end{bmatrix} = \begin{bmatrix} 1 - FC_{PV} & FC_{PV} & 0 \\ 0 & 0 & \eta_{CT} \end{bmatrix} \cdot \begin{bmatrix} P_e \\ P_{PV} \\ P_g \end{bmatrix} \quad (10)$$

Rezultă următoarele ecuații:

$$\begin{cases} L_e = (1 - FC_{PV}) \cdot P_e + FC_{PV} \cdot P_{PV} \\ L_h = \eta_{CT} \cdot P_g \end{cases} \quad (11)$$

Pentru rezolvare, se impune P_{PV} (prin alegerea puterii instalate a panourilor fotovoltaice) și se ține seama de factorul de utilizare a capacității instalate FC_{PV} pentru această tehnologie în condițiile din România [6], rezultând necunoscutele P_e și P_g (tabelul 5).

Tabelul 5

Puterile purtătorilor de energie în scenariul 3

Sarcini necesare [kW]		Durata [h/an]	Sarcini necesare [kW]		Durata [h/an]	Sarcini necesare [kW]		Durata [h/an]	Sarcini necesare [kW]		Durata [h/an]
L_e	25	1600	L_e	20	2400	L_e	18	800	L_e	10	3960
L_h	100		L_h	70		L_h	20		L_h	20	
P_e	23,72		P_e	18,72		P_e	16,72		P_e	8,72	
P_g	111,11		P_g	77,78		P_g	22,22		P_g	22,22	

Scenariul 4:

În această variantă consumurile de energie sunt asigurate din rețelele publice de utilități (tabelul 6).

Tabelul 6

Puterile purtătorilor de energie în scenariul 4

Sarcini necesare [kW]		Durata [h/an]	Sarcini necesare [kW]		Durata [h/an]	Sarcini necesare [kW]		Durata [h/an]	Sarcini necesare [kW]		Durata [h/an]
L_e	25	1600	L_e	20	2400	L_e	18	800	L_e	10	3960
L_h	100		L_h	70		L_h	20		L_h	20	
P_e	25		P_e	20		P_e	18		P_e	10	
P_h	100		P_h	70		P_h	20		P_h	20	

Analiza economică în vederea aplicării diverselor soluții de alimentare cu energie a unei clădiri presupune determinarea valorii nete actualizate a costurilor implicate în realizarea investițiilor și exploatarea instalațiilor pe durata de viață a investiției respective.

Valoarea netă actualizată (VNA) reprezintă proiecția la momentul „0” a tuturor costurilor menționate în funcție de rata de depreciere a monedei considerate [7]:

$$VNA = C_0 + \sum_{k=1}^S C_{Ek} \sum_{t=1}^N \left(\frac{1 + f_k}{1 + i} \right)^t + C_M \sum_{t=1}^N \left(\frac{1}{i + 1} \right)^t \quad (12)$$

în care:

C_0 – costul investiției totale în anul „0” [Euro];

C_E – costul anual al energiei consumate, la nivelul anului de referință [Euro/an];

C_M – costul anual al operațiunilor de mentenanță [Euro/an];

f – rata anuală de creștere a costului energiei (0,1 %);

i – rata de actualizare (7 %);

k – indice corespunzător sursei de energie utilizate;

N – durata fizică de viață a sistemului analizat (15 ani).

Costurile totale evidențiate prin valoarea netă actualizată, pentru fiecare scenariu analizat, sunt prezentate în tabelul 7.

Tabelul 7

Costurile totale comparative pentru scenariile analizate

	Scenariul 1	Scenariul 2	Scenariul 3	Scenariul 4
VNA [Euro]	217191	222014	270214	253147

Costurile minime, pentru profilurile de sarcină ale consumatorului analizat, se realizează în cazul scenariului 1.

4. Concluzii

Întreaga infrastructură de alimentare cu energie a unei clădiri poate fi considerată ca un sistem de noduri de energie interconectate.

Interacțiunea între purtătorii de energie se realizează prin intermediul sistemelor de conversie care transformă energia dintr-o formă în alta.

Această flexibilitate în alimentarea cu energie a clădirii ridică noi semne de întrebare cu privire la funcționarea optimă a sistemului.

Printr-o astfel de abordare pot fi indentificate diverse probleme de optimizare privind utilizarea energiei în clădiri. Astfel, în faza de proiectare sau reabilitare a unei clădiri, pot fi selectate diverse surse în vederea unei cuplări optime pentru satisfacerea consumurilor de energie în clădire (încălzire, răcire, energie electrică).

Referințe

- [1] M. Geidl, G. Andersson, „Optimal power flow of multiple energy carriers”, in IEEE Transaction Power Systems, vol. 22, 2007, pp. 145-155.
- [2] M. Geidl, G. Koepfel, P. Favre-Perrod, B. Klockl, G. Andersson, K. Frohlich, 2007, „Energy hubs for the future” in IEEE Power and Energy Magazine, vol.5, no.1, 2007, pp. 24-30.
- [3] V. Corrado, E. Fabrizio, M. Filippi, „Modelling and optimization of multi-energy source building systems in the design concept phase”, Proceedings of Clima 2007 WellBeing Indoors, REHVA World Congress, June 10-14, 2007, Helsinki, Finland.
- [4] A. Sheikhi, Sh. Bahrami, A.M. Ranjbar, S. Sattari, M. Adami, „Financial Analysis for a Multi-Carrier Energy System Equipped with CCHP”, International Conference on Renewable Energies and Power Quality (ICREQP'13), March 20-22, 2013, Bilbao, Spain.
- [5] A. Sheikhi, A. M. Ranjbar, M. Mahmoody, F. Safe, „CHP Optimize Selection Methodology for an Energy Hub System”, 10th International Conference on Environment and Electrical Engineering, May 8-11, 2011, Rome, Italy.
- [6] *** ANRE (Autoritatea Națională de Reglementare în domeniul Energiei): <http://www.anre.ro>
- [7] *** Mc 001/3-2006, Metodologie de calcul al performanței energetice a clădirilor.

Daylight in retrofitting office building design*

¹Alexandru Mircea Iatan–PhD

²Angel Madalin Dogeanu–PhD Student

¹Technical University of Civil Engineering of Bucharest, Faculty of Building Services,
e-mail: alex_iatan@yahoo.fr

²Technical University of Civil Engineering of Bucharest, Faculty of Building Services,
e-mail: angeld_ro@yahoo.com

Abstract: *Understanding the specifics of sustainable building and determining effective sustainable practices can be confusing. Daylighting analysis is an important component towards creating accurate simulations for sustainable design and visual health. Daylight has been utilized as a design element in buildings throughout history. One of the main reasons for using daylight in recent years is its benefit in reducing energy consumption through its use as a main or secondary illumination source in order to replace the use of electrical lighting. Daylight not only replaces artificial lighting, reducing lighting energy use, but also influences both heating and cooling loads. Planning for daylight therefore involves integrating the perspectives and requirements of various specialties and professionals. Daylighting design starts with the selection of a building site and continues as long as the building is occupied.*

This paper presents a numerical method based on Dialux to predict daylight factors and daylight uniformity factor into a retrofit office building in order to comply green and sustainability standards requirements.

Keywords: daylight factor, daylight uniformity ratio, green building, sustainability development.

1. Introduction

For centuries, daylight was the only efficient source of light available. Architects were dominated by the goal of creating openings large enough to distribute daylight to building interiors. Efficient artificial light sources and fully glazed facades have liberated designers from these constraints of the past. Advanced daylighting systems and the new control systems are another step forward in providing daylight in a user-friendly, energy-efficient manner. These systems need to be integrated into a building's overall architectural strategy and incorporated into the project from the early design stage. The design considerations will be associated with enhancing a building's daylight utilization while achieving maximum energy efficiency and user acceptance.[1]. The energy efficiency and sustainability become a common subject these days increasing the important issues in the field of architecture. Daylighting is recognized as the first step in reducing the energy consumption. A coherent design is reducing the amount of electrical lighting in a building. In addition to reducing the

* Lucrare inclusă în programul conferinței EENVIRO 2014

carbon footprint of buildings, daylighting is known to have positive effects on human health and productivity. All energy standards and green building rating systems have strongly recommended that designers incorporate daylighting strategies into building design. However, this recommendation is all too frequently ignored due to the complexity of daylighting design and to concerns of the potential for thermal and visual discomfort caused by excessive sunlight penetrations and glare. [2]

2. The concept of daylight coefficients

The concept of daylight coefficients, originally proposed by Tregenza and Waters (1983) [3], is to theoretically divide the celestial hemisphere into disjoint sky segments, and to calculate the contribution of each sky segment to the total illuminance at various sensor points in a building,

based on each sensor's position within a given environment and orientation.[4]

Although the sky is changing every minute of a day, typically average sky conditions are used for daylighting calculations. Different models of virtual skies have been developed by the CIE. CIE has mathematically developed 15 different sky conditions, two of which are shown in Figure 1[5],

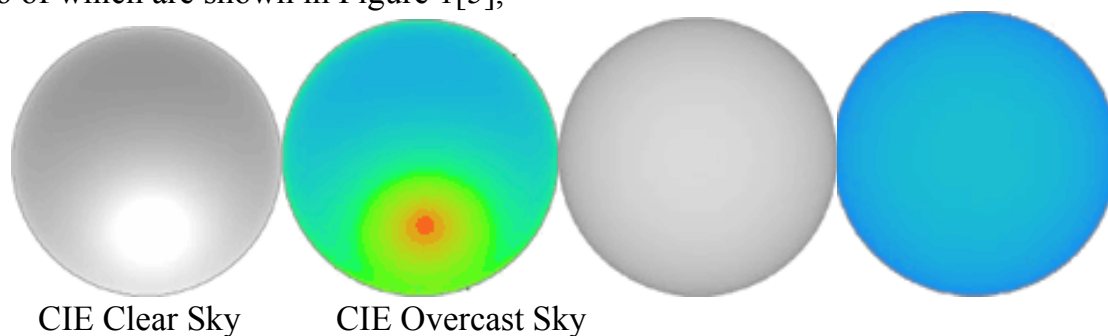


Figure1. CIE sky conditions [6].

where CIE Overcast Sky - completely cloudy sky (100% covered), represent the most widely used sky model for daylight factor calculation and CIE Clear Sky is defined by having less than 30% of clouds covering the sky or no clouds, being useful when visual glare and thermal discomfort studies are performed. [5]

In the past because the computational resources were limited, the luminance of the entire overcast sky was taken as uniform. This type of sky is termed as uniform sky and under this condition the illuminance at a point on a horizontal surface due to an unobstructed hemisphere of overcast sky can be given by:

$$E = L \times \pi \text{ (lux)} \quad (1)$$

Where

L represent the sky luminance in Cd / m^2 .

Nowadays, when the standardized CIE sky was widely adopted and implemented in the simulation software, the diffuse light from a completely overcast sky is calculated when ground is free of snow. The luminance distribution of the CIE sky is not

uniform. The relative luminance L_q depends on the angle θ of elevation q measured with respect to the horizon, and is given by:

$$L_q = L_z \frac{1 + 2 \sin \theta}{3}, \quad (2)$$

Where

L_z represent the sky luminance at the zenith.

This equation shows that :

- (a) Zenith ($q = 90^\circ$) is the brightest region,
- (b) The luminance decreases to 1/3 of that of the zenith towards the horizon
- (c) The luminance is independent of the position of the sun, and therefore the orientation of the windows has no effect on the illumination of the room.

There are two ways to handle daylight quantitatively:

- (a) by using luminous quantities (flux, illuminance), by a set of outdoor conditions and calculating the resulting interior illuminances;
- (b) by using relative values (the daylight factor) which compare indoor to outdoor illuminance. This factor is constant under widely varying outdoor lighting conditions for a given position.

The daylight factor is defined as :

$$DF = \frac{E_i}{E_o} \times 100 \quad (\%) \quad (3)$$

where:

E_i = illuminance due to daylight at a point on the indoors working plane,

E_o = simultaneous outdoor illuminance on a horizontal plane from an unobstructed hemisphere of overcast sky.

In figure 2 we presented all possible paths along which light can reach a point inside a room through glazed windows. [4] As following:

- (a) light from the sky visible at the point considered, this component is named as the sky component (SC),
- (b) light that is reflected from opposing exterior surfaces and then reached the point, this component is known as the externally reflected component (ERC),
- (c) light entering through the window but reaching the point after it reflect from internal surfaces, this component is known as the internally reflected component (IRC).

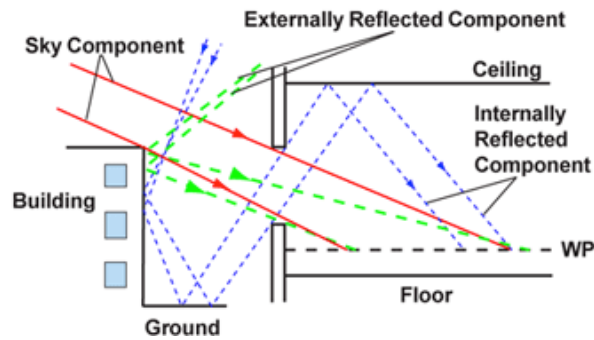


Figure 2. Components of the Daylight Factor. [4]

The sum of the three components gives the daylight factor:

$$DF = SC + ERC + IRC \quad (4)$$

3. Daylight Factors Target

In temperate climates, choosing the value for the daylight factor can have a crucial impact on the energy efficiency of a building. This is mainly for two reasons. First of all the impact is because of the low thermal insulation of glazing that carries a heavy penalty in heating energy consumption matching the minimum of glazed area sufficient to provide adequate day lighting is an important target. Secondly, the short day lit hours of the winter mean that the transition to artificial lighting will occur during the working day and this transition point will be sensitive to the daylight factor and the light level required for functional purposes [7]. There are many methods for finding the components for a specific given point, though they are checking procedures rather than ones, which generate a daylighting design. In order to reach this goal an average daylight factor must be proposed as a design parameter. To determine the factor all three components are calculated simultaneously based on window sizing, enabling daylighting to take a place in the overall design process. [8] Technical recommendations and Standards defining daylighting design parameters and minimum values have been drawn up independently for each country. For example, British Standards settle minimum average daylight factors related to different activities and to supplementary electric lighting as presented in table 1. [9]

Table 1.

Daylighting recommendations in some workplaces. [9]

Activity/ Spaces	Type of daylighting(*)	DF (%)
Teaching	A	5
	B	2
General offices	A	5
	B	2
Laboratories	A	5
	B	2
Drawing offices	A	5
	B	1 (in supplemented area)

(*) A - Full daylighting / B - Supplemented daylighting

There are also recommendations for checking daylight uniformity in table 2 [10]

Table 2.

Recommendation on daylight uniformity. [10]

BS CP 3/64	$DF_{\max} / DF_{\min} < 2$
BS 8206/92	<ul style="list-style-type: none"> - no significant part of the working planes shall lie beyond the no-sky line; - in an interior with one or more windows on one wall only room depth shall not exceed window height and width; - in an interior with rooflights, the spacing/height ratio should not be too great; - in an interior with rooflights, ceiling and floor reflectance should be high enough

In practice is recommended to use the following expression for estimating average daylight factor [11],[12]:

$$DF_m = \frac{A_w \cdot t \cdot \theta}{A_{tot} (1 - r_m^2)}, \quad (5)$$

where:

DF_m = average Daylight Factor,

A_w = total glazed area of windows,

t = glass transmittance,

θ = angle of visible sky,

A_{tot} = total area of all the room surfaces,

r_m = area-weighted average reflectance of room surfaces.

It is also inadequate to use standard average daylight factor because it only provide recommended values that can be used as a partial checking of daylighting quantitative aspects and does not provide natural light distribution, luminance ratio and view. The average daylight factor is a single, broad measure of daylight for the whole room and does not provide any detailed information about distribution and punctual value in different points.[8]

The average daylight factor has other limitations such as not being able to predict glare and luminance ratio and often it is necessary to make use of further daylight control elements to satisfy user visual comfort requirements.

During the design stage it is necessary to take into consideration the different performances of a daylighting system with respect to light distribution and uniformity ratio as they play an important role in architectural daylighting, in this case we are talking in particular case of an office buildings.

Based on a relationship between source and background luminance, the degree of glare caused by any individual light source can be expressed as a glare constant [13]:

$$G_i = k \frac{L_s^{1.6} \Omega^{0.8}}{L_b + 0.07 \omega^{0.5} L_w}, \quad (6)$$

where:

G_i = glare coefficient for each of the component parts of the view through the window (sky, obstruction, ground);,

L_s = luminance in Cd/m^2 of the patch of visible sky, of the obstructions and of the ground seen through the window,

Ω = solid angle subtended by the source, with weighting factors for different areas depending on their direction with respect to the occupant line of sight,

L_b = average luminance in Cd/m^2 of the interior surfaces of the room which contribute to the visual field of an occupant of the room,

ω = total solid angle in steradians subtended by the window,

L_w = average luminance of the window weighted according to the relative areas of sky obstructions and ground,

k = constant depending on measurement units and source.

The glare constants for all sources are then summed to determine the Daylight Glare Index [13]:

$$DGI = 10 \log \sum_{i=1}^n G_i \quad (7)$$

The glare is a comfort sensation, the DGI is based on how groups of people have responded to various levels of brightness, the DGI is influenced by daylight and artificial light, with the glare sensation scored as each individual perceived it. Being a subject test there was created an satisfaction scale at different glare index obtained in different conditions. The scale is having intervals ranging from “just imperceptible” to “just intolerable”. Daylight glare criteria have been defined and compared to those ones for classical electric lighting sources in table 3. [8],[14]

Table 3.
Comparison between artificial source glare indices (IES GI), daylight glare index (DGI) and glare criteria.

MEAN SUBJECTIVE ASSESSMENT OF GLARE	IES GI	DGI
just imperceptible	10	16
	13	18
just acceptable	16	20
	19	22
just uncomfortable	22	24
	25	26
just intolerable	28	28

All the above considerations require for an numerical study showing lighting performances of different rooms based on window options in order to evaluate the relationship between window shape, position and light distribution [8]. When sizing windows should be take into account qualitative aspects such as view out.

4. The case study

The building used in this study is a single floor building built to mid 1980. The building hasn't been finalized, remaining at foundation stage for more then 30 years. Foundations surface is 1800 square meters. On those foundations a new building will be designed as open space business center. The plan view with the new space layout is represented in figure 3.

The virtual room was 64 meters long, 45 meters wide, and 3.2 meters high. On the south orientation the walls was entirely glass with an 89% transmittance value. Light meters were added into work plane area situated at 0.75 meters above floor. The properties of all the elements are given here: ceiling: 80% reflectance walls: 50% reflectance, floor: 20% reflectance, glass wall: 89% transmittance. This virtual space has been tested under CIE overcast skies. From the base case model described above, a 3D model has to be created.

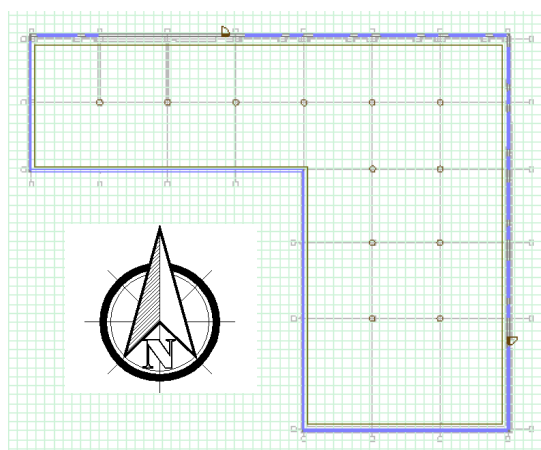


Figure 3. Building new layout plan view.

The computer simulation need a 3D drawing reproducing the material characteristics of which the model was realized so that the model drawing was made with the DIALux software assigning to each geometrical component the properties used in the real model is presented in Figure 4.



Figure 4. Building 3D model view.

The daylight calculation capabilities within DIALux make use of German standard DIN 5043 and CIE Publication 110. Geometric input is limited to certain shapes. Sky choices are somewhat limited but acceptable for diverse ranges of weather conditions. There is an external radiosity and ray-tracing model, POV-Ray (Persistence of Vision 2010).

The geometry of the model and the finishing touches are very simple to have a base model avoiding any influence on the analysis of particular material or geometrical element and deferring the study of single specific case to a separate evaluation. The room building parameters analyzed were the geometry, its glazing system, the reflectance of the room walls and floor, the dimensions of the adjoining spaces and the reflectance of the materials that finish the interior spaces. The study was based on preliminary design hypothesis such as a simple finishing touches, as mentioned above.

5. Simulation results

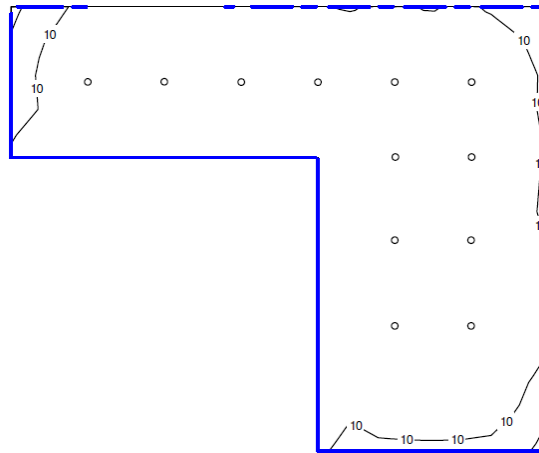


Figure 5. Daylight workplaneisolines.

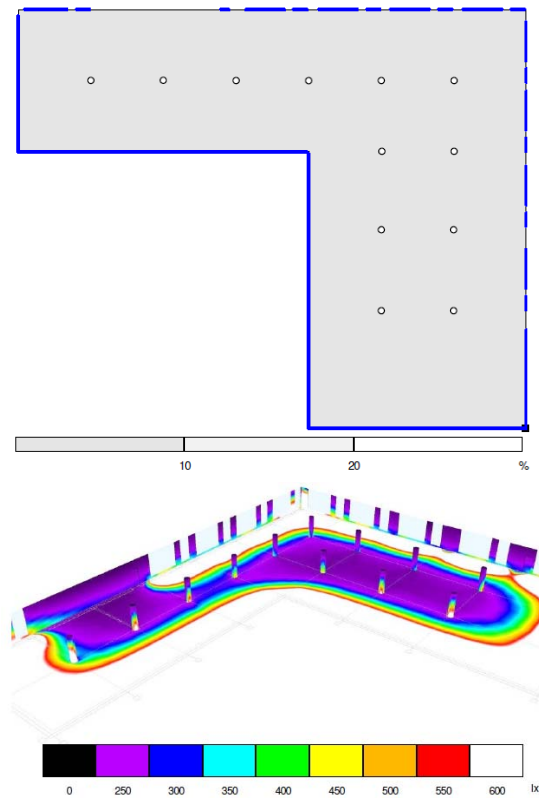


Figure 6. Daylight workplane greyscale(a), 3D rendering colors (b).

- a) reducing windows area by limiting the windows height,
- b) introduction of automatic shading elements,
- c) changing the glass composition to decrease the degree of transparency
- d) changing the glass composition to increase the reflectance.

Thus it follows that the attempt to use the maximum level given by daylight does not necessarily lead to an efficient energy solution, nor in terms of comfort.

Additional measures to be taken are chosen such so there is a balance between the use of day lighting luminance level and interior comfort (regarding energy efficiency of building facilities, with particular reference to HVAC systems and artificial lighting).

6. Conclusions

Today, a large number of buildings are refurbished because of:

- a) a poor indoor environment,
- b) high power level or energy consumption,
- c) the need for a new floor layout.

Daylight design is an important component of building retrofitting components that affect the building performance. Most common retrofit measures are referring to the replacement of windows or of the whole facade.

Building refurbishment is an opportunity to redefine the functional concept in order to meet today's requirements.

Selection of the right glazing is of major importance for a building's daylighting strategy. The combined application of new glass and new daylighting systems, particularly those that provide solar shading, glare control, and the redirection of light, can increase daylight and decrease cooling loads.

Combining daylighting and artificial lighting systems through is a design option in retrofits as well as new construction.

The aim of this study has been to undertake a more comprehensive analysis of daylighting in interior spaces, and to verify the performances of daylighting systems with respect to the luminous environment.

An overall analysis of the luminous environmental quality and its effects on psychological and emotional aspects needs for a subjective survey.

7. References

- [1] Daylight in Buildings, A report of IEA SHC Task 21/ ECBCS Annex 29, July 2000;
- [2] Kensek K., Suk J.Y., "Daylight Factor (overcast sky) versus Daylight Availability (clear sky) in Computer-based Daylighting Simulations", Journal of Creative Sustainable Architecture & Built Environment, CSABE Vol. 1, November, 2011
- [3] Tregenza, P., Waters, "Daylight coefficients. Lighting Research and Technology.", Vol. 15, No. 2, pp. 65 – 71. I. M. 1983;
- [4] Bourgeois D, Reinhart CF, Ward G, "A Standard Daylight Coefficient Model for Dynamic Daylighting Simulations" Building Research & Information 36:1 pp. 68-82, 2008;

- [5] Norvasuo, Markku, "The new CIE general sky standard: daylighting experiences and implications.", The European Council for an Energy Efficient Economy, 2002
- [6] Sky Illuminance. Retrieved March 14, 2010 from www.naturalfrequency.com/wiki/Sky_Illuminance
- [7] Comfortable Low Energy Architecture, website, <http://www.new-learn.info/packages/clear/index.html>;
- [8] C. Aghemo, A. Pellegrino, "Indoor daylighting: assessment of the performances of different window options", Dipartimento di Energetica - Politecnico di Torino, Torino, Italy, 2010;
- [9] BS DD73: Basic data for the design of buildings: Daylight, (British Standards Institution), 1982;
- [10] Torricelli M.C., Sala M., Secchi S., "Daylight - La luce del giorno. Tecnologie e strumenti per la progettazione", Alinea Editrice, Firenze, 1995;
- [11] CIBSE (The Chartered Institution of Building Services Engineers), "Code for interior lighting", 1994;
- [12] CIBSE (The Chartered Institution of Building Services Engineers), "Applications Manual, Window Design", 1987;
- [13] Chauvel P., Collins J.B., Dogianux, Longmore J., "Glare from windows: current view of the problem", Lighting Research & Technology, Vol. 14 (1), 1982;
- [14] N. Baker, A. Fanchiotti, K., Commission of the European Communities, Directorate General XII for Science, Research and Development, Daylighting in Architecture, a European reference book, 1st edition, Brussels and Luxembourg, Steemers, 1993.

Aiming to achieve net zero energy lighting in buildings*

Dr Cosmin Ticleanu, MSL

Building Research Establishment

Bucknalls Lane, Watford WD25 9XX, United Kingdom

ticleanu@bre.co.uk

Abstract: *Energy consumption for interior lighting is rapidly increasing and takes up 17.5% of the total global electricity consumption on average. With European office buildings using 50% of their total electricity consumption for lighting alone, and other shares of electricity of 20-30% in hospitals, 15% in factories, 10-15% in schools and 10% in residential buildings, there is significant potential to reduce energy consumption for lighting. By implementing a combination of key measures, such as minimisation of lighting power density; use of highly-efficient lighting technologies based on renewable energy sources; use of appropriate lighting control systems; and maximisation of daylight use, energy saving targets can be pushed forward to aim at achieving net zero energy lighting in buildings. This paper presents findings from Building Research Establishment projects for public and private buildings to reduce lighting energy consumption whilst improving the quality of the internal luminous environment.*

Keywords: energy performance, interior lighting, daylight, efficient lighting, lighting controls.

1. Current background

Lighting is a large and rapidly increasing source of energy demand in buildings. In 2005 grid-based electricity consumption for lighting was 2650 TWh worldwide, or around 19% of the total global electricity consumption, whilst the electricity consumption for interior lighting alone was estimated at 2438 TWh worldwide, or about 17.5% of the total global electricity consumption (Halonen, Tetri and Bhusal, 2010). Interior lighting accounts for a significant part of the electricity consumption in buildings. According to International Energy Agency (IEA) research, heating is the leading energy consumer in EU commercial buildings, followed by lighting (Fig. 1).

* Lucrare inclusă în programul conferinței RCEPB 2014

Cosmin Ticleanu

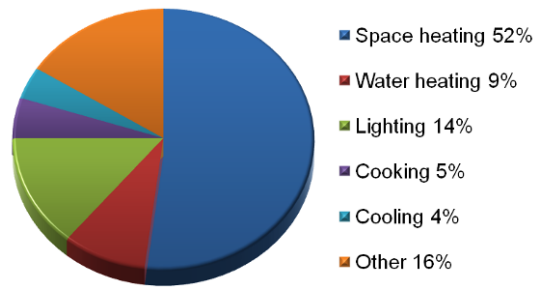


Fig. 1. Energy consumption by end use in EU commercial buildings (source: IEA).

The electricity consumption for interior lighting varies with the type of building. In some buildings, lighting is the largest single category of electricity consumption; office buildings, on average, use the largest share of their total electricity consumption in lighting. 50% of total electricity consumption in European office buildings is used for lighting, 20-30% in hospitals, 15% in factories, 10-15% in schools and 10% in residential buildings (EC, 2011). The heat generated by lighting represents a significant fraction of the cooling load in many internal spaces, and contributes to further consumption of electricity.

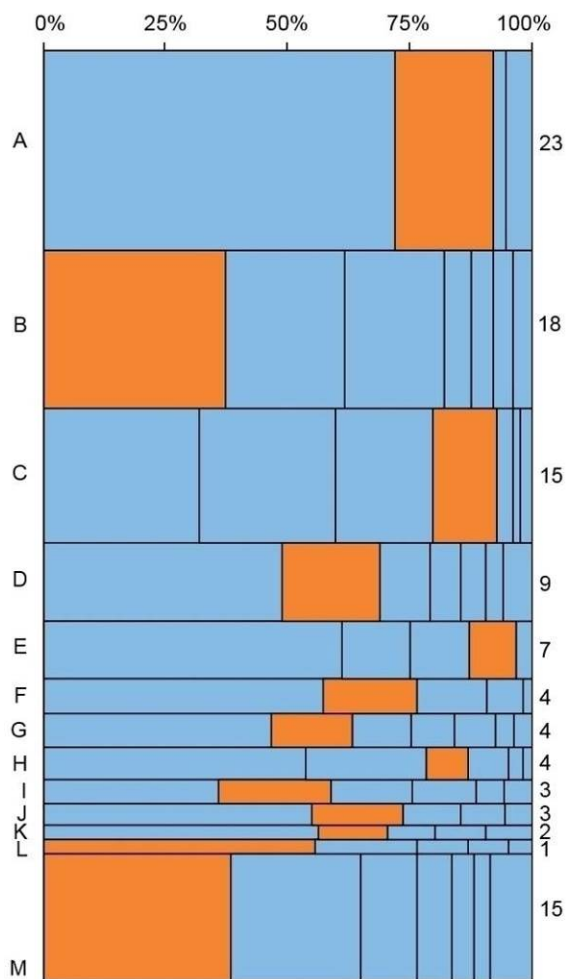


Fig. 2. Emissions by building type and end use (source: Carbon Trust). Figures on the right indicate carbon emissions in MtCO₂; letters on the left indicate building types: A – industrial; B – retail; C – hotels & restaurants; D – commercial offices; E – schools; F – healthcare; G – government estate; H – further & higher education; I – sports; J – heritage & entertainment; K – public offices; L – transport/communications; M – miscellaneous.

Fig. 2 illustrates findings of BRE and Carbon Trust analysis on carbon emissions from different building types and end uses (Carbon Trust, 2011). Carbon emissions from lighting are shown in orange.

Whilst more than 50% of all lamps installed in Europe are still not classed as energy efficient, the potential for improvements and energy savings is significant. Increases in energy price can also act as a driver towards efficiency, and encourage energy-efficient lighting solutions.

The EU is aiming for a 20% cut in Europe's annual primary energy consumption by 2020. In order to increase energy efficiency, the Commission has implemented EU Ecodesign regulations (EC, 2009a; EC, 2009b; EU, 2012a) to gradually remove from the market inefficient products like tungsten lamps, less efficient tungsten halogen, compact fluorescent, and metal halide reflector lamps, all high pressure mercury lamps, less efficient sodium and metal halide lamps, the least efficient LED lamps and magnetic ballasts. The Commission has also implemented Green Public Procurement (GPP) criteria to increase resource and energy efficiency within the public sector (EC, 2012). The GPP criteria also include lighting in buildings covering lamp efficacy and overall power consumption of the whole system. Other Commission measures refer to the use of smart meters that encourage consumers to manage their energy use better, and to the labelling of energy-using products (EU, 2012b).

The Energy Performance of Buildings Directive (EU, 2010) strengthens the requirements for building energy performance by requiring each Member State to establish minimum energy performance requirements for new and existing buildings, and to implement energy certification schemes. The Directive also requires that all new buildings are nearly zero-energy by 2021, with new buildings occupied and owned by public authorities nearly zero-energy by 2019. An approved methodology is employed to determine energy performance which also includes impacts from daylighting and built-in lighting systems.

In the UK, the updated Part L of the Building Regulations (DCLG, 2014) requires that new lighting in office, industrial and storage spaces should have an average luminaire efficacy (the amount of light emitted from the luminaire divided by its circuit wattage) of at least 60 lm/W. Lower efficacy values apply if some types of automatic lighting control are used in some types of space. An alternative, more complex approach uses the Lighting Energy Numeric Indicator (LENI), which is a measure of the energy used for lighting per square metre over the whole year. For lighting in other non-domestic spaces, an average lamp efficacy (the amount of light from the lamps divided by the circuit wattage) of 60 lm/W is required. For display lighting the average lamp efficacy should be at least 22 lm/W. In new dwellings three out of every four light fittings should be low energy, with a lamp efficacy of at least 45 lm/W.

Other energy efficiency initiatives include schemes like BREEAM and the UK Enhanced Capital Allowance (ECA). BREEAM assesses the environmental performance of new and existing buildings, with BREEAM International addressing buildings outside

the UK (BREEAM, 2014). Although it is a voluntary scheme, it is often required by client specifiers. Lighting related credits refer to minimum floor areas being adequately daylight, suitable shading, the right quality of light according to relevant codes and standards, appropriate lighting system zoning and control, separate sub-metering of energy use including lighting, and energy efficient external lighting. The ECA scheme (DECC, 2014) gives tax incentives for companies to install energy-efficient equipment including lighting, by writing off capital costs against Corporation Tax in the first year after installation.

Despite the various measures to increase the efficiency of electric lighting, there is still substantial potential to reduce further the energy consumption for lighting and the associated carbon emissions. Whilst there is a trend in the international community to reduce the electricity consumption for lighting with new technology to below 10 kWh/m² (EC, 2011), the arrival of advanced, optimised daylighting technologies and of state-of-the-art electric lighting technologies using renewable energy sources can help push forward the target by aiming to achieve net zero energy lighting in buildings.

2. Methods to achieve net zero energy lighting

Modern lighting techniques and equipment, and more efficient light sources, provide opportunities for significant reductions in the use of energy, while achieving a greatly enhanced level of illumination and improved visual appeal. Cutting wasted energy for lighting can also reduce overheating, and therefore cut the high cost of air conditioning.

Although lighting products are becoming more efficient, longer occupancy hours and higher light levels have increased the energy used for lighting in buildings. Also, inappropriate control strategies and improper choice of light sources result in energy being wasted.

Key areas for minimising lighting energy consumption in buildings include: minimisation of lighting power density through optimisation of lighting strategies and levels of illuminance; use of highly-efficient lighting technologies; use of appropriate lighting control systems; and maximisation of daylight use. Quality should not be neglected when implementing measures to increase lighting efficiency, and therefore attention should always be given both to the effectiveness and the quantity and quality of lighting.

2.1 Minimising lighting loads

The general illuminance level in a space has a substantial influence on the energy consumption for lighting. Reducing the general illuminance has a direct impact on energy consumption, as the power consumed is roughly proportional to illuminance.

Recent research and consultancy projects carried out by BRE for public and private clients have revealed that illuminance levels in various types of internal space are higher

than those recommended by current relevant standards and guidelines. For example, opportunities to decrease illuminance levels and therefore the lighting energy use have been noted in case of retail buildings. A survey carried out by BRE revealed that the average lighting power density in retail spaces was 36 W/m^2 , compared to $10\text{--}12 \text{ W/m}^2$ in a modern office space with efficient lighting (Ticleanu, Littlefair and Howlett, 2013). Significant energy savings can be achieved by changing the lighting design philosophy so that instead of aiming for an overall level of illuminance the focus falls on the lit effect of the scheme, and hence on delivering lighting to where it is required. Two main techniques are proposed for retail buildings: using the right proportions of task and ambient lighting, so that low illuminance levels are achieved in the bulk of the store, whilst using accent lighting on displays to guide shoppers to key focal areas; and lighting the perimeter of the space to make the whole space look better lit by making the walls brighter. Another possibility is to use daylight to provide some or most of the ambient light levels.

A good practice example is shown in Fig. 3, which illustrates a store that reduced its energy use by 30% and its carbon emissions by 23% by implementing measures that included lower ambient light levels of 300 lux and higher illuminances only on vertical surfaces of the merchandise. In combination with highly-efficient LED lighting, this led to a reduced lighting load of 7 W/m^2 (Ticleanu, Littlefair and Howlett, 2013).



Fig. 3. Lower ambient light levels leading to lower energy consumption (source: Philips Lighting).

These techniques can be employed in a similar manner in other types of space or building, in accordance with standard recommendations. Reducing illuminance levels to the values recommended by relevant standards and codes, and optimising lighting strategies typically lead to significant reduction of lighting power densities (in W/m^2) and normalised lighting power densities (in $\text{W/m}^2.100\text{lux}$), with direct consequences for the energy use for lighting.

2.2 Using highly-efficient lighting technologies

Fluorescent lamps are by far the most popular lamps for lighting non-domestic buildings, although metal halide lamps and even tungsten halogen lamps are widely used in various applications that include accent or display lighting. Metal halide lamps are

also a typical choice for high bay internal spaces. LED technologies are increasingly used following their significant advances in the last years. Various types of luminaires are used for indoor lighting, depending on the type of building.

Given the phase out of inefficient technologies brought about by EU legislation, new alternatives have been developed, with higher luminous efficacy and reduced environmental impacts. New types of lamp include LEDs, highly efficient fluorescent lamps and improved tungsten halogen lamps. Highly efficient compact fluorescent lamps use up to 80% less energy than conventional tungsten lamps, while improved tungsten lamps incorporating halogen technology use 20% to 45% less energy for the same light output than conventional tungsten lamps. The latest developments in compact fluorescent technology include lamps with higher luminous efficacy and lower mercury contents. Recent developments of the metal halide lamp type include ceramic metal halide lamps driven by electronic ballasts that are highly energy efficient. Having the array of wattages expanded to lower values of 20-22W, ceramic metal halide lamps driven by electronic ballasts last up to 20,000 hours and can reach lamp efficacies of up to 104 lm/W.

The most significant technical developments have been made by LED technology, which is increasingly being used for various lighting applications and lasts longer than other light sources. Not only has the variety of LED fittings increased, but the luminous efficacy of LEDs is improving year on year and is now comparable with that of fluorescent lamps. Whilst state-of-the-art white LED lamps have already reached efficacies of 100-150 lm/W, LED lamp efficacy is growing fast and, as shown in Fig. 4, further improvement is expected over the next 5-10 years (IET, 2013). Osram is already claiming a lamp efficacy of 215 lm/W for a T8 replacement LED tube that will be launched in 2015 in both warm white and cool white appearance (Osram, 2014). With a 95% efficiency driver, the claimed system efficacy is 205 lm/W.

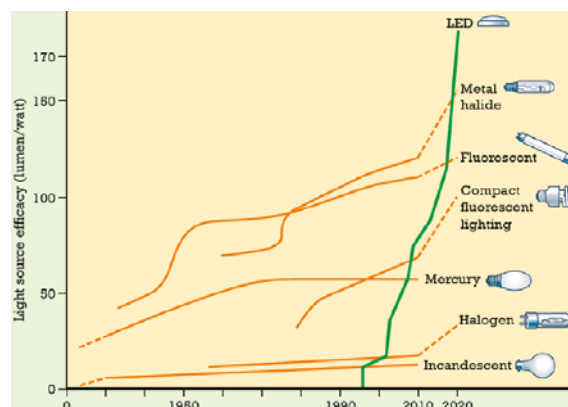


Fig. 4. Accelerated increase in LED lamp efficacy (source: IET).

Other technical developments in lighting include high-efficiency optics for luminaires with increased light output ratio, and optimized lamp-ballast systems consuming less energy and providing longer lamp life.



Fig. 5. LED luminaire rated at 100 lm/W luminaire efficacy (source: Philips Lighting).

In order to reduce the energy consumption for lighting, the overall efficiency of the lighting system should be addressed. There is no sense in placing an efficient lamp in an inefficient luminaire, so the most efficient luminaires should also be used.

2.3 Employing adequate lighting controls

The control strategy for lighting in building is usually set according to the type and complexity of the building and application. It can include various controls ranging from localised manual switching to daylight-based photoelectric dimming and complex management systems.

The choice of lighting controls from simple manual switches and dimming switches to presence detectors and light-level sensors has a large impact on total lighting energy use. However, currently most lighting control systems are under-specified, and electric light is often delivered to spaces where no one is present, or for which there is already adequate daylight. Most spaces are typically lit fully on during occupancy hours and this leads to substantial energy consumption even when sufficient illuminance levels can be provided by incoming daylight. Using photoelectric control linked to daylight sensors in daylighted areas leads to significant energy savings depending on the characteristics of the interior space and the existing lighting systems.

For example, the illuminance measured at various points inside a car showroom display area was in the range 860-5100 lux, which was generated mostly by daylight. However, all electric lighting was maintained fully on continuously during the day and there were neither daylight-linked, nor dimming controls. A multi-gang switch was used to manually control the lighting both in the showroom and other open-space areas. Implementing daylight-based controls of the electric lighting in the car showroom can save 25 MWh of electricity each year, or around 8% of the total electricity used (including all consumers e.g. cooling, small and large power), and 13 tonnes of carbon each year, or around 6% of the total carbon emissions of the showroom.

Research shows that simply providing users with the capacity to control lighting levels in the space they occupy can significantly lower lighting energy use. Effective lighting controls can save 40-60% of the building's lighting energy use (Littlefair, 2014). Energy can be saved after working hours and when work stations are unoccupied, and when daylight is sufficient. Even a short switch off (5 minutes or more) can save energy and money. If dimming is provided, additional savings can be made by dimming lamps early in the maintenance cycle when their output is high. This can typically save around 10% of lighting energy use even in a non-daylit space. With LED lighting the savings can be

higher (15% or more) and the lifetime of the LEDs can be increased due to dimming (Littlefair, 2014).



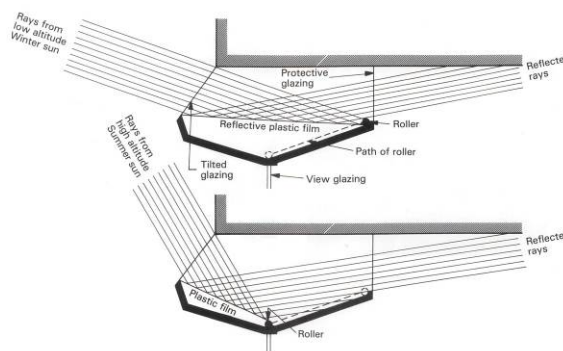
Fig. 6. Examples of user interfaces for lighting controls (source: Helvar).

A wide variety of control types are now available (Fig. 6), with new forms of manual control including wireless and smart phone controls. Occupancy sensing is especially valuable for infrequently used spaces. Photoelectric controls switch or dim the lamps in response to daylight. Time switching is appropriate for buildings with set hours of occupancy. Sophisticated lighting management systems are available which can control the lighting in an entire building, combining all these different control types if required. It is important to take into account the type of space, how it is used and the amount of daylight available.

2.4 Maximising the use of daylight

Daylight has physiological and psychological benefits for building occupants and can improve performance and wellbeing. At the same time it is a freely available light source that can provide high quality lighting to internal spaces at zero costs and with no carbon emissions. However, using daylight successfully requires careful planning and design to avoid associated problems such as glare from direct sunlight or solar heat gains.

Sidelighting can provide a view out that may be appreciated by building occupants and can be integrated in multi-storey buildings. However, the amount of daylight that penetrates into the space depends on the building orientation and the absence of obstructions, and there is a higher risk of glare from direct and reflected sunlight.



Aiming to achieve net zero energy lighting in buildings

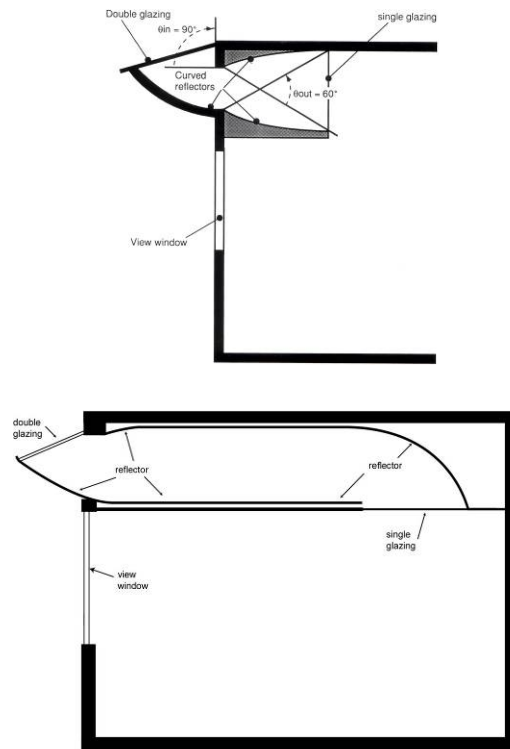


Fig. 7. Sidelighting techniques. From top to bottom: variable-area, light-reflecting assembly; anidolic reflector system; anidolic ceiling arrangement.

The distribution of daylight in the space from sidelighting is uneven, with higher daylight levels in areas nearer to windows and decreasing amounts further away into the space. For this reason, sidelighting is not effective for internal spaces with a deep layout. Advanced sidelighting strategies (Fig. 7) can improve daylight penetration into the depth of the building by redirecting it onto a reflective ceiling. Light shelves, sun-directing glass or anidolic collectors can be installed in the upper part of windows to redirect daylight deeper into the buildings (Littlefair, 1996).

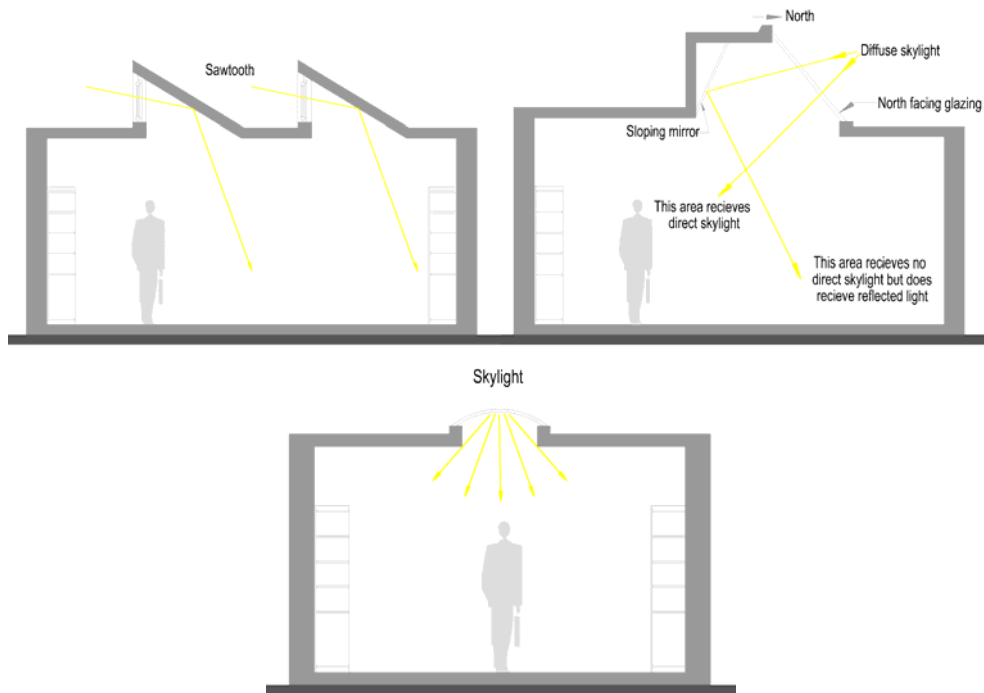


Fig. 8. Toplighting techniques. From top to bottom: northlight; sawtooth; rooflight.

Toplighting strategies (Fig. 8) use openings in the roof to allow daylight penetration into a space: hence their application is limited to single-storey buildings, or to the top floor of multi-storey buildings. However, daylight uniformity is significantly improved throughout the whole space, and there is less impact from obstructions, with maximum available daylight at all times. There is a limited view out, but toplighting strategies in atria and courtyards allow occupants to experience connection to the outside at all times of the day. Because of higher and longer exposure to sunlight, irrespective of orientation, toplighting strategies – other than northlights – typically incur a higher risk of overheating than sidelighting. Soft-coat, low-emissivity glazing with low solar transmittance (g-value) but higher daylight transmittance should be considered for such strategies.

Typically roof apertures over 8–10% of the whole roof area can be sufficient to keep electric lighting turned off during a significant part of the daytime. Substantial savings can be made by capitalising on the availability of natural light, while creating a pleasant, airy atmosphere that is favoured by occupants.

Optical systems are able to redirect or harvest daylight by means of tubular light-guiding systems, fibre optics, or arrays of mirrors and lenses. Daylight-guiding systems (Fig. 9) can lead daylight collected at roof level into internal spaces via highly reflective, mirrored tubes, and are more effective under clear sky conditions, although some of them can deal quite effectively with diffuse skylight. This helps reduce the need for electric lighting during the day. Fibre optic systems rely mainly on direct sunlight, as they are typically integrated within complex arrangements using sun-tracking collectors.

Sophisticated arrangements of mirrors and lenses can be used to direct daylight (mainly direct sunlight) into specific internal areas of interest.



Fig. 9. Daylight guidance systems using light-pipes (source: Monodraught).

Using daylight as a primary light source can potentially save energy by reducing the need for electric lighting. However, over-glazing can lead to high solar heat gains. The aim should be to provide generous levels of daylight with reasonably low associated solar heat gains to avoid using extra energy for cooling. Daylight into internal spaces needs to be controlled, and lighting controls are required to adjust the electric lighting to match daylight variability. Significant energy savings can be achieved by correct zoning of the electric lighting that establishes the groups of luminaires that should be controlled simultaneously, based on different factors that include daylight availability. The electric lighting system needs to be controlled separately in the daylit and non-daylit areas to maximise energy savings while providing the required light levels. Typically, luminaires should be grouped together in each zone that receives a similar amount of daylight.

2.5 Using renewable energy sources

Recent developments in renewable energy technologies, such as photovoltaic panels and wind turbines, have made it realistic to conceive nearly-zero or even zero energy lighting systems, particularly if highly-efficient lighting technologies and adequate controls are used. However, solar or wind powered lighting systems are still not commonly used in buildings due to a number of technical and financial challenges. Although government schemes support the uptake of such technologies by practising attractive feed-in tariffs, payback is typically long (particularly for smaller systems) and electricity generation is strongly affected by climatic conditions. Additional equipment is also required, such as inverters or batteries, and this requires supplementary storage and power optimisation.

Nevertheless, by nature, LED lighting systems are most commonly DC devices, operating from a low voltage of direct current. This makes it easier to integrate them with renewable energy based technologies, whilst achieving a higher system efficiency that allows for net zero energy.

3. Case studies

A number of projects have already been completed or are being assessed in order to reduce the energy consumption for lighting whilst improving the quality of the internal luminous environment.

3.1 Clothes store

Illustrated in Fig. 10, the LED-only scheme delivers an average light level of around 500 lux on the walkways and a light level on specific focal areas of the merchandise of around 900-1000 lux. By using LEDs rated 16W and 50 lm/W, which deliver warm white light of 3000K colour temperature and colour rendering index CRI of 90, the installed lighting load is 17 W/m² (Ticleanu, Littlefair and Howlett, 2013).



Fig. 10. Fully LED-lit clothes store (source: Reggiani).

3.2 Superstore

The use of pre-wired, daylight-based, dimmable $2 \times 73\text{W}$ T5 Eco fluorescent fittings, with adjustable reflector and louvre for precise direction to the point of sale, as shown in Fig. 11, provided a 28% energy saving, 30% reduction in the number of lamps required, and 25% reduction in installation time compared with the previous lighting scheme (Ticleanu, Littlefair and Howlett, 2013).



Fig. 11. Daylight-based, dimmable T5 fluorescent fittings with adjustable reflectors and louvres producing the right light output at the level of the merchandise (source: Whitecroft Lighting).

3.3 Supermarket

The sales area is lit by a combination of ceiling-recessed square modules and round spotlights using LEDs with a colour temperature of 4000K, while chiller cabinets are lit by 4200K CRI 80 LED tubes concealed from the shoppers' view and aimed at the merchandise (Fig. 12). This delivered a well-lit solution at less than 9 W/m² and achieved an energy reduction of approximately 40% (Ticleanu, Littlefair and Howlett, 2013).



Fig. 12. LEDs used for general and display lighting.

3.4 Fashion store

It is proposed to upgrade the lighting in the 2-storey store shown in Fig. 13 from conventional fluorescent and metal halide technologies to warm white LED lighting. The design philosophy is tackled to provide the right amount of light to each type of area (e.g. 300 lux ambient illuminance and a minimum of 500 lux accent illuminance in sales areas) and to minimise the number of luminaires by choosing optimum positions and tilt angles. In so doing, 51% electricity savings and carbon reduction would be achieved, and lighting power density would decrease by 46% to 18 W/m² in sales areas and by 70% to 6 W/m² in fitting rooms. Around 83% of the energy used by the new LED lighting system could be supplied by 100 monocrystalline PV panels rated at 320W_p and 19.6% efficiency covering 163m² of the total roof area available (Topriska, 2012).



Fig. 13. Fashion store to incorporate LED lighting supplied with electricity from roof-mounted PV panels.

3.5 Office building

The office building illustrated in Fig. 14 has been assessed in order to increase its energy efficiency and substantially reduce its carbon footprint. The current lighting system consists of fluorescent fittings using electromagnetic ballasts and is controlled via wall-mounted switches in offices and presence detection in circulation and other communal areas. No daylight-linked controls are used. The total lighting load currently installed is 14.3kW, with an estimated energy consumption of 36,190 kWh/year, whilst the average lighting power density is around 14.7 W/m² throughout the building.



Fig. 14. Glazed façade office building proposed to be lit by a net zero energy lighting system.

The aim is to develop a net zero energy lighting system using highly-efficient LED lighting, adequate lighting controls and roof-mounted PV panels. A change in layout is also considered, as the current cellular offices will be converted into larger open-plan office areas. By using the latest LED lighting systems, the total lighting energy consumption can be reduced by 54% to 16,560 kWh/year, at an estimated normalised lighting power density of 1.5 W/m².100lux on average in office areas and 2.5 W/m².100lux on average in other areas.

Large glazed areas are present on west, south and east façades. By adding daylight-based dimming controls to reduce the light output of electric lighting when sufficient daylight is available to achieve the maintained illuminances during work hours (9.00 to 17.30), the energy consumption for lighting can be further reduced by an additional 29% to 5,740 kWh/year.

Net zero energy lighting can be further achieved by adding an array of grid-connected monocrystalline PV panels rated at 235W_p and 14% efficiency, with a total estimated electricity production of 5,800 kWh/year (Park, 2013). The PV panes would require 50m² of roof area for the installation, and a simple payback period would be 10.5 years.

4. Conclusions

Lighting is a rapidly increasing source of energy demand and takes a significant part of the electricity consumption in buildings. More than half of all lamp technologies installed in Europe are still not classed as energy efficient, and continuous increases in energy prices are expected for the coming years. The EU is aiming for a 20% cut in Europe's annual primary energy consumption by 2020, and the Commission has implemented a number of measures to increase energy efficiency. These are

supplemented by various schemes, standards and codes to reduce carbon footprint and energy use.

In this context, where various drivers towards energy efficiency exist, the potential for improvements and energy savings in lighting of buildings is substantial.

Although there is a trend in the international community to reduce the electricity consumption for lighting with new technology to below 10 kWh/m², recently developed daylighting technologies and state-of-the-art electric lighting technologies using renewable energy sources can give the potential for net zero energy lighting in buildings. This can be possible if such technologies are integrated into optimised design strategies such as minimising lighting power density through optimising lighting strategies and levels of illuminance; use of highly-efficient lighting technologies; use of appropriate lighting control systems; and maximising daylight use.

REFERENCES

BREEAM, 2014, Building Research Establishment Environmental Assessment Method. Available online at: <http://www.breeam.org/>

Carbon Trust, 2011, *Lighting: Bright ideas for efficient illumination*. London: The Carbon Trust.

DCLG, 2014, Approved Document L - Conservation of fuel and power, UK Building Regulations. Department for Communities and Local Government. Available online at: <http://www.planningportal.gov.uk/buildingregulations/approveddocuments/partl/approved>

DECC, 2014, Enhanced Capital Allowance Scheme. Available online at: <https://etl.decc.gov.uk>

EC, 2009a, Commission Regulation (EC) No 244/2009 of 18 March 2009 implementing Directive 2005/32/EC of the European Parliament and of the Council with regard to ecodesign requirements for non-directional household lamps. *Official Journal of the European Union*, L76:3-16.

EC, 2009b, Commission Regulation (EC) No 245/2009 of 18 March 2009 implementing Directive 2005/32/EC of the European Parliament and of the Council with regard to ecodesign requirements for fluorescent lamps without integrated ballast, for high intensity discharge lamps, and for ballasts and luminaires able to operate such lamps, and repealing Directive 2000/55/EC of the European Parliament and of the Council. *Official Journal of the European Union*, L76:17-44.

EC, 2011, Green Public Procurement Indoor Lighting Technical Background Report. Brussels: European Commission.

EC, 2012, Green Public Procurement Criteria for Indoor Lighting. Available online at: http://ec.europa.eu/environment/gpp/pdf/criteria/indoor_lighting.pdf

EU, 2010, Directive 2010/31/EU of the European Parliament and of the Council of 19 May 2010 on the energy performance of buildings. *Official Journal of the European Union*, L153:13-35.

EU, 2012a, Commission Regulation (EU) No 1194/2012 of 12 December 2012 implementing Directive 2009/125/EC of the European Parliament and of the Council with regard to ecodesign requirements for directional lamps, light emitting diode lamps and related equipment. *Official Journal of the European Union*, L342:1-22.

EU, 2012b, Commission Regulation (EU) No 874/2012 of 12 July 2012 supplementing Directive 2010/30/EU of the European Parliament and of the Council with regard to energy labelling of electrical lamps and luminaires. *Official Journal of the European Union*, L258:1-20.

IET, 2013, *Code of Practice for the Application of LED Lighting Systems*. London: The Institution of Engineering and Technology.

Halonen, L., E. Tetri and P. Bhusal (Eds), 2010, *Guidebook on Energy Efficient Electric Lighting for Buildings*. Espoo: Aalto University.

Littlefair, P., 1996, *Designing with innovative daylighting*. Bracknell: IHS BRE Press.

Littlefair, P., 2014, *Selecting lighting controls*. BRE Digest 498. Bracknell: IHS BRE Press.

Osram, 2014, Osram constructs the world's most efficient LED lamp. Press Release, 28 March 2014. Available online at: http://www.osram.com/osram_com/press/press-releases/_trade_press/2014/osram-constructs-the-worlds-most-efficient-led-lamp/index.jsp

Park, S., 2013, *Investigation of LED alternatives in an office building*. Dissertation submitted for the MSc in Building Services Engineering with Sustainable Energy, Brunel University, September 2013.

Ticleanu, C., P. Littlefair and G. Howlett, 2013, *The essential guide to retail lighting: Achieving effective and energy-efficient lighting*. Bracknell: IHS BRE Press.

Topriska, E., 2012, *Investigation of LED alternatives in retail lighting*. Dissertation submitted for the MSc in Building Services Engineering with Sustainable Energy, Brunel University, September 2012.

Fluid flow and heat transfer simulations for a box double-skin façade in Brasov, Romania*

Gabriel NASTASE¹, Robert GAVRILIUC², Alexandru SERBAN¹,
Ioan BOIAN¹,

¹Civil Engineering Faculty, Transylvania University, str. Turnului nr. 5, Brasov, Romania

²Building Services Faculty, Technical University of Civil Engineering, Bucharest, Romania

trznasa@gmail.com

Abstract: *CFD – Computational Fluid Dynamics Method is the modern scientific method, for prediction of fluid flow, heat and mass transfer and other related phenomena, by numerical solving the mathematical equations governing those phenomena, such as the law of mass, momentum and energy conservation. CFD method is very useful when it comes to conceptual studies for new model of buildings, detailed development of certain parts of a building, useful for solving problems that appear during construction or exploitation of a particular system that is part of a building etc. CFD analysis complements the numerical modeling and experimental modeling, reducing the effort and cost for experiment and data acquisition systems. This paper presents a few results for heat transfer and fluid flow, made on a box double-skin façade, in Brasov, Romania, as a part of a PhD thesis.*

Keywords: *heat transfer, fluid flow, box double-skin façade, convection, heating, cooling, energy.*

1. Introduction

This article presents a few results for heat transfer and fluid flow obtained from a box window double-skin façade (DSF) model, made after a real model developed in situ, on the ground floor of the Civil Engineering Faculty in Brasov, part of Transylvania University from Brasov, on the south façade of the building. The real model serve as a basis for all the measurements made with the goal of modeling and then validate processes within the system and ultimately determine the impact of such façade on a building placed in Brasov, Romania. The experimental model is part of a PhD thesis and consists of a so-called "box window"-type double-skin façade connected with the experimental room by an indoor air curtain; it is manually controlled, having a forced air circulation in summer. The venetian blinds shading system is placed inside the cavity, in the median area (see Figure 1).

* Lucrare inclusă în programul conferinței RCEPB 2014

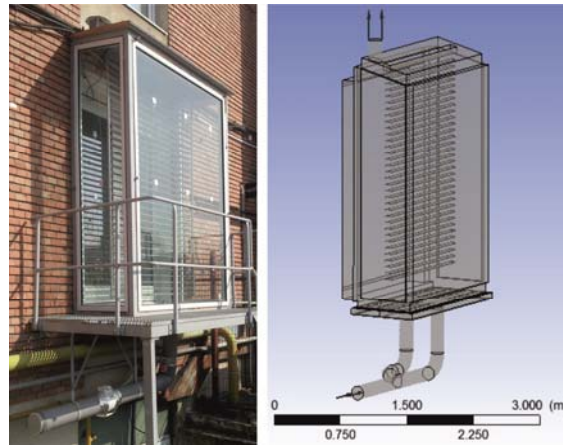


Fig. 1. Box double-skin façade experimental model (left). Simulation model in 3D (right)

The energy performance of a double-skin façade in general is influenced by the convective heat transfer coefficients, inside the cavity, which may vary depending on the strategy chosen for the ventilation (natural or mechanic) and depending also whether or not the solar radiation is present. The article is mainly focused on fluid flow and heat transfer, considering forced convection inside the cavity, during the summer, when venting superheated air is required, in order to maintain a good climate in the experimental room. The study highlights also the influence of the angle of the slats from the shading system on air flow, inside the cavity, by constructing 5 distinct cases: without the shading device and with shading device having the slats positioned at 0° , 25° , 45° and 65° . All the simulations are made in ANSYS 15 – Fluid Flow (CFX) Module and Steady State Heat Transfer Module.

2. General characteristics of experimental model

The experimental model to be presented in this study was built on the ground floor of the Civil Engineering Faculty in Brasov, on the south facade of the building. The model has an outer envelope consisting of a 10 mm secure glass in direct contact with exterior, placed at a distance of 1 m from an insulating double-glazed window 4-16-4 mm, which is the inner envelope. The outside air flows between the two glazing: during the winter the free convection transfers the solar heat gain to the interior space and during the summer through forced convection the superheated air is evacuated. Because of the greenhouse effect inside the cavity mechanical ventilation was required in order to extract the solar heat and evaluate this hot air flow that can be used for other purposes. The mechanical ventilation is provided by a duct fan VENTS TT150, common to the two input fresh air circuits, in the cavity, one in front of the shading system and the other behind it, as can be seen in Figures 1 and 2.

Box window double-skin façade and experimental room dimensions are presented in Table 1:

Table 1.

Box window double-skin façade and experimental room dimensions

Area	Length [mm]	Width [mm]	Height [mm]
Box DSF	1500	1000	2500
Experimental room	3600	2000	3000

To control daylight and solar radiation that enters the experimental room and improve working conditions for occupants, inside the cavity was installed in the middle area, a venetian horizontal blinds system, having shaped sides roll, made of special aluminum alloy enamel, 80 mm wide, UV resistant and weatherproof. The system is operated by means of a 220/240 V electric motor, 50 Hz, placed on the top of the shutter. The system has fully retractable blinds allowing maximum natural light in low light conditions and easy access for cleaning windows inside facade.

3. Fluid flow simulations

The fluid flow simulations presented in this paper concern only forced air circulation in the façade cavity, during the summer season. The purpose of fluid flow simulations is to determinate the medium cavity air velocity. As main input condition for simulations was used the measured air velocity in supply duct of the façade mechanical ventilation system, which was 4,5 m/s.

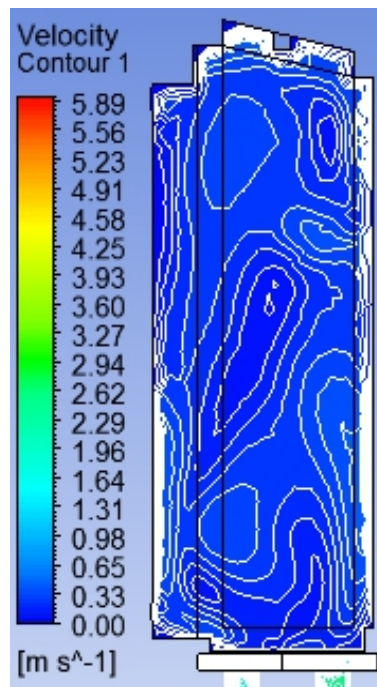


Fig. 2. Velocity contours inside cavity in case of shading system fully rose

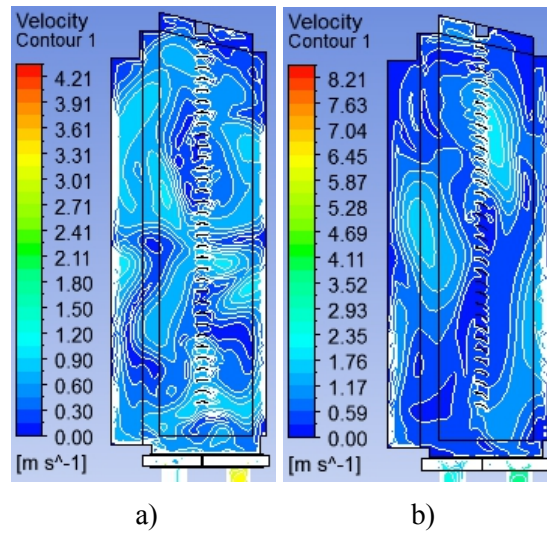


Fig. 3. Velocity contours inside cavity in case of shading slats positioned at 0° (a) and at 25° (b)

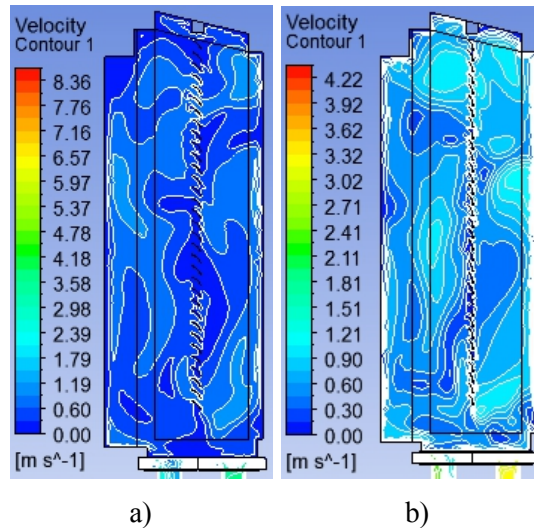


Fig. 4. Velocity contours inside cavity in case of shading slats positioned at 45° (a) and at 65° (b)

Figures above show a mid-section plane with velocity contours, first in case of shading system fully raised (Figure 2) and then with shading slats positioned at 4 different angles 0°, 25°, 45° and 65° (Figures 3 and 4). If it's taken into consideration only the wide cavity area the medium velocities are those presented in table 2.

Table 2.

Medium velocities obtained					
Case	I	0°	25°	45°	65°
Velocity [m/s]	0,26	0,52	0,71	0,54	0,62

As expected the smallest velocity is in the first case and all others are higher but all of them are less than 1 m/s.

More simulation work has still to be done in order to check the validity of models with respect of achieving more than 100 iterations and other operating conditions, i.e.

different outside/inside air temperatures as well as different values for solar radiation, this work being in progress.

4. Heat transfer simulations

The heat transfer simulations presented in this paper have been performed in steady state conditions, having as input conditions extreme climatic data for winter and summer. Boundary conditions for the two cases are presented below, in Figures 5 and 6.

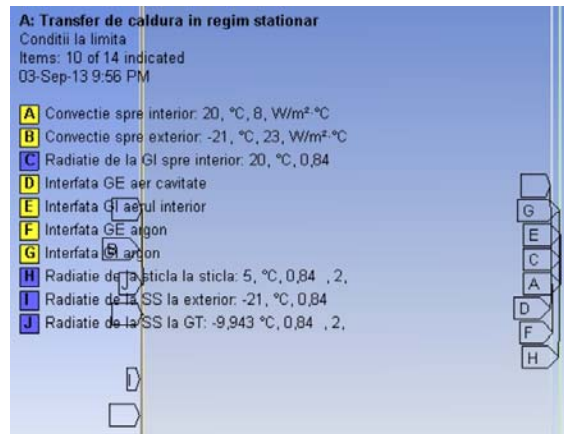


Fig. 5. Boundary conditions for the winter season

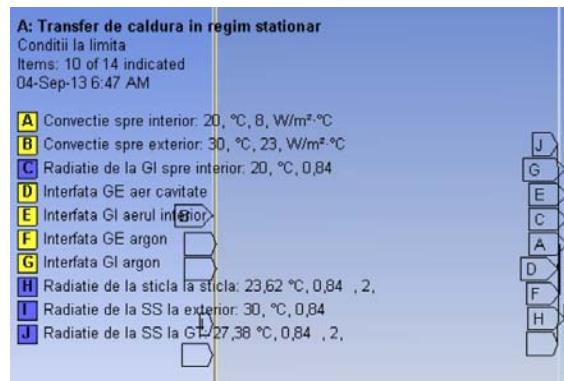


Fig. 6. Boundary conditions for the summer season

The results for heat transfer simulations are presented as temperatures and total heat fluxes for both cases winter and summer.

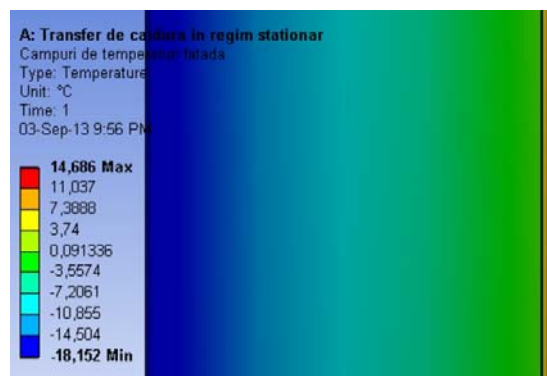


Fig. 7. Temperature distribution for winter season

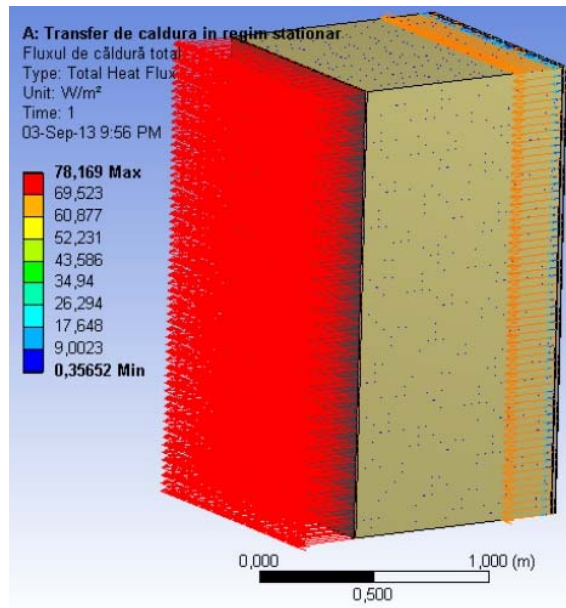


Fig. 8. Total heat flux for winter season

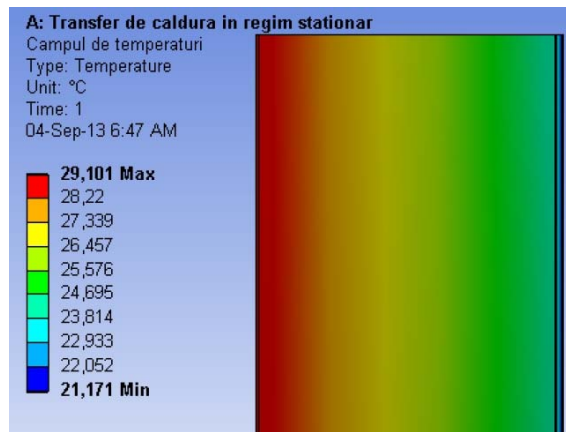


Fig. 9. Temperature distribution for summer season

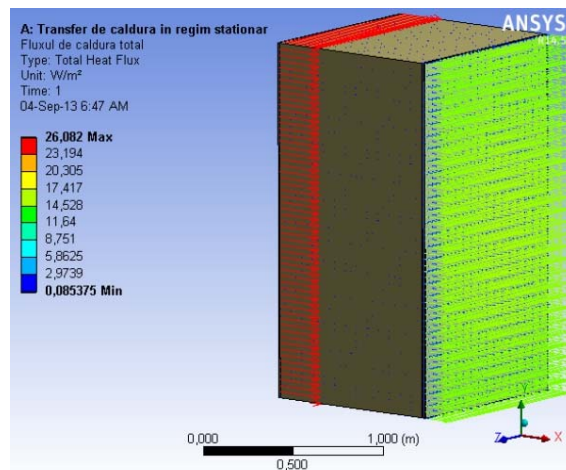


Fig. 10. Total heat flux for summer season

If it is to compare these results for heat transfer with those for a double pane window system (4 mm glass – 16 mm argon – 4 mm glass) keeping the same other conditions the results would be like those in Figures 11 and 12.

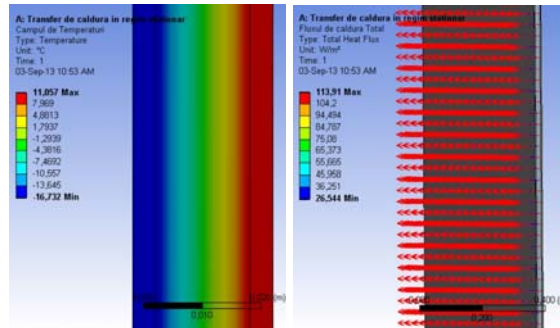


Fig. 11. Heat transfer simulation results for temperatures (left) and total heat flux (right), winter season in case of double pane window

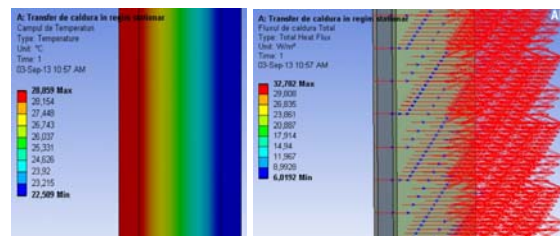


Fig. 12. Heat transfer simulation results for temperatures (left) and total heat flux (right), summer season in case of double pane window

If all figures above are analyzed we can say that in case of winter season the surface temperature inside experimental room is with 3,6°C higher in case of double-skin façade, comparing to the double pane window, this leading to a lower heat flux in case of double-skin façade. In this case the decrease in heat flux is about 31%.

In case of summer season the surface temperature inside experimental room is with 0,24°C higher in case if double pane window, comparing to the double-skin façade. In this case the decrease in heat flux is about 19%.

5. Conclusions

The complexity of the double skin façade considering elements which may vary from case to case depending on the location of the building, the local climate conditions, etc., the problem that arises in heat transfer is to evaluate the heat flux through the entire system, according to its geometric configuration, and the way the air flows through the cavity for different elements bounding the cavity i.e. their thermophysical properties.

These simulations are intended to be a starting point for modelling the same phenomenon with the entire double skin façade system, in transient condition and considering solar radiation. Such simulations should be run on a workstation in order to achieve over 600 iterations in a shorter period of time with more accurate results.

REFERENCES

- Năstase G., Gavriiuc R., Șerban A., – Box window double-skin faade. Experimental model in Brasov, Romania, *Advances in Environment Technologies, Agriculture, Food and Animal Science ISSN 2227-4359*, 2013;
- Năstase G., Șerban A. – Box window double-skin faade. Heat transfer validation through inner envelope. Conferina CIBV 2013, ISSN 2065-2127, Editura Universitații Transilvania din Brașov, 2013;
- SR EN ISO 12631:2013 – Performana termica a faadelor cortina. Calculul coeficientului de transfer termic, *Asociaia de Standardizare din Romania - ASRO*, martie 2013;
- Năstase G., Gavriiuc R., Șerban A., Horneț M. – Office buildings with double-skin facade in Europe, Conferina CIBV 2012, ISSN 2285-7656, ISSN-L 2248-7648, Editura Universitații Transilvania din Brașov, 2012;
- Năstase G., Gavriiuc R. – “Transferul de caldura printr-un geam dublu tip termopan”, Conferina Naionala de Instalații, Sinaia 2012;
- Adrian Bejan – “Convection Heat Transfer. Third edition”, *Editura John Wiley & Sons, Inc.*, 2004;
- Florea Chiriac, Aureliu Leca, M. Pop, Adrian Badea, L. Luca, Nicolae Antonescu, D. Peretz - Procese de transfer de caldura și de masa în instalațiile industriale, *Editura Tehnica*, 1982;
- E. Sandu, A.M. Bianchi, C. Mihaila, V. Caluianu, N. Antonescu – Termotehnica și aparate termice, *Editura Didactica și Pedagogica*, 1982;
- Ansyes Design Modeler Training Manual, version 12, 1st Edition, *ANSYS INC*, 2009;
- Ansyes Design Modeler Workshop Supplement, version 12, 1st Edition, *ANSYS INC*, 2009.
- ANSYS SIMULATION SOFTWARE, versiunea 14.5 – Steady State Thermal;
- Ansyes Design Modeler Training Manual, version 12, 1st Edition, *ANSYS INC*, 2009;
- Ansyes Design Modeler Workshop Supplement, version 12, 1st Edition, *ANSYS INC*, 2009;
- Ansyes Workbench – Mechanical Intro (Beta) Training Manual, version 12, 1st Edition, *ANSYS INC*, 2009;
- Ansyes Workbench – Mechanical Intro (Beta) Workshop Supplement, version 12, 1st Edition, *ANSYS INC*, 2009;
- Ansyes Meshing Application Introduction Training Manual, version 12, 1st Edition, *ANSYS INC*, 2009;
- Kent L. Lawrence – ANSYS Workbench Tutorial, ANSYS Release 10, ISBN: 1-58503-269-7, SDC Publications;
- ANSYS Thermal Analysis Guide, Ansyes release 10, *ANSYS INC*, august 2005;
- ANSYS 14.5 HELP, *ANSYS INC*, 2013

Ecoshopping: energy efficient & cost competitive retrofitting solutions for retail buildings*

Dr A. J. Lewry, CEng, MIMMM, CEnv, SOE; and Dr E. Suttie, CEng, MIMMM

Sustainable Energy Team, Building Research Establishment Ltd., UK. Lewrya@bre.co.uk

Abstract: *“EcoShopping” project aims to build a holistic retrofitting solution for commercial buildings to reduce primary energy consumption down to less than 80kWh/m² per year and increase the proportion of Renewable Energy systems (RES) to more than 50% using state of the art solutions.*

The project intends to use and integrate available products and technologies along with a network of low-cost equipment to accurately monitor the environmental and occupancy parameters to have better control of the Building Management System and full exploitation of the Building Thermal Mass, which serves as a “Thermal Battery” and stores the RES directly without using battery, tank or other expensive storage material and simplifying the system structure.

Keywords: ECOSHOPPING: energy efficient, retrofitting, Retail sector, shopping buildings.

The “EcoShopping” project (<http://ecoshopping-project.eu/>) aims to produce a systematic methodology and cost effective solutions for retrofitting commercial buildings. By improving the insulation and lighting system; integrating additional RES based HVAC systems; exploiting the building as thermal storage (“mass”); developing an intelligent automation control unit; and improving maintenance and commissioning technologies; the energy efficiency of the commercial building is expected to have an overall enhancement of about 58%.

The “EcoShopping” platform will integrate other existing HVAC systems, such as heating, ventilation, air conditioning, etc. and will interoperate with other ICT- based subsystems (e.g. for security, protection, gas-detection, safety and comfort). The control and management of automation systems will be based on advanced algorithms where the platform will be capable of learning from previous operations and situations; by means of a semi-automatic process of retraining from Internet-based repositories, which allows configuration, personalization and dynamic adaptation to the characteristics of the building and the weather.

The project cost is 4.10 million €; starting in September 2013 with a duration of 4 years.

* Lucrare inclusă în programul conferinței RCEPB 2014

The phasing of the project is shown in figure 1 and this paper will present the initial results of Work Package 2.

The overall objectives of the project are:

- To reduce primary energy consumption down to less than 80kWh/m² per year and increase the proportion of RES (Renewable Energy Sources) to more than 50%.
- To investigate a retrofitting solution with innovative thermal insulation solutions and Day lighting technologies.
- To develop and install a RES direct powered DC variable speed heat pump and increase the Building Thermal Mass with a view to reducing the energy consumption.
- To integrate the Intelligent Automation Unit (IAU) concept with a Mobile Robot.
- To develop a solution for automatically identifying and predicting failures; and inefficiencies in HVAC system performance.
- To carry out a continuous assessment through the entire project.

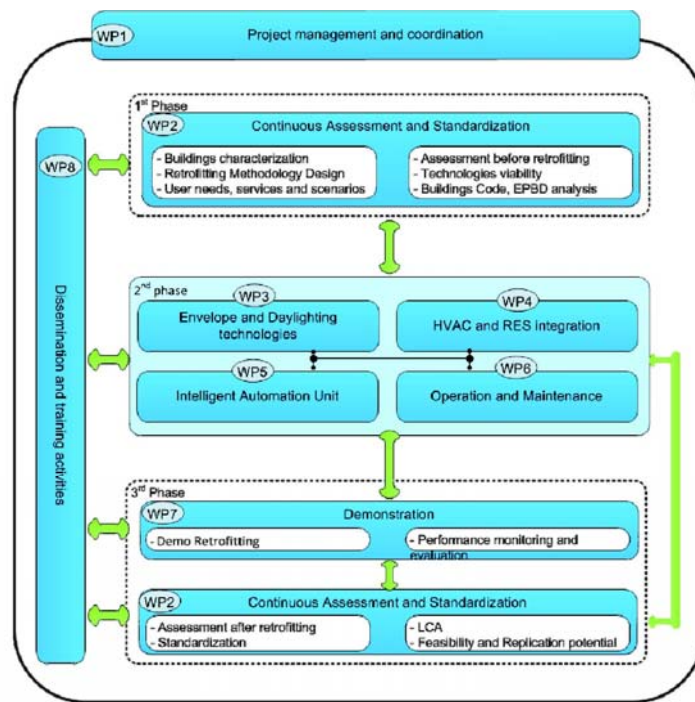


Fig.1. Ecoshopping work packages and phasing

The case study

IKVA Shopping Centre is a retail mall in the city of Sopron in Győr-Moson-Sopron County of Hungary. It was built in 1979 and has approximately 3,700 square meters leasable area. It is located within the city centre, in the outskirts of the Castle district. This part of the city has a historic atmosphere and a strong touristic appeal.

The IKVA was built within the framework of a large scale urban development plan together with the Fenyő Shopping Centre next to it.

IKVA is a freestanding building. It is linked with an open passageway to the Fenyő Shopping Centre. Access from the parking lot and also from street level is ensured with a pedestrian ramp and staircases. From the bridge there is a direct access to the retail space on the ground floor. There is an open hallway around ground level store floor. Next to the building there is a city block which consists of mid-rise residential buildings with additional retail and service functions. A wide pedestrian passageway points directly to the Shopping Centre from the south.

IKVA due its larger department store size and its downtown location makes it ideally suited to meet the demands of larger retailers. Main part of the retail area consists of large open spaces with only a few pillars, which allows various uses.

Operation time: 0800-1900, 220 working days plus 0800-1300, 52 weeks*1 day which gives 2680 operational hours/year total.

The building has 2 main sections: common area, which consists of 2 storeys plus an open parking lot on ground level, and service/office area with 3 storeys and a basement. Geometry of the building follows functional separation recognizably. Service and visitor access is well-separated. The building has a reinforced skeleton structure, 25 cm thick reinforced concrete envelope and a flat roof with bituminous waterproofing and polystyrene insulation. There is no insulation on the external walls which results together with the large aluminium frame single-glazed portals in common areas a high overall heat transfer coefficient. Maximum height is 14.90 m.

Pre-retrofit building assessment

The survey has identified three HVAC systems:

- Heating system: 3 Viessmann Vitodens condensing boilers.
- Cooling system: local split air conditioners.
- DHW: only some local, electrical water heater.
- Ventilation: 2 AHUs, but these are operated only in summer, 2 hours per day. The heating pipe for heat exchanger of AHU was cut off so the AHU has no heating capability.
- Lighting system: Mainly fluorescent lighting with some tungsten. Many of the fittings are inoperative.
- There is only the basic level of control (on/off for time control plus thermostats) with maintenance staff carrying out this function.

Energy usage and calculations

Natural gas and electricity consumption was collected for the last 3 years:

- Natural gas: ~ 30.000 m³/annum;
- Electricity: ~124.000 kWh/annum.

The first step was to carry out a static calculation in accordance with Hungarian legislation (Energy Performance of Buildings: 7/2006. (V.24.) TNM directive) which is harmonised with the EPBD (Energy Performance Building Directive, 2002).

The calculation expresses the primary energy consumption of the heating, domestic hot water, cooling, ventilation and lighting systems.

The primary energy factors in Hungary are: $e=2.5$ for electricity, $e=1.0$ for natural gas.

Static calculation

Primary energy consumption per systems:

- Heating: 93.71 kWh/m²/annum;
- Cooling: 11.49 kWh/m²/annum;
- Lighting: 62.5 kWh/m²/annum.

The Primary energy consumption was calculated as **167.7 kWh/m²/annum which gave an E rating on the Energy Performance Certification (EPC).**

When comparing actual to model consumption the following observations were made:

- Calculated natural gas consumption is 31.400 m³/annum; which is close to the real consumption (30.000 m³/annum).
- Calculated electricity consumption for lighting and HVAC is 96.000 kWh/annum. The real energy consumption much higher (124.000 kWh/annum), this is due to the additional usage of office equipment, IT technology, etc.

Target value for the IKVA case study is 80 kWh/m²/annum; which is just over a 50% reduction in energy usage and would give an EPC rating of an “A”. This is an ambitious target but one that is thought to be achievable.

The Ecoshopping consortium

The consortium consists of:

- EnergoSys Inc (Hungary);
- Fraunhofer Institute for Digital Media Technology IDMT (Germany);
- Solintel M&P (Spain);
- Austrian Institute of Technology (AIT);
- Intelligent Sensing Anywhere (ISA - Portugal);
- Novamina (Croatia);
- IZNAB Sp. z o.o.(Poland);
- GeoClimaDesign (GCD - Germany);
- National Research Council (CNR - Italy);
- Symelec (Spain);

- Building Research Establishment (BRE – UK);
- R.E.D. s.r.l. (Italy);
- Yaşar University (Turkey);
- National Taiwan University of Science and Technology (NTUST);
- LaGross Ltd.(Hungary);
- Ancodarq (Spain).

This consortium gives the project a wide range of expertise in terms of the construction process and technology areas.

The project is Co-funded by the European Commission within the 7th Framework Programme but has its own website and marketing with the following logo:



Work Package 2: Continuous assessment and standardisation

The first deliverable is an assessment of national building codes, EPBD implementation and standards identified (Lewry, A. J. and Garrido, M. D. C., 2013). This report compares and analyses the national building codes for non-domestic buildings from European countries (Austria, Croatia, Germany, Hungary, Italy, Poland, Portugal, Spain and the UK) within the project. It concludes that building codes lay down minimum levels of performance for building fabric elements and building services; but not renewables. The energy performance of non-domestic building as designed is calculated holistically by the use of approved software and this should be used to for quantifying options. The codes do not attempt to prompt best practice. In the context of this project this points to the best fabric u-values identified should be used as the backstop (minimum) performance levels and the static calculation method being used to assess the design options; the reasoning being that these are the most appropriate in terms of local construction methods and climate.

Best Practice for Technology areas was identified as lying within the EU Green Public Procurement (GPP) criteria and the UK's Enhanced Capital Allowance (ECA) scheme and it's Energy Technology List (ETL).

It is proposed that heat pumps are part of the refurbishment and their performance should match or exceed those laid down in the criteria of the GPP or ETL. This lays down best practice performance for Heat pumps, in terms of a Coefficient Of Performance (COP) in Heating mode and an Energy Efficiency Ratio (EER) in Cooling mode for:

- Air source: gas engine driven split and multi-split (including variable refrigerant flow);

- Air Source: Packaged Heat Pumps;
- Air Source: Split and Multi-Split (including Variable Refrigerant Flow) Heat Pumps;
- Air Source: Air to Water Heat Pumps;
- Ground Source: Brine to Water Heat Pumps;
- Water Source: Split and Multi-Split (including Variable Refrigerant Flow) Heat Pumps;

An example of the criteria is shown in Table 1.

Table 1:

UK ETL performance criteria for Water source: split and multi-split (including variable refrigerant flow) Heat Pumps.

Product Category	Heating mode (COP)	Cooling mode (EER)
Water source: single split (non-VRF) heat pumps	>3.70	>3.30
Water source: dual split (non-VRF) heat pumps	>3.70	>3.30
Water source: multi-split (non-VRF) heat pumps	>3.70	>3.30
Water source: split or multi-split variable refrigerant flow (VRF) heat pumps	≥4.10	>3.50

The ETL also contains criteria for Heat pump dehumidifiers; Heat pump driven air curtains and CO₂ Heat Pumps for Domestic Hot Water Heating.

Building Controls

The report and the documents it references (Lewry, A. J., 2014) recognise that the control of energy in non-domestic buildings is generally poor, despite the availability of a range of tried and tested systems incorporating both mature and innovative technologies. The installation of HVAC zone controls, optimising controllers (for Wet Heating Systems) and lighting controls is encouraged by the building codes, but their specifications are basic. As controls are one of the most effective solutions in realising energy savings, they should always be part of a refurbishment. The European standard on the Energy performance of buildings — Impact of Building Automation, Controls and Building Management (BS EN 15232, BSI, 2012), should be used as the methodology for estimating their effect.

EN 15232 has a series of classes describing the energy performance – see Figure 2.

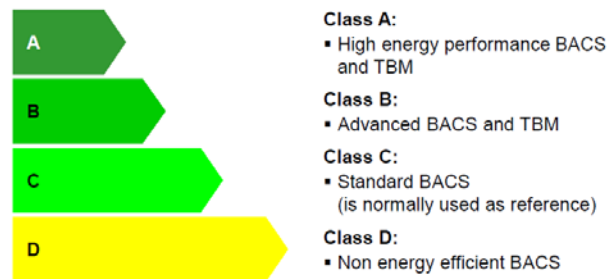


Figure 2: Energy performance classes

Note: Building Automation and Controls Systems (BACS) and Technical Building Management Systems (TBM) in the UK are known as Building Management System (BMS) and Building Energy Management System (BEMS) respectively.

To put this into context Class C is what would be required by the current UK building regulations published in November 2013 (UK Non-Domestic Building Services Compliance Guide).

The UK Energy Technology List (ETL) currently has criteria for:

- Heating, Ventilation and Air Conditioning (HVAC) controls (now Building Environment Zone Controls);
- Hot Water Systems Optimising controls (now Heating Management Controllers);
- Lighting controls; and
- Variable Speed Drives (VSDs).

The ETL Building Environment Zone Controls criteria are close to representing good practice when all the criteria are imposed. The criteria above fall slightly short in that summer/winter change over functionality and a requirement for 365 day programming, as defined in BS EN 15500 (BSI 2008), have not been included. Joining these together would represent good practice and a specification based on this would probably meet the requirements of Class B of EN 15232, a step up from the building codes but this still falling short of the most efficient operation of a building.

The indicative savings that can be achieved from the implementation of the EN 15232 classes are shown in the table 2. This considers Class D of the standard as the baseline; the reason for this is that the majority of buildings will be at this level or below.

If we look at the wholesale and trade service buildings line we can see that fitting Class C controls could realise 35.9% savings, whilst an additional 17.3% can be achieved through Class B controls. Pre-programmable BEMs would satisfy the Class B criteria but in order to achieve Class A of the standard, programmable BEMs would be required and then the final 8.3% of energy savings may be realised.

Table 2:

Indicatives savings for increasing the class of building controls from Class D of EN 15232

Non-residential building types	% savings from D			
	D	C (Reference)	B	A
	Non energy efficient	Standard	Advanced	High energy performance
Offices	0.00	33.77	47.02	53.64
Lecture hall	0.00	19.35	39.52	59.68
Education buildings (schools)	0.00	16.67	26.67	33.33
Hospitals	0.00	23.66	30.53	34.35
Hotels	0.00	23.66	35.11	48.09
Restaurants	0.00	18.70	37.40	44.72
Wholesale and retail trade service buildings	0.00	35.90	53.21	61.54
Other types: - sport facilities - storage - industrial buildings - etc.		N/A		
* These values highly depend on heating / cooling demand for ventilation.				

This indicates that approximately 62% of savings for a retail building can be achieved by fitting EN 15232 Class A controls (a programmable BEMs) which would achieve the target for the building without other measures.

Lighting controls are also included within the ETL but are technology specific; the specification covers products that are specifically designed to switch electric lighting on or off, and/or to dim its output. In addition to the functionality covered by the Building Environment Zone Controls described above, lighting controls cover presence detection and daylight detection – with and without dimming.

The result is that this could be used as an off the shelf specification for the building control systems.

Building Controls and zoning

The way a non-domestic building is subdivided into zones will influence the predictions of energy performance and how you set up the control of the building. Therefore, the zoning rules must be applied when assessing a non-domestic building for controls. The end result of the zoning process should be a set of zones where each is distinguished from all others in contact with it by differences in one or more of the following:

- The activity attached to it;
- The HVAC system which serves it;

- The lighting system within it;
- The access to daylight (through windows or rooflights).

To this end, the suggested zoning process within a given floor plate is as follows:

1. Divide the floor into separate physical areas, bounded by physical boundaries, such as structural walls or other permanent elements.
2. If any part of an area is served by a different HVAC or lighting system, create a separate area bounded by the extent of those services.
3. If any part of an area has a different activity taking place in it, create a separate area for each activity.
4. Divide each resulting area into “zones”, each receiving significantly different amounts of daylight, defined by boundaries which are:
 - At a distance of 6m from an external wall containing at least 20% glazing;
 - At a distance of 1.5 room heights beyond the edge of an array of rooflights if the area of the rooflights is at least 10% of the floor area;
 - If any resulting zone is less than 3m wide, absorb it within surrounding zones;
 - If any resulting zones overlap, use your discretion to allocate the overlap to one or more of the zones.

An example of this approach is given in Figure 3. Once the zoning has been carried out consideration can be given to placement of sensors (temperature, occupancy and light levels) with a view to controlling these zones in terms of the services provided.

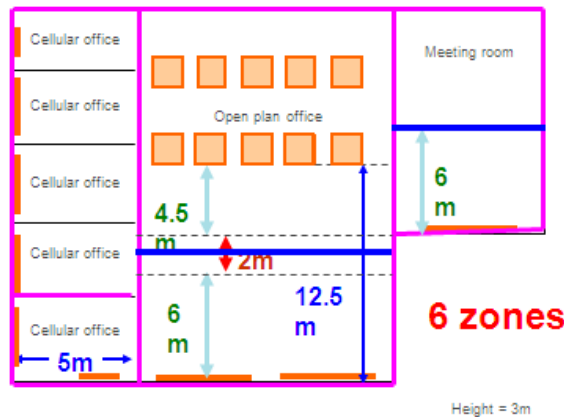


Figure 4: an example of a small office zoned by activity and then daylighting

Daylighting Standards

The only comprehensive standard found, for non-domestic buildings, was the British Code of Practice for daylighting (BS 8206-2, BSI 2008). This standard gives recommendations regarding design for daylight in buildings. It includes recommendations on the design of electric lighting when used in conjunction with daylight.

BS 8206-2 describes good practice in daylighting design and presents criteria intended to enhance the well-being and satisfaction of people in buildings, recognizing that the aims of good lighting go beyond achieving minimum illumination for task performance.

This revision of BS 8206-2 has been prepared to take account of the publication of two European standards (BS EN 12464-1, BSI, 2-11; BS EN 15193, BSI, 2007). In particular, some of the manual calculations that appeared in the 1992 edition have been omitted and a new annex on climate-based daylight modelling has been added along with a new clause on daylighting and health.

Simple graphical and numerical methods are given for testing whether the criteria are satisfied, but these are not exclusive and computer methods may be used in practice. Sunlight and skylight data are given.

In addition a new BRE guide (Ticleanu, C., Littlefair, P. and Howlett, G., 2013) provides essential guidance on how to achieve effective and energy-efficient retail lighting

Best practice guidance for daylighting in non-domestic buildings has also been identified along with the need to carry out an energy audit first in order to identify the most appropriate technology areas for any refurbishment.

Energy auditing and whole building energy savings

There is a new European standard for energy auditing (BS EN 16247-1, BSI, 2012) which should be used to identify opportunities for savings and barriers to implementation. Then the data collected can also be used to create meaningful improvement targets through the application of data analysis (Lewry, A. J., 2013).

For a case study such as this it is essential that the methodologies are comparable with those already in use and that technologies match or exceed best practice criteria already published. In addition, producing auditable numbers is essential to showing transparency in how the energy savings claimed are justified.

However, refurbishment is not treated consistently and for major works it is suggested the EU GPP criteria of an 20% improvement on the building regulations for new build is aimed for or at least the same performance as the minimum new build criteria, as laid out in the building codes, is reached.

If this is not technically feasible a minimum performance increase, such as achieving a final rating in the top quartile of energy performance should be considered. The top quartile level defined by analysing the database of Energy Performance Certificate (EPC) ratings within the country in which the non-domestic building is situated.

From earlier you can see that this project is far more ambitious and aims for an **EPC “A” rating**.

Best practice guidance

Best practice guidance on low carbon refurbishment of non-domestic buildings has also

been identified; this covers both the refurbishment process and the use of renewable technologies (Carbon Trust, 2008). The guidance is structured around a roadmap for the refurbishment process, identifying the key intervention points during the preparation, design, construction and use phases of the project – Figure 5.

Phase	Low Carbon Refurbishment Process	Page	RIBA Work Stages		
Prepare 	Commit to a low carbon refurbishment	7	Preparation		
	Establish a low carbon vision for the refurbishment	7		Approval	
	Develop a low carbon outline brief	7	Design		
	Establish the current carbon footprint of the building	8		Design brief	
	Set carbon targets for the refurbishment	8		Design	
	Undertake a pre-refurbishment assessment	8			Concept
	Consult stakeholders	10		Design development	
	Consider a budget for low carbon elements	10			Technical design
	Appoint a carbon champion	11		Pre-construction	
	Choose an appropriate design team	11			
	Empower the design team	12		Tender documentation	
	Design 	Keep the low carbon theme up front		13	
Develop an integrated low carbon design		13	Construction		
Encourage exploration of a wide range of low carbon options		14		Mobilisation	
Allow flexibility in design		15	Construction to practical completion		
Use energy modelling data		16		Post practical completion	
Use whole life costing to support low carbon solutions		17			Post practical completion
Manage the budget and scope		17		Use	
Approve the integrated design		18			Make sure the occupants understand the building
Include targets in contracting arrangements	18	Make sure the building operator understands the building			
Construct 	Ensure effective project management	18	Conduct a post-occupancy evaluation		
	Choose an appropriate contractor and subcontractors	19	Check energy use and comfort conditions and make changes		
	Get buy-in from site workers	19	Make the most of the low carbon building		
	Monitor site progress against objectives	20			
Use 	Ensure high quality commissioning	20			
	Set up energy monitoring	20			
	Make sure the occupants understand the building	21			
	Make sure the building operator understands the building	21			

Figure 5: Good practice roadmap for the Low Carbon refurbishment process

For renewables, the ETL has best practice performance criteria for Heat pumps; Solar Thermal; Combined Heat and Power; Biomass boilers and room-heaters.

The UK Feed-in Tariff (FIT) for generating electricity on-site, Renewable Heat Incentive (RHI) and the Microgeneration Certification Scheme (‘MCS’) contains technology requirements for:

- Solar thermal systems;
- Solar PV systems;
- Small and micro wind turbines;

- Heat pump systems;
- Biomass systems;
- CHP;
- Micro-hydro systems;
- Bespoke Building Integrated Photovoltaic (PV) Products.

These give full product specifications to the current EN and ISO standards. An example of the product certification scheme requirements for solar photovoltaic modules is given in Appendix 15.

MCS includes minimum performance requirements for heat pumps (COPs) and biomass (efficiency) and every MCS installation standard includes a methodology for estimating the annual energy performance of renewable energy systems. For example PV has the MCS Guide to the installation of PV systems which contains a method for estimating the annual electricity generated (AC) in kWh/year of the installed system.

Conclusions

This study identifies that building regulations and their associated codes lay down minimum levels of performance for non-domestic buildings but do not attempt to prompt best practice. However, the building codes laid down the minimum performance (“backstop”) requirements for building fabric elements and building services; the exception being true renewables, i.e. solar, hydro and wind based technologies, where there were generally no performance criteria. This project aims to match the best of these backstop U-values and exceeded them wherever possible.

The building codes approach the energy performance of non-domestic building holistically where the overall performance of the building as designed is calculated by the use of approved software. This gives an asset rating which is then deemed as a pass or fail when compared to the performance level required by the individual building code, normally in terms of a target kWh/m²/annum. The Primary energy consumption was calculated as **167.7 kWh/m²/annum which gave an E rating on the Energy Performance Certification (EPC). Target value for the IKVA case study is 80 kWh/m²/annum; which is just over a 50% reduction in energy usage and would give an EPC rating of an “A”.** This is an ambitious target but one that is thought to be achievable.

Best practice performance criteria were identified for the majority of technology areas. The project proposes the use of heat pump technology and the performance of said technology should match or exceed the best practice performance criteria described in the UK’s Enhanced Capital Allowance (ECA) scheme and its Energy Technology List (ETL).

The control of energy in non-domestic buildings is generally poor and controls are one

of the most effective solutions in realising energy savings. They should always be part of a refurbishment and EN 15232 used as the methodology for estimating their effect. Indicative savings of 62% may be realised by the installation of an advanced Building Energy Management system (BEMs).

For a case study such as this it is essential that the methodologies are comparable with those already in use and that technologies match or exceed best practice criteria already published. In addition, producing auditable numbers is essential to showing transparency in how the energy savings claimed are justified.

REFERENCES

Energy Performance Building Directive (EPBD) implementation and its current recast, Directive 2002/91/ec of the European parliament and of the council of 16 December 2002 on the energy performance of buildings, <http://eur-lex.europa.eu/LexUriServ/LexUriServ.do?uri=OJ:L:2003:001:0065:0065:EN:PDF>

Energy Performance of Buildings: 7/2006. (V.24.) TNM directive, customized calculation methods (EPBD)
http://net.jogtar.hu/jr/gen/hjegy_doc.cgi?docid=A0600007.TNM

Lewry, A. J., and Garrido, M. D. C., Deliverable D2.1 Assessment of national building codes, EPBD implementation and standards identified, EcoShopping - Energy efficient & Cost competitive retrofitting solutions for Shopping buildings, European Commission within the 7th Framework Programme, V1, 17th January 2014. http://ecoshopping-project.eu/document/D2.1%20Assessment%20of%20national%20building%20codes,%20EPBD%20implementation%20and%20standards%20identified_17-01-14x.pdf

EU Green Public Procurement (GPP) criteria -
http://ec.europa.eu/environment/gpp/gpp_criteria_en.htm.

UK's Enhanced Capital Allowance (ECA) scheme and its Energy Technology List (ETL) -
<https://etl.decc.gov.uk/etl/site.html>.

Lewry, A. J., Understanding the choices for building controls, BRE IP 1/14. Bracknell, IHS BRE Press, 2014.

BS EN 15232 (2012): Energy performance of buildings — Impact of Building Automation, Controls and Building Management, British Standards Institute.

UK Non-Domestic Building Services Compliance Guide (NDBSCG) 2013.
http://www.planningportal.gov.uk/uploads/br/domestic_building_services_compliance_guide.pdf.

BS EN 15500 (2008): Control for heating, ventilating and air-conditioning applications — Electronic individual zone control equipment, British Standards Institute.

BS 8206-2 (2008): Code of Practice for daylighting, British Standards Institute.

BS EN 12464-1(2011): Light and lighting - Lighting of work places - Indoor work places, British Standards Institute.

BS EN 15193 (2007): Energy performance of buildings, Energy requirements for lighting, British Standards Institute.

Ticleanu, C., Littlefair, P. and Howlett, G., The essential guide to retail lighting: Achieving effective and energy-efficient lighting (FB 56), IHS BRE Press, 2013.

BS EN 16247-1 (2012): Energy audits - Part 1: General requirements, British Standards Institute.

Lewry, A. J., Energy surveys and audits – A guide to best practice. BRE IP 7/13, Bracknell, IHS BRE Press, 2013.

CTV 038 (2008), Low Carbon Refurbishment of Buildings - A guide to achieving carbon savings from refurbishment of non-domestic buildings, Carbon Trust, free download from <http://www.carbontrust.com>.

UK Feed-in Tariff (FIT) for generating your electricity on-site - <https://www.gov.uk/feed-in-tariffs>.

Renewable Heat Incentive (RHI), <https://www.gov.uk/government/policies/increasing-the-use-of-low-carbon-technologies/supporting-pages/renewable-heat-incentive-rhi>.

Guide to the Installation of Photovoltaic Systems, Microgeneration Certification Scheme ('MCS'), 10 Fenchurch Street, London EC3M 3BE, 2012, www.microgenerationcertification.org.